DEVELOPMENT OF THE AUTONOMOUS DIODE LASER WEEDING ROBOT

by

CANICIUS JOSEPH MWITTA

(Under the Direction of Glen Rains and Kyle Johnsen)

ABSTRACT

Weed control in agricultural fields poses a major challenge for farmers due to the significant losses that can be caused by weeds, impacting productivity. Herbicides have been the most effective weed control solution, in addition to other conventional methods like mechanical and manual weeding. However, the emergence of herbicide-resistant weed populations, concerns regarding herbicides' negative impact on the environment, and the labor-intensive nature of these conventional weed control methods threaten the ability of the agricultural industry to keep up with the growing demand. Furthermore, evidence shows that labor costs in agriculture are increasing rapidly due to labor shortages. All these factors necessitate alternative weed control solutions that are less labor-reliant, cost-effective, with minimal impact on the environment and crop health. Lasers have emerged as a viable weed control solution due to their capacity to precisely target weeds. Small autonomous robotic platforms employing lasers can be used to target weeds in their early growth stages and eliminate them.

In this study, an autonomous robot that employed a diode laser for weed elimination was designed and implemented. The robot utilized a combination of visual servoing for motion control, the Robot Operating System (ROS) for coordination, and a Finite State Machine to manage its states, actions, and transitions. Data from sensors such as GPS, encoders, stereo

cameras, and IMUs were utilized for weed detection, robot navigation, and control of the robotic manipulator arm. An Extended Kalman Filter (EKF) sensor fusion algorithm was employed to fuse sensor data for robot localization. Furthermore, the robot employed deep learning for weed detection, weed tracking, and path detection between cotton rows. It then used the Dynamic Window Approach (DWA) path planning algorithm for navigation. A 2D Cartesian manipulator arm was used to position the laser diode attached to a rotating pan-and-tilt mechanism for precise weed targeting. Experiments conducted in a cotton field showed that the robot was able to effectively navigate autonomously between cotton rows, detect and track weeds, and eliminate them with laser beam treatment. These results provide strong evidence of the feasibility of autonomous weed elimination using low-cost diode lasers on small robotic platforms.

INDEX WORDS: Laser weeding, Weeding Robotics, Machine Vision, Deep Learning, Precision Agriculture, Visual Servoing, Autonomous Navigation, ROS, Finite State Machine, PID Control, Weed tracking, Weed detection, RTK-GNSS, Ackerman-Steering Robot, Dynamic Window Approach

DEVELOPMENT OF THE AUTONOMOUS DIODE LASER WEEDING ROBOT

by

CANICIUS JOSEPH MWITTA

B.S., University of Dar es Salaam, Tanzania, 2011

M.S., University of Edinburgh, United Kingdom, 2016

A Dissertation Submitted to the Graduate Faculty of The University of Georgia in Partial Fulfillment of the Requirements for the Degree

DOCTOR OF PHILOSOPHY

ATHENS, GEORGIA

2023

DEVELOPMENT OF THE AUTONOMOUS DIODE LASER WEEDING ROBOT

by

CANICIUS JOSEPH MWITTA

Major Professors:	Glen Rains
	Kyle Johnsen
Committee:	Javad Mohammadpour
	Eric Prostko
	Changying Li

Electronic Version Approved:

Ron Walcott
Vice Provost for Graduate Education and Dean of the Graduate School
The University of Georgia
December 2023

DEDICATION

To my late mother, to whom I owe everything. I pray for her to continue resting in peace.

ACKNOWLEDGEMENTS

It is a blessing to have experienced and talented mentors for guidance. I would like to express my special appreciation to my advisor, Dr. Glen Rains. Firstly, for providing me the opportunity to work on my dream field; secondly, for his guidance, advice, support, and encouragement throughout my research. Thanks for showing me the right direction and your timely reviews of my work. I look forward to future collaborations.

I would like to thank Dr. Kyle Johnsen for agreeing to be my co-advisor and for his guidance and support on my research.

My special thanks and appreciation go to Dr. Eric Prostko for his tremendous support and knowledge in weed research, which significantly informed my research. Thank you for your timely responses and reviews of my research.

I would also like to thank my committee advisors, Dr. Javad Mohammadpour and Dr. Changying Li, for their guidance. I appreciate your feedback on my research.

My thanks also go to Dr. Kadeghe Fue for his collaboration and for his early work on the rover. Many thanks to Mr. Shekhar Thapar for assisting in the building of the robot, Mr. John Paulk for technical support, and my lab mates Mr. Denis Kiobia and Mr. Peter Ngimbwa for their assistance in the field.

I am grateful for my dad, sister, and brother who have always supported and encouraged me to pursue my dreams. Thank you for your love and support.

Finally, my sincere thanks and appreciation to Cotton Incorporated and Georgia Peanut Commission for providing funding for the project.

TABLE OF CONTENTS

Page

LIST OF TABLES

Page

LIST OF FIGURES

Page

CHAPTER 1

INTRODUCTION

1.1 **Background and Significance of This Study**

Invasive weeds in agricultural fields pose a major threat to agriculture production because they compete for crucial resources with crops. Weeds are known to cause higher potential yield losses in crop production than pathogens and animal pests (Oerke, 2006), thereby posing a significant threat to food security (Délye et al., 2013). This makes weed control in an agricultural field a crucial predictor of productivity.

Weed control in agricultural environments can be a challenging and expensive process. Herbicides have been the most effective method for controlling weeds in agricultural fields, in addition to other conventional methods such as mechanical weeding, and manual weeding. Despite their popularity, several challenges have been associated with these methods, including:

- Emergence of herbicide-resistant weed populations, which hinder weed control efforts (Powles et al., 1996; Shaner, 2014)
- Potential negative impacts of herbicides on the environment (Colbach et al., 2010)
- Inefficiency of mechanical weeding approaches and the potential for interfering and injury to crops (Fogelberg & Gustavsson, 1999)
- High labor costs associated with manual weeding (Bastiaans et al., 2008; Schuster et al., 2007)

- Labor shortages in agriculture, leading to rapidly increasing labor costs (Guthman, 2017; Richards, 2018; Zahniser et al., 2018). This is exacerbated by the labor-intensive nature of conventional weeding methods.

To sustain the world's rapid population growth, agricultural production needs to keep up. Without alternative methods of controlling weeds that are less labor-reliant and chemical dependent, agricultural production will fall short of demand.

Advances in technology, such as the emergence of faster portable processors, artificial intelligence (AI), robotic technology, modern computer vision algorithms and equipment, modern mechanics, and others, provide an opportunity for small autonomous robotics adoption to address most of these weeding challenges, as well as other farming tasks. Autonomous robotic weed control addresses the challenges of labor requirements, costs, and efficiency. However, an effective high-precision weed removing method is needed to address the other challenges such as chemical impact and crop interference. Laser technology has emerged as a potential solution for precise targeted elimination of weeds. Treating weeds with laser beams has proved effective in eliminating them or hindering their growth (Heisel et al., 2001; Kaierle et al., 2013; Marx et al., 2012; Mathiassen et al., 2006; Mwitta et al., 2022). Narrow beams from lasers can remove both inter-row and intra-row weeds with precision targeting. To make the system small and energy efficient, diode lasers were selected for this research. Diode lasers emit the beam by passing current through a semiconductor. They have the advantage of being small, widely available, inexpensive, requiring low voltage and low current. Their uniqueness in size, weight, costs coupled with their high efficiency and reliability, makes them easier to integrate in systems (Bachmann, 2003), as opposed to other types of lasers available in the market, such as CO_2 and Fiber lasers. CO_2 lasers are relatively bulky, and require more power, and a separate cooling

system when operating in an outside environment, while fiber lasers are the most powerful and most expensive of the three.

Small autonomous robotic platforms that employ diode lasers can be utilized in agricultural environments to target weeds in their early stages of growth and eliminate them. Due to their low operating costs, the robots can be utilized multiple times to deal with weeds as they emerge, as well as performing other farming tasks such as planting, harvesting, and scouting.

1.2 Objectives

The primary objective of this dissertation was to develop an autonomous diode laser weeding robot and assess its weed control performance in an actual agricultural field.

The specific objectives were as follows:

1. Conduct a review of robotic weeding in agriculture.
2. Conduct experiments to evaluate diode laser performance in weed elimination.
3. Develop a real-time deep learning model for weed detection.
4. Create a path planning and navigation strategy for the robot to maneuver between crop rows.
5. Develop algorithms for robot localization, and integrate sensing, path planning, navigation, and end-effector manipulation.
6. Test the robot in a real-world agricultural environment.

1.3 Research Contribution and Dissemination

The models, algorithms, and system hardware developed in this study are open source. They can be adopted by other researchers, the industry, or enthusiasts to develop inexpensive autonomous laser weeding robotic platforms. The codes from this study are shared freely in our Github accounts; https://github.com/UGA-AgRobotics and https://github.com/Cannyjm

This study contributes to the efforts of precision weeding development. With the robot successfully tested in the field, the study stands as one of the earliest implementations of autonomous diode laser weeding in agricultural industry. Apart from the developed robot, the methods and results have been presented and published in various conferences and workshops, one article has been published and three others are to be submitted. The publications that are presented in this dissertation are as follows:

1. Mwitta, C., Rains, G. C., and Prostko, E. (2022). Evaluation of Diode Laser Treatments to Manage Weeds in Row Crops. Agronomy, 12(11), 2681.
2. Mwitta, C., Rains, G., and Prostko, E. (2023). Evaluation of inference performance of deep learning models for real-time weed detection in an embedded computer. (to be submitted)
3. Mwitta, C., and Rains, G. (2023). The integration of GPS and Visual navigation for autonomous navigation of an Ackerman steering mobile robot in cotton fields. (to be submitted)
4. Mwitta, C., Rains, G., and Prostko, E. (2023). Autonomous Diode Laser Weeding Mobile Robot in Cotton Field Using Deep Learning, Visual Servoing and Finite State Machine. (to be submitted)

1.4 Overview of the Dissertation Chapters

The dissertation consists of seven chapters. Chapter 1 introduces the significance of this study and describes the objectives and research contributions of this dissertation.

Chapter 2 provides a brief overview of other studies in robotics in agriculture, autonomous weeding, laser weeding as well as looking at current available commercial autonomous weeding systems in agriculture industry.

Chapter 3 introduces a study on the viability of using inexpensive low-powered diode lasers for weed elimination. The robot needs to kill weeds or stunt their growth using these laser diodes. Laser diodes with different power were tested on their ability to kill weeds of different species, different stem diameters, and at different treatment durations. Analysis on the effect of laser power, weed diameter, treatment time and weed species to the survival of the weed was performed.

Chapter 4 compares three deep learning algorithms on their weed detection performance in an embedded computer. Since the robot uses an embedded computer, it is important to know the ideal weed detection deep learning model for optimal performance. Deep learning models were trained on 11 species of weeds and testing experiments were conducted to determine their detection performance. Comparison analysis was performed to determine the best model for optimal weed detection performance.

Chapter 5 evaluates different autonomous navigation strategies of the robot in cotton field. GPS navigation, visual navigation, and a combination of both were tested. The robot must be able to localize itself and navigate autonomously in the field. Various methods and techniques were created utilizing deep learning, path planning, path tracking, and sensor fusion to navigate the robot between cotton rows. Experiments were conducted in the field, and analysis was performed on the effectiveness of each of the navigation approaches.

Chapter 6 introduces a working autonomous laser weeding robot and evaluates its performance on weed elimination in a cotton field. The robot utilizes finite state machine to control the autonomous processes, such as weed detection using YOLOv4-tiny, navigation using deep learning and GPS, arm manipulation for positioning the laser diode to target weed stems, and laser manipulation.

Chapter 7 presents research conclusions, limitations, and future research studies.

CHAPTER 2

LITERATURE REVIEW – AGRICULTURAL ROBOTS AND LASER WEEDING

A substantial body of research has been devoted to agricultural robots, especially weeding robots, and more recently, the impact of lasers on weed control. This chapter provides a concise overview of the trends in designing and developing agricultural robots, with a specific emphasis on weeding robots and the innovative concept of laser weeding.

2.1 **Agricultural Robots**

The process of designing and developing agricultural robots presents unique challenges, primarily due to the demanding nature of the outdoor operating environment. Factors such as weather conditions, unpredictable terrain, fluctuations in light intensity, field obstacles, and unforeseen issues can complicate the robot development process. To be effective, a robotic system in agriculture must meet several key criteria, including safety, cost-effectiveness, reliability, and the ability to perform tasks in unstructured agricultural settings while maintaining work quality comparable to current methods (Bechar & Vigneault, 2016).

Despite these challenges, autonomous robots hold substantial potential for positively impacting agriculture. As demonstrated by (Pedersen et al., 2006) in their economic feasibility study, autonomous robotic applications in high-value crops offer greater economic viability when compared to conventional systems. In terms of designing and developing agricultural robots, (Bechar & Vigneault, 2016) concluded that autonomous agricultural robots would typically comprise four primary sub-systems: Mobility and steering, Sensing and self-localization, Path planning and guidance, and Manipulators and end effectors. This literature

review was conducted with these sub-systems in mind, providing a comprehensive perspective on the subject.

2.1.1 Sensing in Agricultural Robotics

Sensors play a crucial role in various aspects of agricultural robots, including tasks like plant detection, navigation, mapping, localization, guidance, and measurement of environmental parameters. They are instrumental in supporting decision-making, enabling task activation, execution, and performance evaluation within robotic systems (Bechar & Vigneault, 2016).

Imaging has been one of the most widely employed sensing techniques for localizing robots in agricultural fields and detecting objects. Imaging technologies like visible light, infrared, fluorescence, spectroscopy, and structural topography have proven to be key in agricultural research (Rahaman et al., 2015). Additionally, other sensors such as 2D and 3D imaging (Zhao et al., 2012), digital cameras (RGB), thermal sensors, multispectral and hyperspectral cameras, light detection and ranging (LIDAR), sound navigation and ranging (SONAR) have been utilized for various sensing tasks in the fields (Deery et al., 2014; Safren et al., 2007; Sankaran et al., 2015).

In terms of navigation, many robots utilize wheel encoders to monitor the wheel rotations and Inertia Measurement Units (IMUs), which combine accelerometers, gyroscopes, and sometimes magnetometers to track orientation, sensor acceleration, and angular velocity. Agricultural robots commonly incorporate Global Navigation Satellite Systems (GNSS) sensors, which rely on a satellite-based navigation system to provide position, velocity, and timing information. A combination of these sensors is frequently employed in autonomous robotic weeding systems.

2.1.2 Steering and Mobility in Agricultural Robots

Navigation in agricultural robots is the process of directing the vehicle in a desired orientation at an appropriate speed (Bechar & Vigneault, 2016). Most robots achieve this by making contact with the soil using wheels or legs. However, various mobility methods have been implemented to address the specific conditions of the agricultural field or the robotic operation (Fue, Porter, Barnes, & Rains, 2020). Figure 2.1 illustrates examples of agricultural robots with different navigation mechanisms.

Wheels are a popular choice for navigating fields quickly and efficiently. However, in dense areas with numerous stems and branches, robotic legs may be more suitable. The emergence of drones offers an alternative means of field navigation without direct contact with the soil, but this technology is primarily used for surveying and spraying. In some cases, robots move along rails for high-speed navigation or swing over plants, particularly on extremely wet soil surfaces, where wheeled robots might encounter difficulties. Several studies such as one conducted by (Zhang et al., 2013), have relied on RTK (Real-Time Kinematics)-GNSS and IMUs to navigate through fields, especially in areas where GNSS signal is not obstructed. Others have employed autonomous row-following techniques using either camera vision (A. Sivakumar et al., 2021) or LIDAR (Barawid et al., 2007; Hiremath et al., 2014).

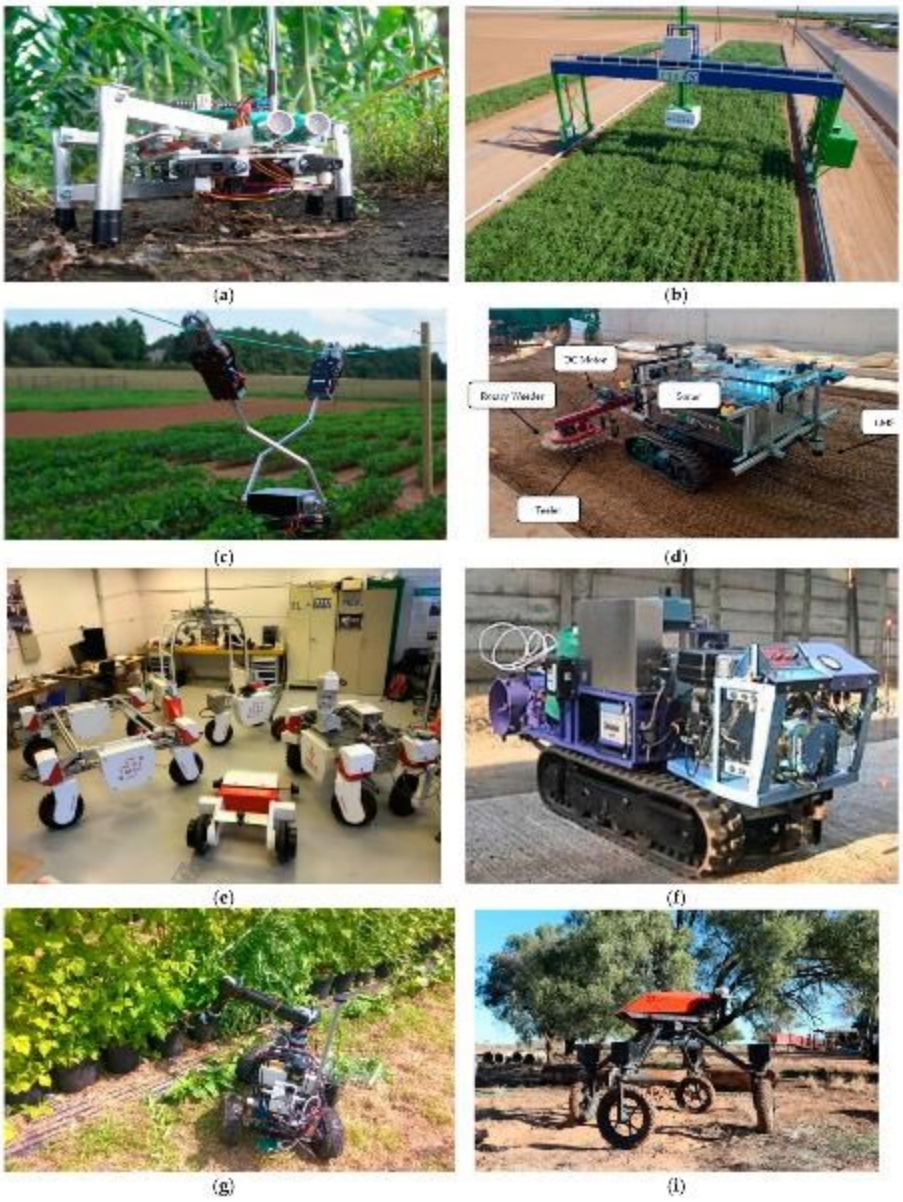

Figure 2.1. From (Fue, Porter, Barnes, & Rains, 2020), some agricultural robots with different navigation mechanisms; (**a**) AgAnt (source: cleantechnica.com), (**b**) Fraunhofer Institute for Production Systems and Design Technology IPK dual-arm robot (source: agromarketing.mx), (**c**) Tarzan swing robot (Davies et al., 2018; Farzan et al., 2018) (**d**) Weeding Robot (Reiser et al., 2019) (**e**) Thorvald II Agricultural Robotic System Modules (Grimstad & From, 2017) (**f**) Fuji industry Robot (source: fuji.co.uk) (**g**) RAL Space Agribot with robot arm weeding raspberries

(source: autonomous.systems.stfc.ac.uk) (**i**) SwagBot, omnidirectional electric ground vehicle (source: confluence.acfr.usyd.edu.au)

2.1.3 Path Planning in Agricultural Robotics

Path-planning involves finding a quality path from source to destination while avoiding collision with obstacles (Bhattacharya & Gavrilova, 2008). It is considered a sub-task of navigation (Bechar & Vigneault, 2016). In agricultural fields, path-planning mainly involves robots moving either over rows of plants or between rows of plants. In addition to that, path-planning involves the plan for movement of manipulators to the target. Several path planning algorithms for robotic systems have been developed such as sampling-based algorithms, grid-based search algorithms (like in (Jensen et al., 2012)) which divide the exploration environment into a collection of grid cells, sampling-based algorithms (like in (Mahmud et al., 2019)) which sample random valid configurations and add them to a tree or graph structure to be queried for a path solution, and velocity-based path planning algorithms like dynamic windows approach (like in (Li et al., 2022)) which navigate using a collision avoidance strategy taking into account the dynamics of the robot.

2.1.4 Manipulation and End-Effector in Agricultural Robots

A manipulator is an arm-like electromechanical device capable of movement within confined spaces, typically equipped with a tool known as an end-effector. Manipulators are classified based on several metrics, including the degrees of freedom, type of joint, link length, and offset length (Kondo & Ting, 1998).

The primary function of a manipulator is to position the end effector for effective interaction with a targeted task object and to orient the end effector to perform the task (Bechar & Vigneault, 2016). End effectors can take various forms, such as grippers (as demonstrated by

Hannan et al., 2007), physical penetrators that enter the target object (as shown in Cao et al., 2003), suction objects (as reported by Monta et al., 1995), or those with adhesive force capabilities (Monkman, 1995; Rodríguez et al., 2012; Tai et al., 2016). Agricultural robots may employ a combination of these end effectors to fulfil various tasks.

2.2 **Autonomous Weeding Robots**

Numerous studies have delved into the development of weeding robots, showcasing a range of complexity and innovation. Some relatively simple robots, like the automatic weed detection and smart sprayers between the crop rows (Aravind et al., 2016), or the plant and weed identifier robot utilizing a deep learning model faster R-CNN (Shah et al., 2021), have been explored. Other studies have successfully created working prototypes of weeding robots, exemplified by the work of (Bawden et al., 2017) and (Sujaritha et al., 2017). In the case of (Bawden et al., 2017), they detailed the design, development, and testing of a modular robotic platform. This involved creating technical specifications based on farmers' insights and then combining the robotic platform with a weeding array that integrated vision and a combination of chemical and mechanical methods for weed removal. Meanwhile, (Sujaritha et al., 2017) proposed a robotic model for weed detection in sugarcane fields, employing leaf textures extraction and a fuzzy real-time classification technique.

To address the uncertainty of agricultural environments, various techniques have been applied. (McCool et al., 2018) combined mechanical and spraying mechanisms in their autonomous weed management robot, Agbot II, which used color segmentation for weed detection. (Blasco et al., 2002) eliminated weeds through electric discharge after identifying them with machine vision algorithms. (Pérez-Ruíz et al., 2014) introduced an autonomous mechanical weeding robot designed to remove intra-row weeds using movable hoes, while

(Florance Mary & Yogaraman, 2021) employed deep learning for weed detection in their autonomous robot and then drilled the weeds to the ground.

Most weeding robots employ cutters, plows, and spraying nozzles as end effectors. Laser technology has recently emerged as a promising solution for precise weed elimination. Studies such as (Heisel et al., 2001; Kaierle et al., 2013; Marx et al., 2012; Mathiassen et al., 2006; Mwitta et al., 2022) have demonstrated that laser beam treatments can effectively eliminate weeds or inhibit their growth.

2.2.1 Autonomous Laser Weeding Robots

Laser weeding robots are equipped with laser systems as their end-effector, utilizing laser beams to target and eliminate weeds. The development of autonomous laser weeding robots is still relatively new and under investigation. For instance, (Xiong et al., 2017) created a prototype of an autonomous laser weeding robot that utilized color-segmentation for weed identification, fast path-planning algorithms, and two laser pointers to target weeds in an indoor environment, achieving an impressive hit rate of 97%. However, there have been relatively few instances of such applications in outdoor field environments.

2.2.2 Commercial Autonomous Weeding Robots

A few robotic companies have made significant strides in developing weeding technology to assist farmers in safeguarding their crops. Notable examples include:

- Ecorobotix (https://ecorobotix.com/en/avo/) – created an autonomous robot for precise herbicide application. This technology is designed to reduce the quantity of chemical treatment required in agriculture, acknowledging that although chemical treatments have faced criticism, they remain efficient. The primary objective is to decrease the reliance on chemicals applied to fields.

- Naio Technologies (https://www.naio-technologies.com/en/home/) - combined various mechanical weeding techniques, including cutters and plows, with the aid of camera vision and sensors to position tools as close as possible to crops. This approach offers an alternative to herbicides, but involves soil tillage, which can disturb and kill non-targeted organisms.
- Vitbot (https://vitibot.fr/article_presse/bakus-attaque-les-vignes-champenoises/) - follows a similar approach to Naio Technologies, utilizing a combination of mechanical weeding techniques and vision-based tools for precision weeding in vineyards.
- Rootwave (https://rootwave.com/) - developed an innovative and environmentally friendly solution for weed control. This non-chemical method employs electric bolts, delivering up to 8kV electricity to weeds, effectively boiling them from the inside. It offers a reduced carbon emissions approach that is non-invasive and is harmless to non-targeted organisms.

These companies represent a growing trend toward more sustainable and precise weeding technologies, reducing the reliance on chemical treatments and minimizing the impact on the environment.

2.2.2.1 Laser Weeding by Carbon Robotics

Carbon Robotics (https://carbonrobotics.com/) is one of the pioneering companies in the field of commercial autonomous laser weeding. Their robot employs multiple 150W CO_2 lasers, a powerful computer, GNSS, and computer vision technology to effectively eliminate weeds.

While this technology offers a promising solution for weed control, it's essential to note that it comes with certain challenges. The high-powered, complex nature of the system makes it

relatively expensive, power-hungry, and complicated to operate. This complexity may raise safety concerns for individuals who aren't well-versed in advanced technology.

CHAPTER 3

EVALUATION OF DIODE LASER TREATMENTS TO MANAGE WEEDS IN ROW CROPS[1]

[1]Mwitta, C., Rains, G., and Prostko, E., (2022). *Agronomy*., 12(11):2681. Reprinted here with permission of the publisher.

3.1 **Abstract**

Herbicides have been the primary weed management practice in agriculture for decades. However, due to their effects on the environment in addition to weeds becoming resistant, alternative approaches to weed control are critical. One approach is using lasers, particularly diode lasers because of their portability, low power demand, and cost effectiveness. In this research, weeds' response to diode laser treatments was investigated. Three experiments were conducted. The first experiment involved treating two species of weeds with four different laser powers to determine the time it takes to sever the weed stem. The second experiment involved monitoring the status of two species of weeds for a week after treating them with two lasers at constant application times of 1 s, 2 s, and 3 s. The third experiment was a repeat of the second with higher laser powers and shorter treatment times. The results showed diode lasers have a potential to be an effective weed controlling tool. Weed stem diameter, laser power, treatment duration, and distance between laser and weed were all statistically significant in weed mortality, with weed species having no significance. Furthermore, it was found that weed management is possible by exposing the stem of the two weed species between 0.8 and 2.65 mm diameter to a laser beam dosage without necessarily severing it, with 80% effectiveness at 0.5 s treatment time, and 100% effectiveness using a 6.1 W laser for 1.5 s.

3.2 **Introduction**

Weed management in agricultural fields is an important whilst challenging endeavor. Weeds are causing a tremendous economic loss in agriculture by reducing crop yield (Oerke, 2006; Pimentel et al., 2000) which make them a major threat to food security (Délye et al., 2013).

Treating weeds with chemical herbicides has been the most effective and most used method of weed management (Buhler et al., 2000; Gianessi & Reigner, 2007). However, there is a growing concern that herbicides are becoming ineffective as weeds become resistant. There are also environmental and health concerns with the overuse and mishandling of chemicals (Mehdizadeh et al., 2021). The alarming rate at which herbicide-resistant weed populations has been increasing, combining with herbicide costs, have made farmers seriously question the use of herbicides as the primary weed control mechanism (Macé et al., 2007; Richter et al., 2002; Wise et al., 2009). Mechanical non-chemical weed control methods like cultivation and hand pulling are generally more labor-intensive (Bastiaans et al., 2008), and in addition, they can increase soil erosion and leaching of plant nutrients (Ahlgren, 2004). All these reasons necessitate research into alternative methods of weed management.

Advances in technology, like the emergence of faster portable processors, artificial intelligence, advances in robotic technology, modern computer vision algorithms and equipment, modern mechanics, deep learning technology, and others, have provided an ample opportunity to explore smart and precision methods of weeding. A broad range of new tools for precision agriculture are growing at a rapid rate, technologies such as geo-positioning services from satellite systems, yield monitors and mapping software, geographical information systems (GIS), automatic guidance and steering of vehicles, have been implemented over the past decades (Christensen et al., 2009).

The introduction of deep learning technology and image processing in agriculture have made real-time weed detection possible (Behmann et al., 2015; dos Santos Ferreira et al., 2017; Hasan et al., 2021; Yang, 2000; Yu et al., 2019). Precision weed elimination may be achieved using a robotic platform by targeting the individual weeds detected by these deep learning

models. Research of targeted weed elimination such as, mechanical weed removal using robotic cutters (McCool et al., 2018) and precision spraying (Berge et al., 2012; Gerhards & Christensen, 2003; Yang, 2000) have been successfully conducted to prove the potential of robotic weeding.

Lasers have emerged as one of the solutions that have a potential to be effective in targeted elimination of weeds. Treating weeds with laser beam can be efficient in controlling the growth of weeds (Coleman et al., 2021; Heisel et al., 2001, 2002; Kaierle et al., 2013; Marx et al., 2012; Mathiassen et al., 2006; Wöltjen et al., 2008). Using narrow CO_2 laser beams (output powers of 4 W, 10 W, and 20 W), Heisel et al. (Heisel et al., 2001) were able to cut weed stems, while using diode lasers (5 W and 90 W), Mathiassen et al. (Mathiassen et al., 2006) showed laser beam can raise the temperature of the water in the plant cells and delay or stop its growth without the need to cut the stem completely. Woltjen et al. (Wöltjen et al., 2008) studied the effects of both CO_2 and diode lasers treatments on plants and discovered different degrees of effectiveness in hindering the growth of plants. Furthermore, using a 25 W fiber-coupled diode laser Coleman et al. (Coleman et al., 2021) demonstrated the potential of lower energy laser in controlling weeds at different growth stages.

Weed management using lasers is a relatively new endeavor, there are not many systems currently in the market that have implemented this technology, however, several solutions have recently been implemented combining laser equipment, weed detection and robotics to control weeds (e.g., https://carbonrobotics.com, accessed on 15 June 2022; https://welaser-project.eu, accessed on 15 June 2022; https://weedbot.eu, accessed on 15 June 2022).

Targeted narrow laser beams have the potential of removing not only the inter-row weeds but also the intra-rows weeds with proper detection, localization and laser targeting hardware and software. In addition, effects on soil health and non-targeted organisms will be minimized,

avoiding interference with other crop activities, and preserving beneficial organisms (Andreasen et al., 2022).

The main objective of this study was to investigate the effectiveness of low power diode lasers on killing weeds. Diode lasers (Figure 3.1) emit the beam by passing current through a semiconductor. They have the advantage of being small, widely available, inexpensive, requiring low voltage and low current. Their uniqueness in size, weight, costs coupled with their high efficiency and reliability, makes them easier to integrate in systems (Bachmann, 2003), as opposed to other types of lasers available in the market, such as CO_2 and Fiber lasers. CO_2 lasers are relatively bulky, and require more voltage, current and a separate cooling system when operating in an outside environment while fiber lasers are the most powerful and most expensive of the three. Since the aim is to use the laser in a robotic platform (Figure 3.2), CO_2 and fiber lasers present a more challenging setup in terms of portability and costs. Furthermore, looking at laser safety, the laser beam turns into heat energy when it hits a surface. High energy lasers can potentially ignite materials and can cause thermal injury to a person (Andreasen et al., 2022). Using diode lasers of low output power present less operational danger than the high-powered and more complicated CO_2 and fiber lasers; however, it can still cause damage to the eyes on exposure, so, proper caution wearing protecting glasses is necessary (Andreasen et al., 2022).

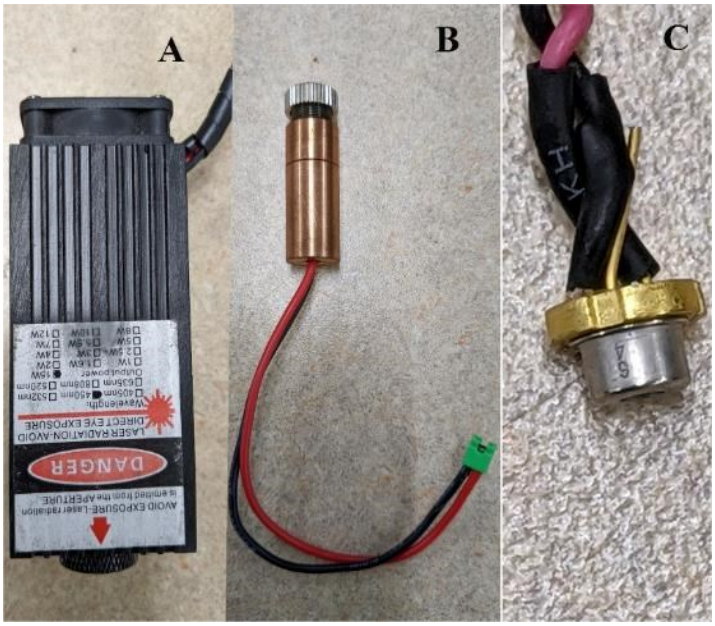

Figure 3.1. Diode lasers. (**A**) diode laser with heat sink enclosure including a fan, (**B**) diode laser without a cooling fan, and (**C**) exposed diode laser.

Figure 3.2. Robotic platform for laser weeding.

3.3 **Materials and Methods**

In this study two phenomena of diode lasers treatments on weeds were investigated. The first investigation aimed to find how effective are laser diodes with different power outputs in completely severing the stems of different weed species and determine the factors that affect the severing effectiveness, since cutting the weed stem completely ensures its elimination. On the other hand, it has been demonstrated that, it is not necessary to cut the weed stem completely for the weed to die, a laser beam can raise the temperature of plant cells, disrupt their structure and kill or stunt their growth (Mathiassen et al., 2006; Wöltjen et al., 2008), so, the second set of experiments aimed to investigate the effectiveness of diode lasers exposure for different durations in killing or stunt the growth of weeds without necessarily severing the weed stem.

3.3.1. Diode Lasers

Six blue laser diodes were tested in this study. Each of the lasers had an output power of less than 10 W, which is on the lower energy end on most of the laser weed studies. The laser diodes were divided into three classes based on their output power. Each diode laser power output was measured at about 5 cm from the laser lens using a Gentec Pronto-50-W5 (Gentec Electro-Optics, Inc. Quebec City, QC, Canada) portable laser power meter. The first class consisted of the lowest energy laser diodes of the group; a 1.2 W laser diode (Nichia M140, 450 nm wavelength, 2.5 mm beam spot diameter) and a 1.35 W laser diode (Nichia M140, 450 nm wavelength, 2.5 mm beam spot diameter). The second class consisted of a 4.2 W 450 nm laser diode with a spot diameter of about 2.5 mm (Nichia NUBM49) and a 4.5 W 450 nm laser diode with a spot diameter of about 2.6 mm (Nichia NUBM4B). The third class consisted of a 5.1 W 450 nm (Nichia NUBM44) and 6.1 W 450 nm (Nichia NUBM47) with 2.5 mm spot diameter each. These laser diodes were fixed with G-8 lenses to focus the beam.

3.3.2. Weed Species

Seedlings from two weed species Palmer amaranth (*Amaranthus palmeri*) and smallflower morningglory (*Jaquemontia tamnifolia*) were collected from the University of Georgia research fields near Ty Ty, GA (31.50973° N, 83.65588° W), then planted in pots and transferred to a greenhouse (Figure 3.3). Four 8 by 16 seedling pot trays were used for planting these weeds about 2 weeks after their emergence. The weeds were grown for another week before laser treatment (about 3 weeks after emergence).

Figure 3.3. Collected weeds in the pots in greenhouse before treatment. Small flower morningglory (**A**), and Palmer Amaranth (**B**).

3.3.3. Experiment 1 – Severing the Stem

The first experiment aimed to investigate how long it takes for low-power diode lasers to sever the weed stem and what factors affect the effectiveness of the diode lasers.

Four diode lasers, 1.2 W, 1.35 W, 4.2 W, and 4.5 W were used to treat weed stems of the two weed species until they were severed. The laser diodes were placed at three different distances of 5 cm, 10 cm, and 15 cm from the weed stems.

The laser was setup as in Figure 3.4; an Arduino Uno microcontroller (Open-source electronics platform) controls the laser beam through TTL (Transistor to Transistor Logic) signal sent to the constant current source laser driver. A button press-and-hold turns the laser diode on and hits the weed stem until it cuts through. Once the weed stem is severed, the button is released, and the Arduino records the duration the button was pressed.

The laser beam hit the weed perpendicular to the stem at approximately the center of the stem.

This was arranged as a factorial experiment with 4 laser output powers, 2 weed species, and 3 distances between the laser and the weed stems, for a total of 24 individual treatments. The experiment was replicated 5 times.

The data for laser power, distance between the laser diode and weed stem, diameter of the stem, weed species, and treatment duration were recorded for each treatment. The diameter of stem at the point of the laser application was measured using an electronic caliper. Statistical analysis of the data was done by performing the analysis of variance (ANOVA) on the linear regression model of the data with a continuous dependent variable (time taken to sever the stem) using R programming language (Andy Bunn, 2017) at 5% significant level and means compared using *t*-test and Tukey method since the dependent variable (time taken to sever stem) is continuous.

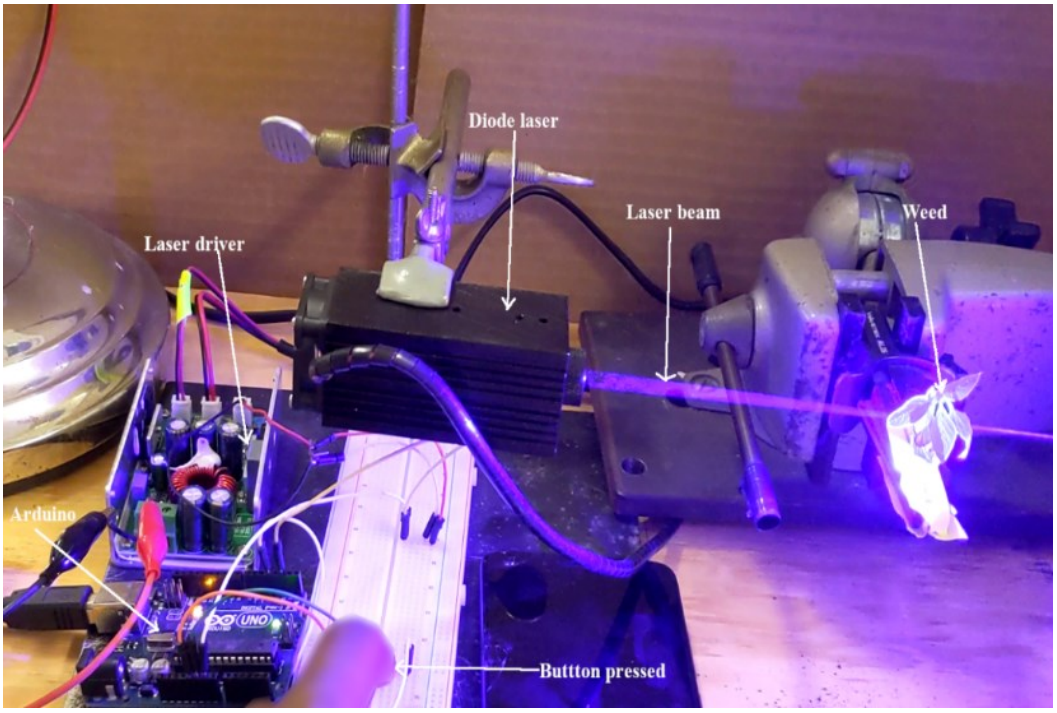

Figure 3.4. Laser setup to cut the weed stem completely.

3.3.4. Experiment 2 – Time Limited Laser Treatment

This experiment aimed to investigate the effect of laser diodes when directed to weed stems for fixed time durations without necessarily severing the stem.

Since there was no difference in effects of the laser diodes within the classes (Section 3.1), only two diodes were used for this experiment; 1.2 W and 4.2 W, and since the diodes were more effective between 5 cm and 10 cm from the weed stem, the laser diodes were placed at approximately 5 cm and perpendicular to the weed stems.

Weed stems of the two weed species were treated with laser beams from the two laser diodes for the fixed durations of 1, 2, and 3 s. The weeds were treated while inside the pots to not interfere with their normal growth (Figure 3.5), the untreated weeds in the pots were left as a control group. The laser side setup was the same as in Figure 3.4, except now the treatment

duration was fixed, so, once the button was pushed, the weed stem would be exposed to the laser beam for the set duration or dosage.

The experiment was arranged as a factorial experiment with 2 laser output powers, 2 weed species, and 3 treatment times for a total of 12 individual treatments and was replicated 5 times.

The data for laser power, diameter of weed stem, treatment duration, and weed species were recorded for each treatment. The weeds were monitored for a week, then the status of each treated weed was recorded (killed/survived). Since the dependent variable (status) of our data was categorical with two levels (killed/survived), the statistical analysis was done on a logistic regression model of the data using R programming language (Andy Bunn, 2017) by fitting a generalized linear model with binomial family and evaluated at 5% significant level.

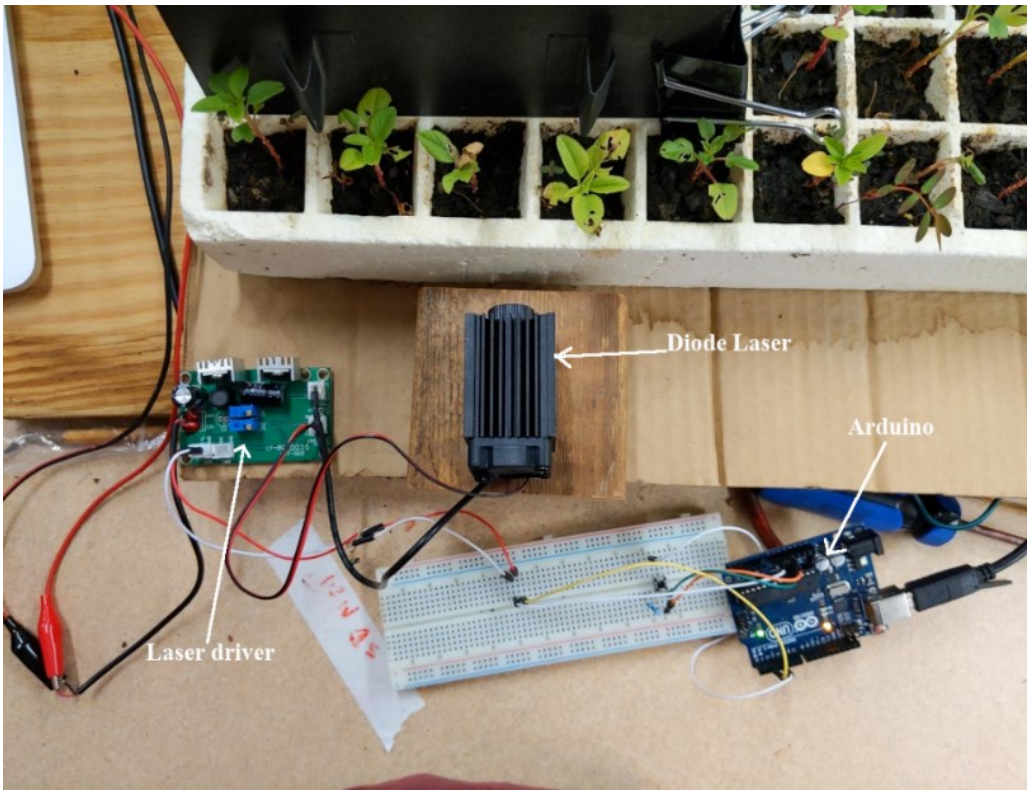

Figure 3.5. Weeds in the pots being treated by a diode laser.

3.3.5. Experiment 3 - Time Limited Laser Treatment with More Power

For the laser diodes to be effective on a weeding robot in the field, the treatment time needs to be as short as possible. The 3 s treatment time which was the most effective using the 4.2 W diode laser in Section 3.2 would not be efficient in a field application. So, we investigated the effect of increasing the laser output power and lowering the treatment time. Like in experiment 2, the two species of weeds inside the pots were treated with laser beams from laser diodes positioned about 5 cm and perpendicular to the weed stems, but now the laser powers were 5.1 W and 6.1 W, and the treatment duration was 0.5, 1, and 1.5 s.

This was designed as a factorial experiment with 2 laser output powers, 3 treatment times, and 2 weed species for a total of 12 individual treatments and was replicated 5 times.

The data for laser power, weed species, diameter of weed stem, and treatment duration, were recorded for each treatment. The weeds were monitored for a week, then the status of each treated weed was recorded (killed/survived/stunted). Stunted status was added to the experiment results due to the observations in experiment 2. Statistical analysis was done on a multinomial logistic regression model of the data using the package ***nnet*** in R programming language (Andy Bunn, 2017) at 5% significant level since the dependent variable is categorical with more than two levels (killed/survived/stunted).

3.4 **Results**

3.4.1. Experiment 1 Results

The mean treatment time for each laser power shown in Table 3.1 demonstrates the effectiveness of the lasers as power is increased. Analysis of variance of a model with R^2 value of 91.7% showed that, the effects of laser power, diameter of stem, and distance between laser diode and stem were all significant, however, weed species effect was not significant in

determining the time taken to cut the stem completely. Figure 3.6demonstrates the effect of laser power on the treatment time in which the lower power lasers (1.2 W, 1.35 W) had slower response (about 5 s) than the high-power ones of 4.2 W and 4.5 W (about 2 s), the distance between laser and weed had a minor effect on the treatment duration, especially at 15 cm, while it seemed to have approximately the same effect at 5 cm and 10 cm. Small flower morningglory was cut quicker than Palmer amaranth, however, that is attributed to the difference in average diameter between the two species (Figure 3.6 D).

Multiple comparisons for the laser power treatment means showed no statistical difference between the effect of 1.2 W and 1.35 W laser, as well as no statistical difference between the effect of 4.2 Wand 4.5 W laser treatments.

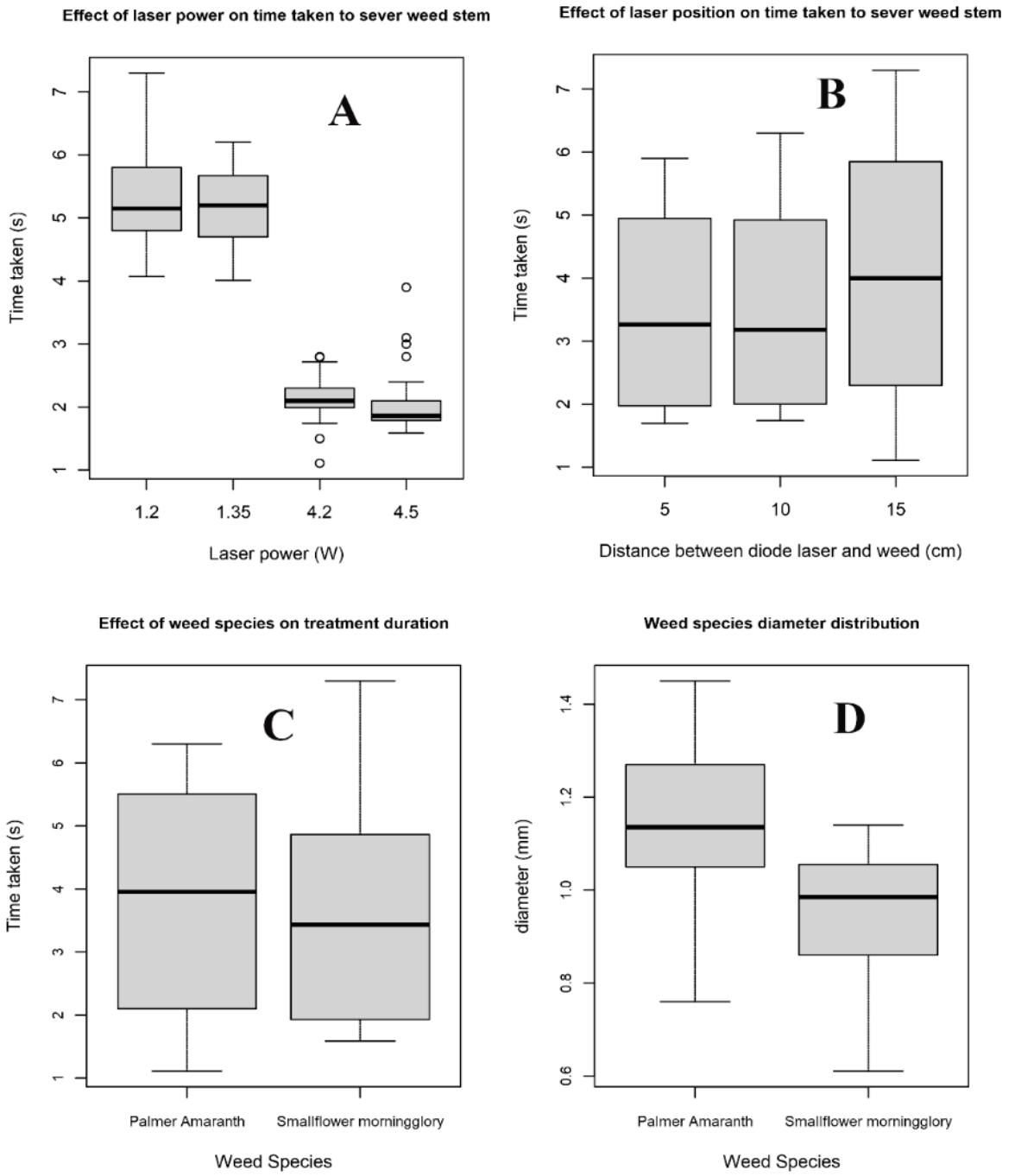

Figure 3.6. Box and whisker plots of the time taken to cut the weed stem vs. three factors, and the diameter data for each weed species. (**A**) shows the laser power effect where the error bars for first class (1.2 and 1.35W) lasers overlap significantly, likely, the second class (4.2 and 4.5W) lasers overlap, while the two classes not overlapping, hence the statistical significant

difference between the classes while no difference within classes, (**B**) shows the effect of distance between laser diode and weed stem where the error bars overlap more between 5 and 10cm with less overlap at 15cm which caused the statistical difference, (**C**) represents the effect of species where the error bars overlap with no statistical difference, and (**D**) represents the diameters data for each weed species with palmer amaranth having slightly higher average diameter than smallflower morningglory.

Table 3.1. Mean time taken by each diode laser to sever weed stems at 5, 10, and 15 cm.

Laser Power	**Distance**	**Time (s)**	
(W)	**(cm)**	**Mean**	**Standard Deviation**
1.2	5	4.84	0.29
	10	5.23	0.69
	15	6.05	0.76
1.35	5	4.97	0.55
	10	4.94	0.47
	15	5.46	0.65
4.2	5	2.1	0.11
	10	2.04	0.19
	15	2.25	0.60
4.5	5	1.83	0.09
	10	1.95	0.16
	15	2.38	0.79

3.4.2. Experiment 2 Results

Results shown in Figure 3.7 and Table 3.2 demonstrate only 15% of the weeds were killed using 1.2 W laser when treated for 1 s and 2 s, while 70% of the weeds were killed when treated for 3 s. The 4.2 W laser killed 40% of weeds when treated for 1 s, 70% of weeds when treated for 2 s, and 100% when treated for 3 s. The laser power, diameter of the stem, and treatment duration were all significant, while the weed species was not significant. Diameter of the stem played a significant role in determining whether the weed was killed or survived, that is, Palmer amaranth was killed more than small flower morningglory because of the overall lower average stem diameter as demonstrated in Figure 3.8. Some treated weeds were not killed but appeared to have stagnated in their growth and some slightly wilted.

Table 3.2. Percentage of weeds killed after 1 week of monitoring

Treatment Time (s)	**Laser Power (W)**	**Weeds Killed (%)**
1	1.2	10
	4.2	40
2	1.2	20
	4.2	70
3	1.2	70
	4.2	100

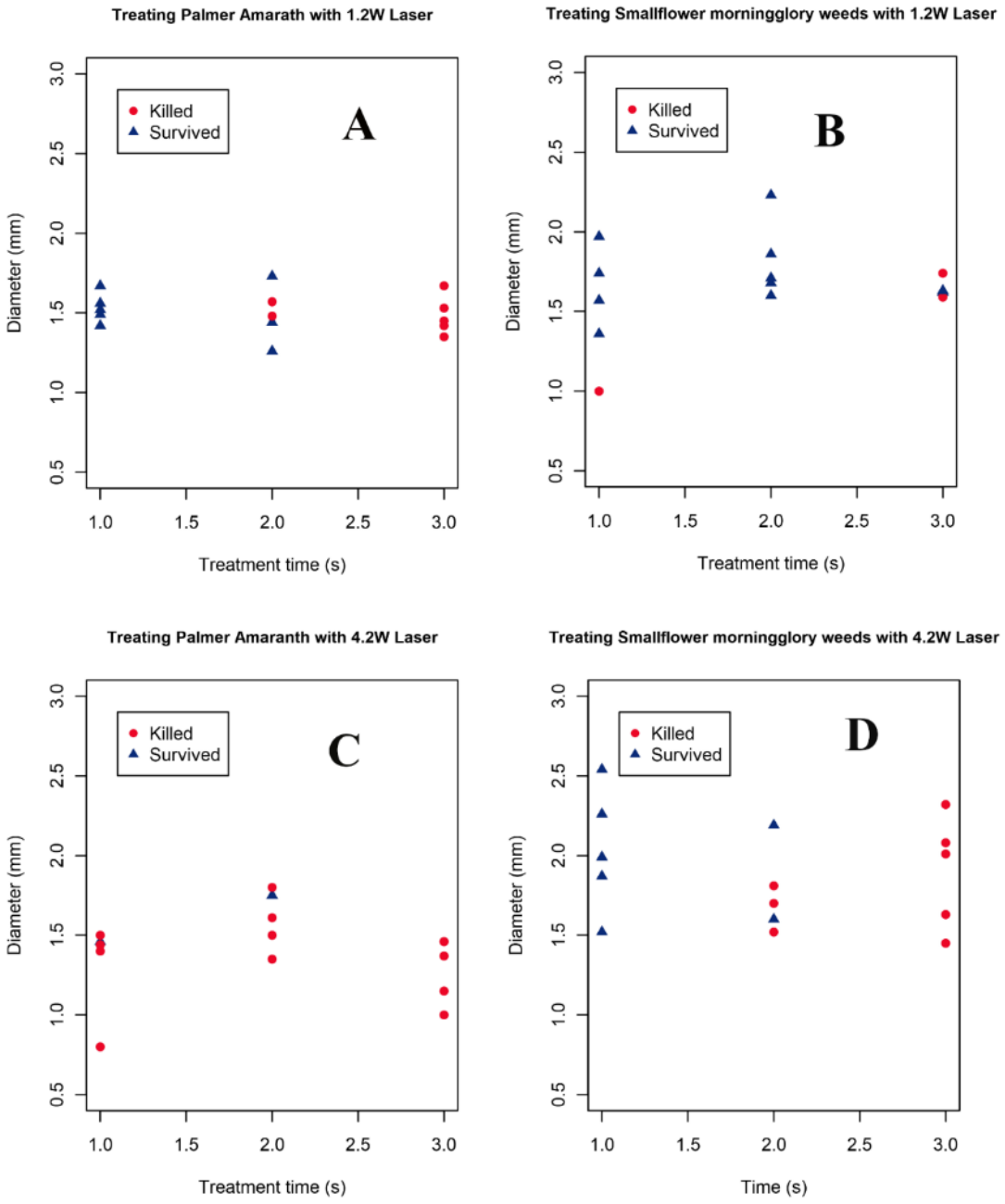

Figure 3.7. Status of weeds after 1 week of monitoring. (**A**) using 1.2 W laser on Palmer amaranth, (**B**) using 1.2 W laser on smallflower morningglory, (C) using 4.2 W laser on Palmer amaranth, (**D**) using 4.2 W laser on smallflower morningglory.

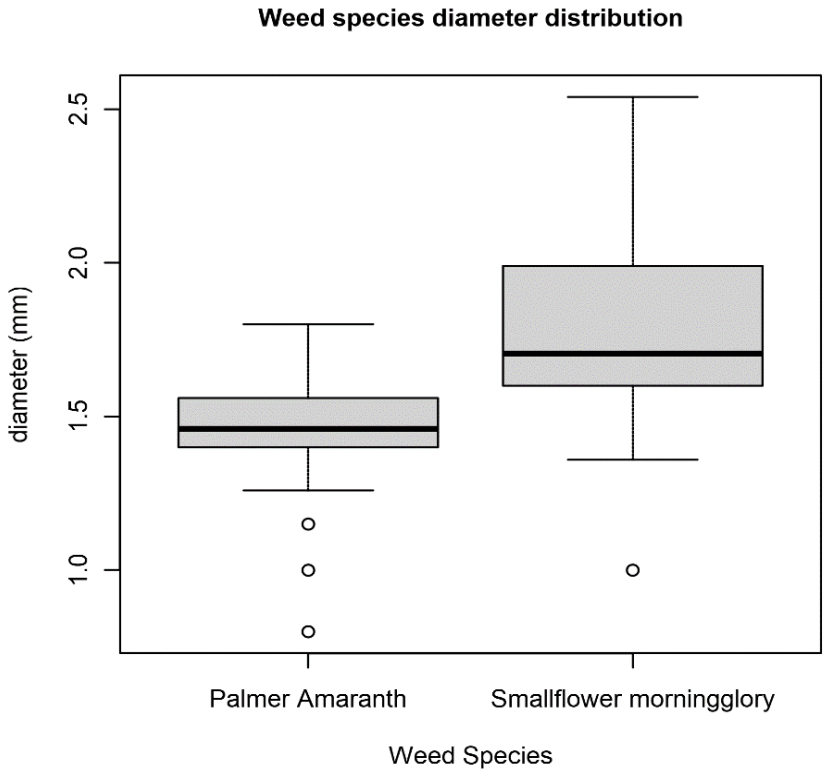

Figure 3.8. Differences in diameter between weed species tested in Experiment 2 where smallflower morningglory have slightly higher average diameter than palmer amaranth and the error bars slightly overlap to imply a possible statistical difference.

3.4.3. Experiment 3 Results

Figure 3.9 and Table 3.3 show the 5.1 W diode laser was 66.67% effective overall (kill/stunt) for the treatment times, while the 6.1 W diode laser was 80% effective for treatment durations of 0.5 s, and 1 s, but 100% effective for the 1.5 s duration. The diameter of stem and treatment duration were significant while there was no statistical difference between the laser powers. The species of the weed did not have any influence on the results.

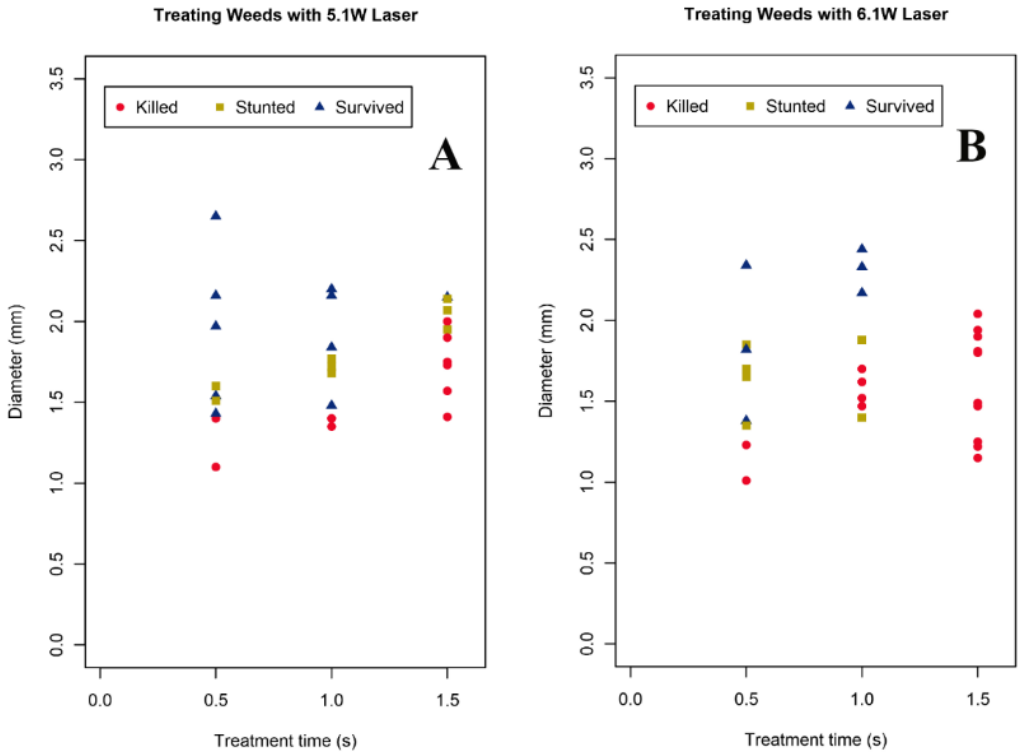

Figure 3.9. Status of weeds after 1 week of monitoring. (A) using 5.1 W laser, (B) using 6.1 W laser.

Table 3.3. Percentage of weeds killed or stunted after 1 week.

Treatment Time (s)	**Laser Power (W)**	**Weeds Killed (%)**	**Weeds Stunted (%)**
0.5	5.1	40	20
	6.1	40	40
1	5.1	40	20
	6.1	60	20
1.5	5.1	60	20
	6.1	100	0

3.5 **Discussion**

The experiments conducted in this study proved that diode lasers can be an effective weed controlling tool. Increasing the diode laser power increased the possibility of killing the weed, this is however affected by the weed stem diameter, the bigger the weed stem, the more difficult to kill. In addition, the more time the weed is exposed to the laser beam, the more laser energy (J) it absorbs which in turn increases the likelihood of it being killed or stunted. Corresponding results from studies which focused on broadleaf weeds at early growth stages (Kaierle et al., 2013; Marx et al., 2012; Mathiassen et al., 2006; Wöltjen et al., 2008) reported similar observation that increasing in laser dosage has the effect of reducing the growth rate (stunt) or kill with variability in the required energy, however, under these studies the laser was positioned vertically targeting the apical meristem of the weed, which might affect the weed response to the treatment. Investigations involving cutting the weed stem with laser by Heisel et al. (Heisel et al., 2001)found that stem thickness was an important factor. Further investigation by Heisel et al. (Heisel et al., 2002)found that more energy was needed as stem thickness increased, which corresponds with our findings.

Using the data from experiment 2 and experiment 3, Figure 3.10 demonstrates the effect of laser energy (J) which is a product of laser power (W) and the treatment time (s) to the weeds of different diameters. Most of weeds which were exposed to high energy were killed, but as the energy goes down, the effect of diameter become more prevalent.

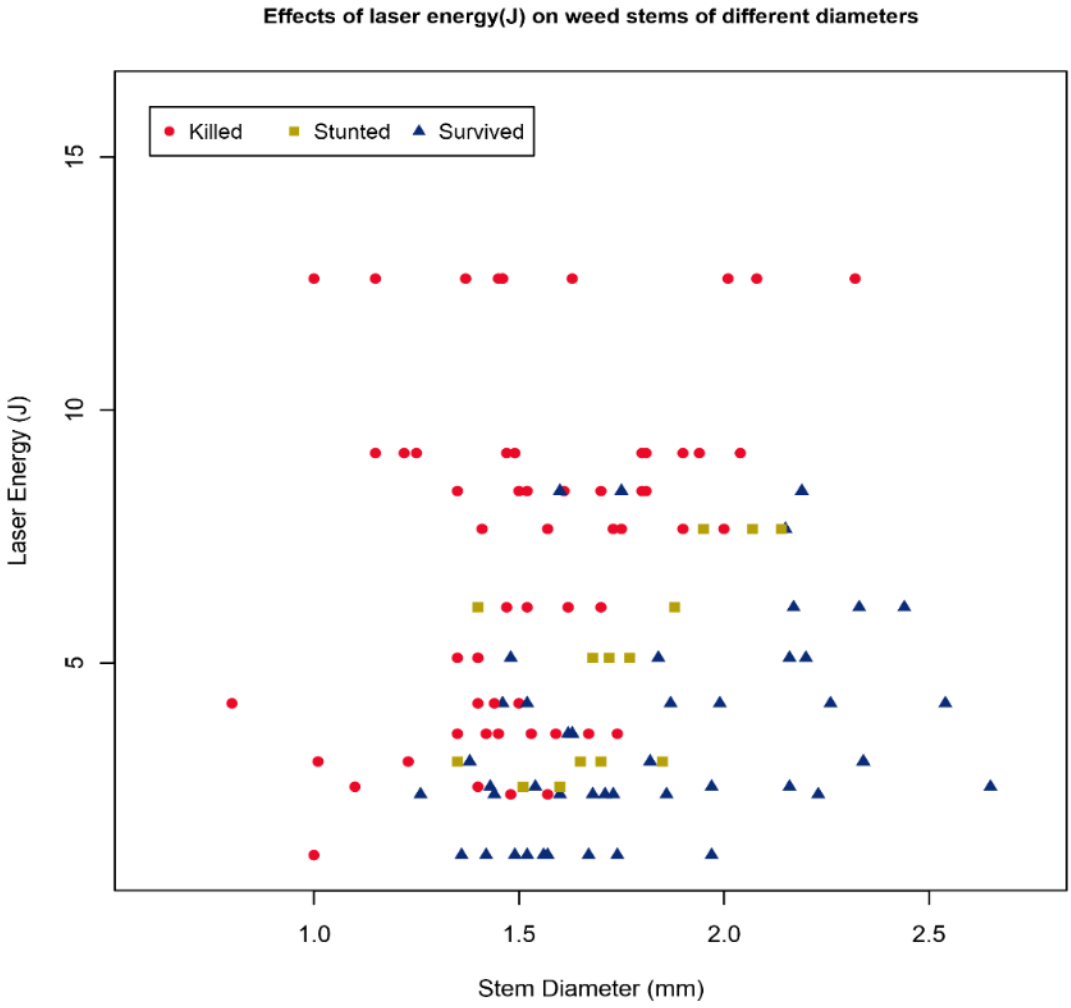

Figure 3.10. Effects of laser energy (power × treatment time) on weed stems of different diameters.

3.6 **Conclusions**

Six diode lasers were tested on their effectiveness in killing or stunting weeds. Three experiments were conducted. The first experiment aimed to determine the time taken to cut the weed stem completely, this experiment showed that weed species was not statistically significant, while the laser power, stem diameter, and distance between weed and laser diode were statistically significant on the survival of the weed. The second experiment demonstrated

that weeds may be killed when exposed to a laser beam for a certain duration even when the stem was not cut completely; in addition, the experiment confirmed the conclusion from the first experiment on the significance of laser power and stem diameter, as well as the treatment duration. The third experiment showed that with more powerful diode laser, the treatment time can be reduced significantly for the laser to be effective in the field. With a target treatment time of 0.5 s, a 6.1 W laser was 80% effective in eliminating the weeds.

Due to their portability and low power demand, multiple diode lasers can easily be accommodated on a small robotic system. Treating the weeds with multiple laser beams at once, or in succession, and using a backstop to prevent the beam from hitting non-target plants may be an effective and safe way to reduce the treatment time while avoiding using a single high-powered laser. Future testing will investigate field performance on a small autonomous rover using machine vision for laser aiming and control in addition to observing the laser effect on crops.

CHAPTER 4

EVALUATION OF INFERENCE PERFORMANCE OF DEEP LEARNING MODELS FOR REAL-TIME WEED DETECTION IN EMBEDDED COMPUTER[2]

[2]Mwitta, C., Rains, G., and Prostko, E. To be submitted to *Sensors*

4.1 **Abstract**

The knowledge that precision weed control in agricultural fields can reduce waste and increase productivity has led to research into autonomous machines capable of detecting and removing weeds in real-time. One of the driving factors to weed detection is to develop alternatives to herbicides, which are becoming less effective as weed species develop resistance. Advances in deep learning technology have significantly improved the robustness of weed detection tasks. However, deep learning algorithms often require extensive computational resources, typically found in powerful computers that are not suitable for deployment in robotic platforms. Most ground rovers and UAVs utilize embedded computers which are portable but limited in performance. This necessitates research into deep learning models that are computationally lightweight enough to function in embedded computers for real-time applications while still maintaining a base level of detection accuracy. This paper evaluates the weed detection performance of three real-time capable deep learning models: YOLOv4, EfficientDet, and CenterNet, when run on a deep learning-enabled embedded computer, Nvidia Jetson Xavier AGX. It tests the accuracy of the models in detecting 13 different species of weeds and assesses their real-time viability through their inference speeds on an embedded computer compared to a powerful deep learning PC. The results showed that YOLOv4 performed better than the other models, achieving an average inference speed of 80ms per image, and 14 frames per second on a video when run on an imbedded computer, while maintaining a mean average precision of 93.4% at a 50% IoU threshold. Furthermore, recognizing that some real-world applications may require even greater speed, and that detection program would not be the only task running on the embedded computer, a lightweight version of YOLOv4 model, YOLOv4-tiny was tested for improved performance in embedded computer. YOLOv4-tiny impressively

achieved an average inference speed of 24.5ms per image and 52 frames per second, albeit with a slightly reduced mean average precision of 89% at a 50% IoU threshold, making it an ideal choice for real-time weed detection.

4.2 Introduction

Invasive weeds in agricultural fields provide competition for crucial resources to crops. In most crops, weeds cause a higher loss in production than pathogens, and animal pests (Oerke, 2006), underscoring the importance of control. Weed control has proven to be a significant challenge. Herbicides have been the go-to method of controlling weeds for decades (Buhler et al., 2000; Gianessi & Reigner, 2007) , in addition to other common solutions like mechanical weeding (Hamill et al., 2004; Rueda-Ayala et al., 2010; Timmons, 1970) and even hand-picking.

The evolution of herbicide-resistant weed populations threatens agricultural productivity (Powles et al., 1996; Shaner, 2014). In addition to that, herbicides and other conventional methods of weed control such as mechanical are labor intensive and expensive (Culliney, 2005). Technology provides an opportunity to increase efficiency in control and reduce costs. Weed control solutions that automate the entire process or part of the process such as automatic sprayers (Culliney, 2005; Gerhards & Oebel, 2006; Utstumo et al., 2018), precision mechanical weed controllers (Bawden et al., 2017; Sori et al., 2018) have been researched and implemented.

Precision weed control methods demand knowledge on the types and location of weeds in the field; therefore, weed detection solutions are essential for this task. Research into weed detection technologies has resulted in various solutions that have proven valuable for precision weed control. Some solutions have used infrared spectroscopy (Shapira et al., 2013), fluorescence (Longchamps et al., 2010), or computer vision (Nguyen Thanh Le et al., 2019;

Zheng et al., 2017; Zhu & Zhu, 2009). The availability of low-cost high resolution cameras and advances in computing hardware have sparked interest in computer vision solutions, Some scholars have used a combination of simple image-processing techniques which utilize extraction of features like color, shape, or texture and machine learning algorithms like Support Vector Machines or random forest to identify weeds; For example (Nguyen Thanh Le et al., 2019; Zheng et al., 2017; Zhu & Zhu, 2009) used a combination of image feature extraction and support vector machines to discriminate weeds from crops. While these methods perform well in stable environments, they may not be robust in harsh outdoor conditions with changes in illumination, occlusions, and shadows. Progress in deep learning technologies has led to an increase in use of convolutional neural networks (CNNs) for weed detection and classification, achieving impressive results. For instance, (Asad & Bais, 2020; Chechliński et al., 2019; dos Santos Ferreira et al., 2017; Peteinatos et al., 2020) used CNN frameworks to detect weeds in crop fields with a great level of stability and accuracy. Individual weed detection makes it possible to implement weed removal solutions that can precisely target individual weed species without interfering with other plants in the field. These solutions include methods like spot spraying (Allmendinger et al., 2022), electricity (Sahin & Yalınkılıc, 2017), or lasers (Mwitta et al., 2022).

Researchers have compared the effectiveness and efficiency of different deep learning models in detecting different weed species, aiding informed decision-making for field implementation. For example, (A. N. V. Sivakumar et al., 2020) compared two deep learning models single shot detector (SSD) and Faster RCNN on their detection performance on UAV imagery and found Faster RCNN to be the superior model. In another study, (Chen et al., 2022) evaluated 35 deep learning models on 15 weed species, establishing a benchmark for weed

identification. Most of the performance evaluations and comparisons for deep learning models have been conducted on powerful computers capable of handling the computational demand of deep learning, however, given our focus on robotic applications, many solutions require portable computers which are often less powerful. For real-time applications in the agricultural fields, robotic platforms such as ground rovers, and UAVs usually use embedded computers which are not comparable to most powerful GPU enabled computers used for deep learning tasks.

This paper compares the performance of three single-stage deep learning models which are lightweight enough for real-time applications: YOLOv4 (Bochkovskiy et al., 2020), EfficientDet (Tan et al., 2020), and CenterNet (Duan et al., 2019). The comparison focuses on real-time detection of thirteen (13) common species of weeds found in cotton and peanut fields. The comparisons are made in a deep learning computer with powerful GPUs (RTX 2080Ti) against an embedded deep learning enabled computer (Nvidia Jetson Xavier AGX). These models were chosen due to their reputation as state-of-the-art object detection models for real-time applications. Detecting multiple species of weeds individually can help in decision-making in real-time of a way to remove the weed, for example if a robotic platform is doing spot spraying and encounter herbicide resistant weed, an alternative method can be employed.

4.3 **Materials and Methods**

4.3.1. Data Collection

More than 5,000 color or RGB (Red, Green, Blue) images of 13 different weed species; Palmer amaranth (*Amaranthus palmeri*), smallflower morningglory (*Jaquemontia tamnifolia*), sicklepod (*Senna obtusifolia*), crabgrass (*Digitaria spp.*), Florida beggarweed (*Desmodium tortuosum*), Florida pusley (*Richardia scabra*), pitted morningglory (*Ipomoea lcunos*), goosegrass (*Eleusine indica*), crowfoot-grass (*Dactyloctenium aegyptium*), purple nutsedge

(*Cyperus rotundus*), yellow nutsedge (*Cyperus esculentus*), ivyleaf morningglory (*Ipomoea hederacea*), and Texas panicum (*Urochloa texana*), seen in Figure 4.1, were collected from University of Georgia research fields near Ty Ty, GA (31.509730N, 83.655880W) and near University of Georgia Tifton campus, GA (31.473410°N 83.530475°W), using smartphone cameras or hand-held digital cameras. Images were captured at early stages of weed growth (from 1 to 3 weeks) at different angles and times of the day.

Figure 4.1. Examples of images of 13 weed species

4.3.2. Data Labelling

More than 3,500 images were labelled using an open-source annotation tool LabelImg (https://github.com/HumanSignal/labelImg). This tool allows for drawing of boundaries around

objects in images to identify them and creates records that indicate the object's location in the image, as seen in Figure 4.2. Labelling was conducted in both PASCAL VOC (Everingham et al., 2010) format for TensorFlow models training and YOLO (Redmon et al., 2016) format for YOLO model training in Darknet.

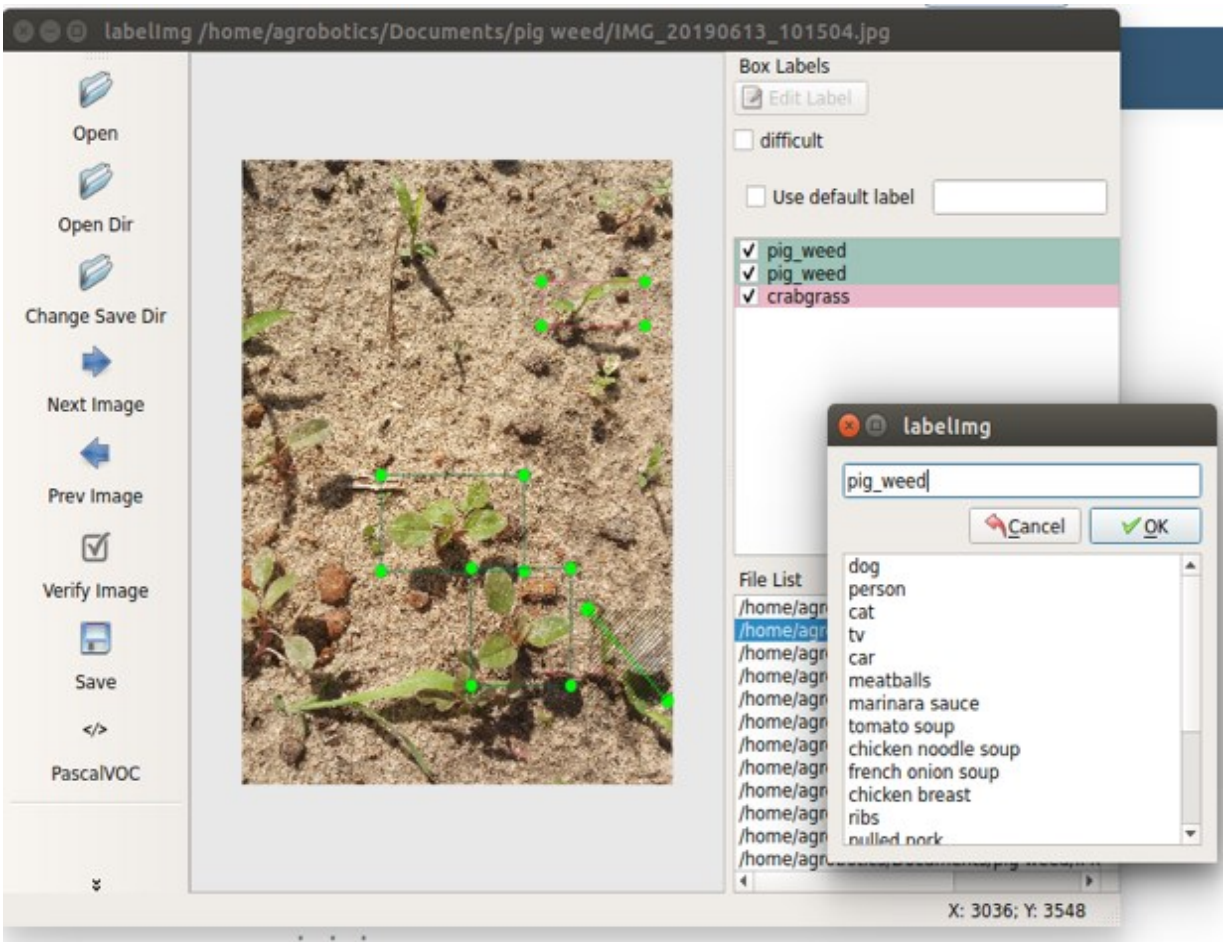

Figure 4.2. Example of labelling weed image using LabelImg

4.3.3. Train-Test Split

The labelled data was divided into training set (60%) for training the models to learn the features, validation set (20%) to validate the model's precision and avoid overfitting, and testing set (20%) for benchmarking, as shown in Figure 4.3.

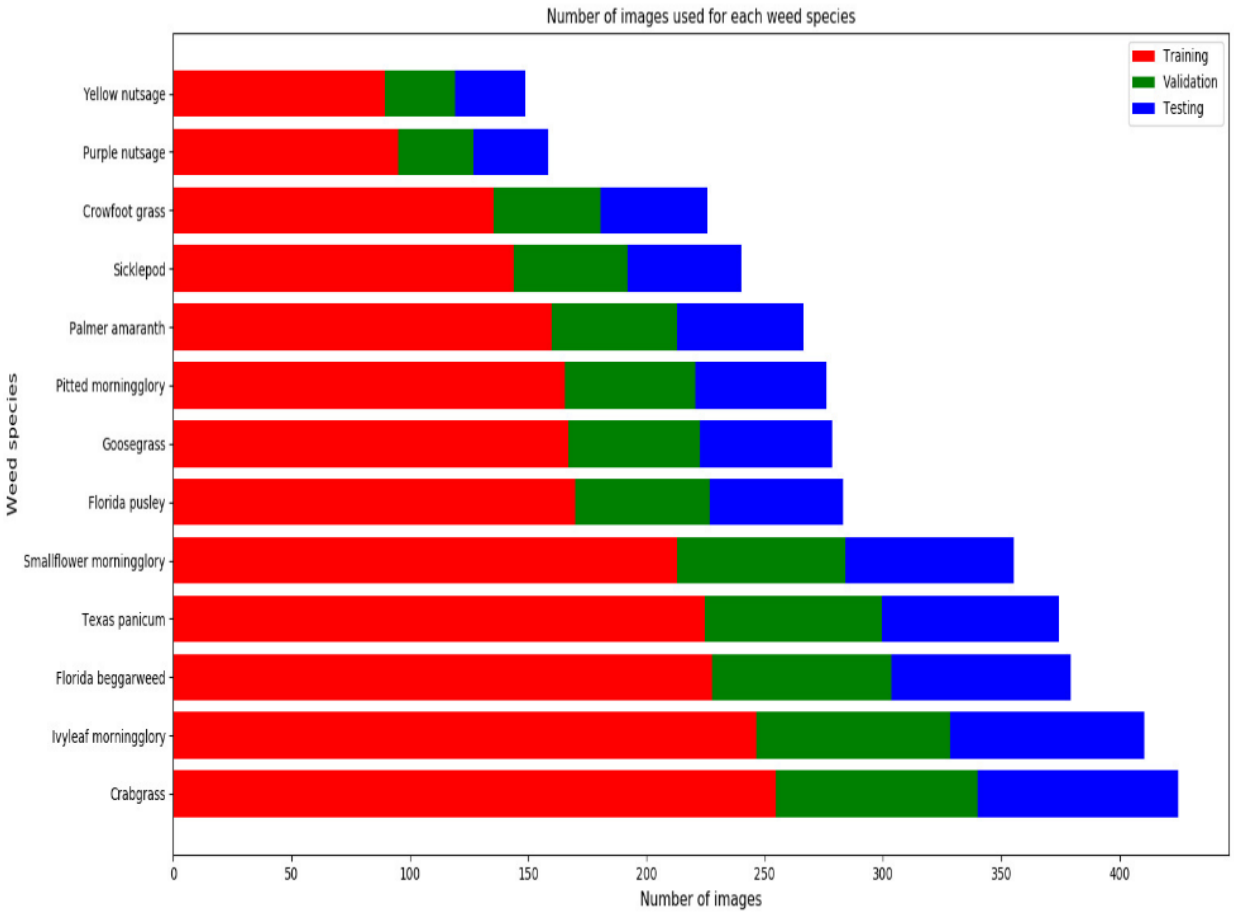

Figure 4.3. Labelled dataset split.

4.3.4. Data Augmentation

Since deep learning models rely heavily on extensive data for improved accuracy and to prevent overfitting, any additional data is valuable. Data augmentation involves techniques that add slightly modified copies of the existing data to the training set to enhance the size and quality of training data (Shorten & Khoshgoftaar, 2019).

The training data was augmented through techniques such as rotation, shear, blurring, cropping and others using an open-source image augmentation library CLoDSA (https://github.com/joheras/CLoDSA). This increased the training set to more than 67,000 images.

4.3.5. Training

Training was conducted using transfer learning, a technique of transferring knowledge between different but related domains (Zhuang et al., 2021). In deep learning, this is accomplished by reusing previously trained models for new problems to reduce training time and enhance the performance of targeted models. In training, the models take labelled images of different resolutions and then change the resolution to the required model input size.

4.3.5.1. YOLOv4

YOLOv4 (You Only Look Once version 4) is a real-time object detection model developed as a continuation of previous YOLO versions to address their limitations. It is a single stage object detection model trained to analyze the image only once and identify a subset of object classes. The YOLO network architecture is renowned for its speed in object detection, and YOLOv4 has prioritized real-time detection.

YOLOv4 training was conducted under the darknet environment (Redmon, n.d.), which is an open-source neural network framework that supports object detection and image classification tasks and serves as the basis for YOLO algorithm. As part of transfer learning, YOLOv4 training started with pre-trained weights which were originally trained on MS-COCO (Microsoft Common Objects in Context) dataset (Lin et al., 2014) which contains a wide range of 80 object classes. Training was conducted on training set while evaluated on the validation set. When the mean average precision of the model evaluated on validation set was not increasing, the training was stopped, as seen in Figure 4.4. The best weights with the highest mean average precision were taken as the designated weed detection model.

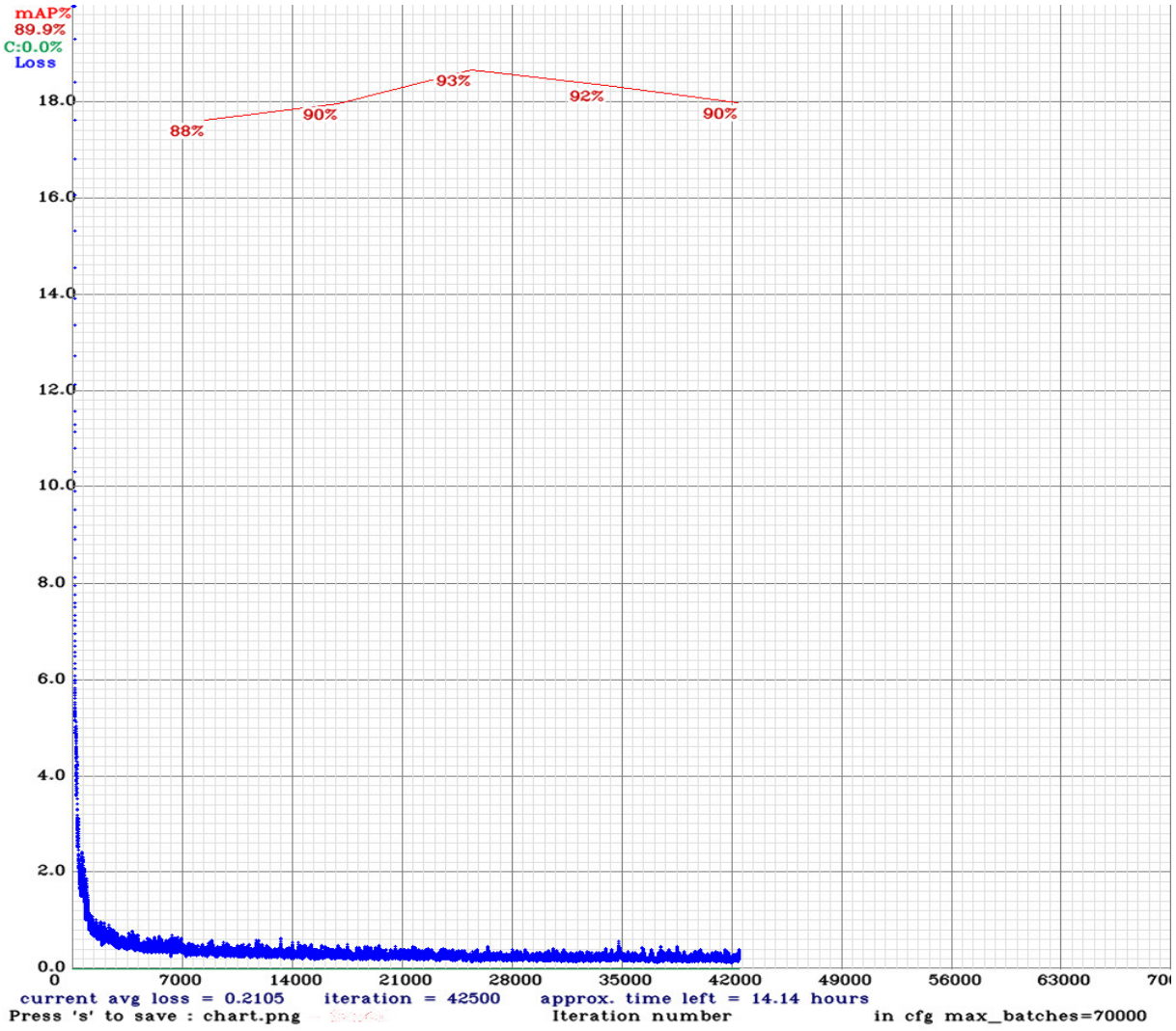

Figure 4.4. YOLOv4 training on darknet platform

4.3.5.2. EfficientDet

EfficientDet is a real-time object detection model written in Tensorflow (Abadi et al., 2016) and Keras (François Chollet, 2015), which utilizes a weighted bi-directional feature pyramid network (BiFPN) to learn input features while incorporating multi-scale feature fusing for box/class prediction.

A pre-trained model (EfficientDet D0 512x512) from a collection of pre-trained models, trained on the COCO 2017 dataset provided by Tensorflow 2 Detection Model Zoo (TensorFlow, 2022) , served as the starting point for training the EfficientDet weed detection model. The

training was done while monitoring the validation loss (Figure 4.5), average precision (Figure 4.6), and recall (Figure 4.7), and stopped when the loss was not decreasing and precision and recall not increasing (around 30K).

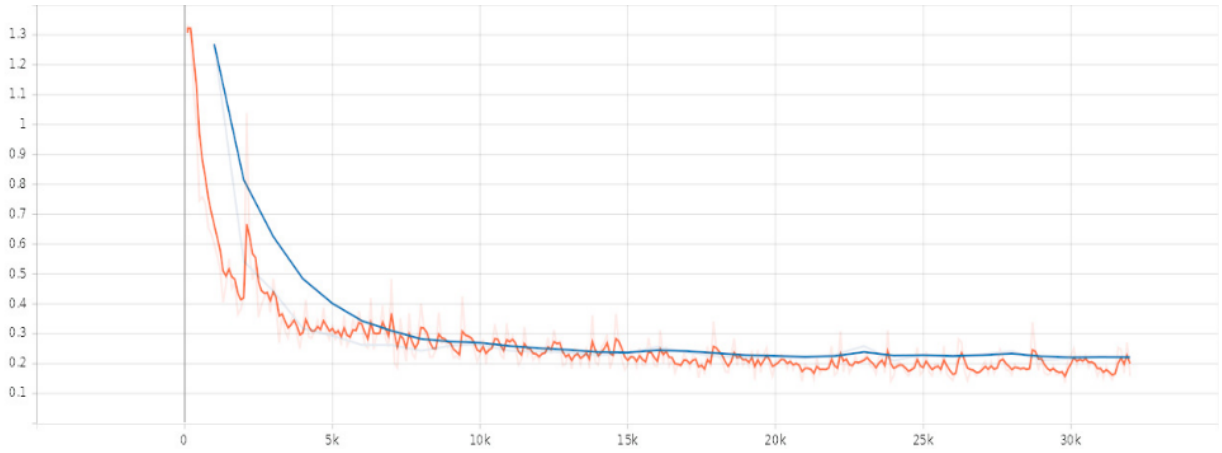

Figure 4.5. EfficientDet - Total Loss against number of training steps - training loss (orange), and validation loss (blue)

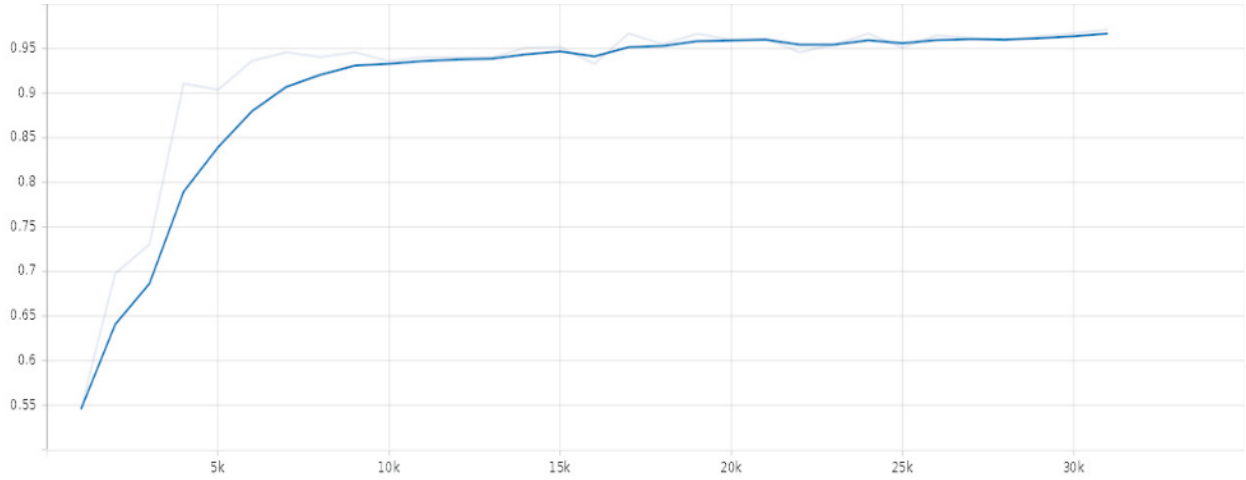

Figure 4.6. EfficientDet - Precision (mAP@0.5) against number of training steps

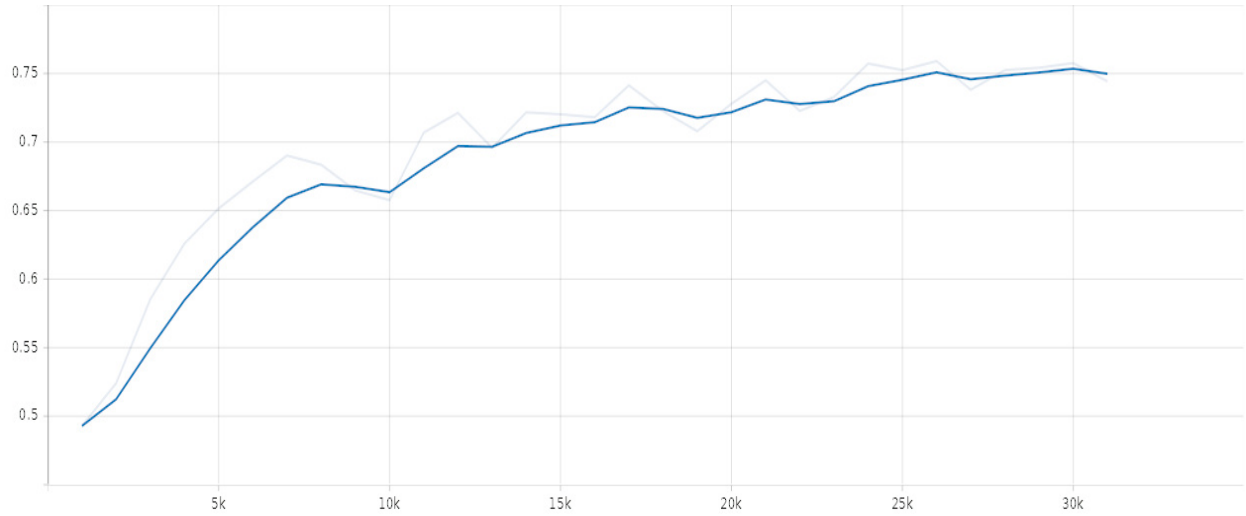

Figure 4.7. EfficientDet - Recall against number of training steps

4.3.5.3. CenterNet

CenterNet represents objects as a set of keypoints, reducing the need for anchor boxes and simplifying the process by predicting the bounding boxes directly.

The training of the CenterNet model utilized a pre-trained model (CenterNet Resnet101 V1 FPN 512x512) from Tensorflow 2 Detection Model Zoo which was trained over Resnet101 (Rao et al., 2017) backbone as the starting network. Total validation loss (Figure 4.8), precision (Figure 4.9), and recall (Figure 4.10) were monitored during the training. Table 4.1 shows the architecture differences between the models used in this study.

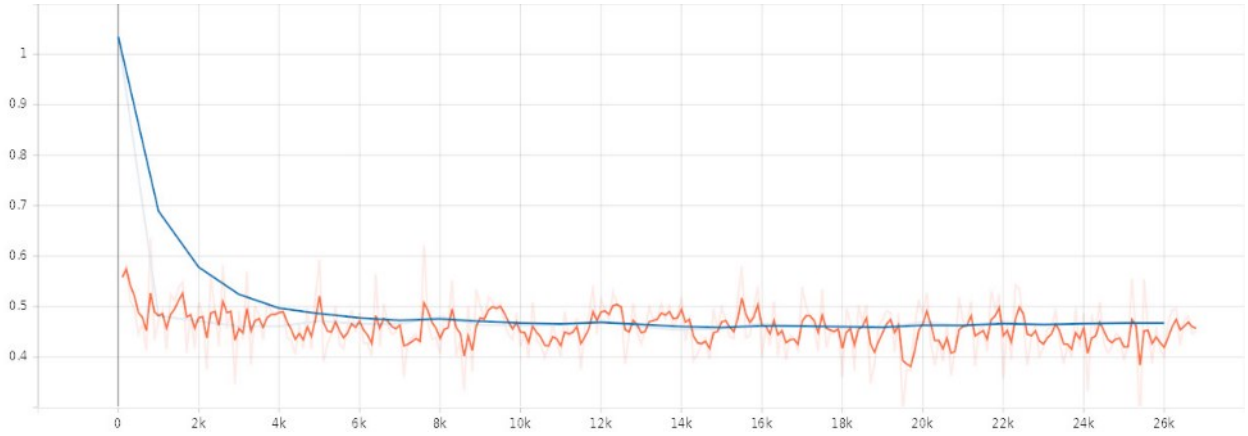

Figure 4.8. CenterNet -Total Loss against number of training steps - training loss (orange), and validation loss (blue)

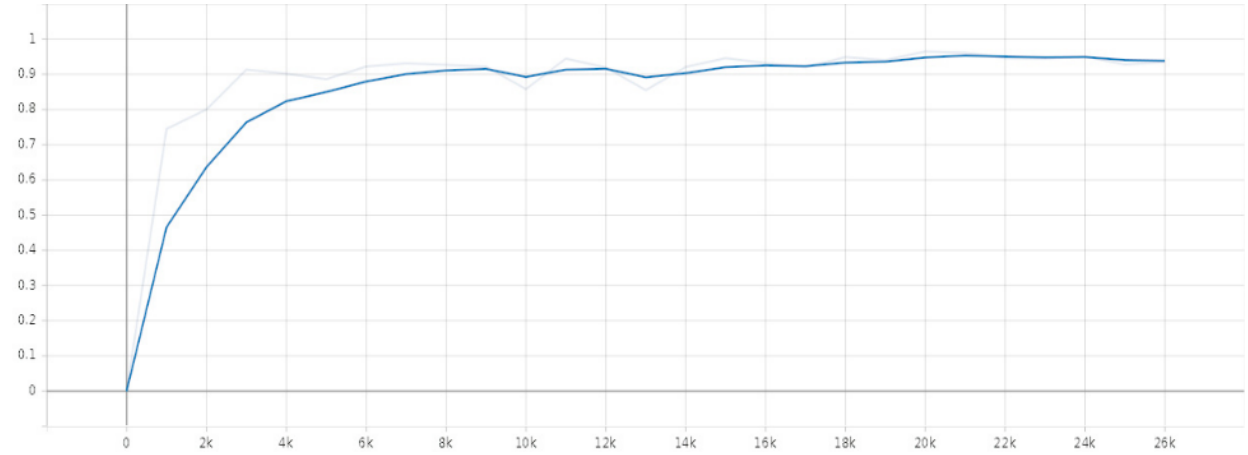

Figure 4.9. CenterNet - Precision (mAP@0.5) against number of training steps

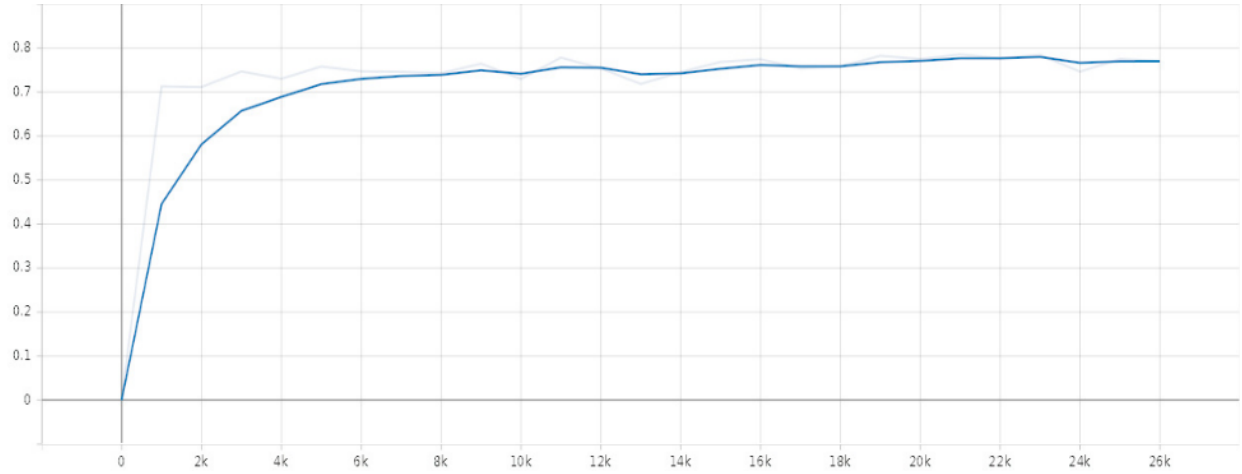

Figure 4.10. CenterNet - Recall against number of training steps

Table 4.1. Architecture comparisons for the models used in this study.

	YOLOv4	**EfficientDet**	**CenterNet**
Number of stages	one stage	one stage	one stage
Backbone	CSPDarknet53	EfficientNetB0	Resnet101
Number of layers	53	237	101
Object detection method	Anchor-based	Anchor-based	Anchor-free
Input size	416x416	512x512	512x512

4.3.6. Platforms

The weed detection models were trained on a deep learning capable computer equipped with 32–cores Intel I9 CPU, Nvidia RTX 2080 Ti GPUs (4352-CUDA cores), and 128GB RAM. Inference speed and accuracy was compared between the deep learning computer and an artificial intelligence (AI) embedded computer designed specifically for autonomous machines, Nvidia Jetson Xavier AGX (Figure 4.11) equipped with 8-core NVIDIA Carmel Arm®v8.2 64-

bit CPU 8MB L2 + 4MB L3, 512-core NVIDIA Volta architecture GPU with 64 Tensor Cores, and 32 GB of RAM.

Figure 4.11. Nvidia Jetson Xavier AGX

4.3.7. Evaluation Metrics

As the focus lies on the inference of the detection models, several metrics were compared when running on the two platforms. Model accuracy metrics such as, precision, and recall, which are summarized by the average precision (AP) value, mean average precision (mAP) evaluated under different Intersection over Union (IoU) thresholds, and speed metrics such as inference time and frames per second (fps), were considered.

Precision measures how well the positive predictions match the ground truth.

$$Precision = \frac{True\ positives}{True\ positives + False\ positives}$$

Recall measures how many relevant predictions are made out of all predictions.

$$Recall = \frac{True\ positives}{True\ positives + False\ negatives}$$

The **Average precision** (AP) represents the weighted average of all precisions at each precision-recall curve threshold where the weight is the increase in recall. This value summarizes the precision-recall curve into a single value.

$$AP = \sum_{k=0}^{k=n-1} [Recalls(k) - Recalls(k+1)] \times Precisions(k)$$

$$Recalls(n) = 0, Precisions(n) = 1, n = Number\ of\ thresholds$$

Intersection over Union (IoU) indicates the overlap of the predicted bounding box coordinates to the ground truth box, as shown in Figure 4.12. When the predicted bounding box closely resembles the ground truth box the IoU would be higher. In deep learning object detection models, multiple bounding boxes are predicted for objects, only those with higher IoU than a threshold are considered as positive predicted boxes.

$$IoU = \frac{Area\ of\ Overlap}{Area\ of\ Union}$$

Mean average precision (mAP) represents the average of weighted means of precisions at each IoU threshold. It is calculated by averaging the Average Precision (AP) for each class across a number of classes.

$$mAP = \frac{1}{N} \sum_{i=1}^{N} (AP)_i$$

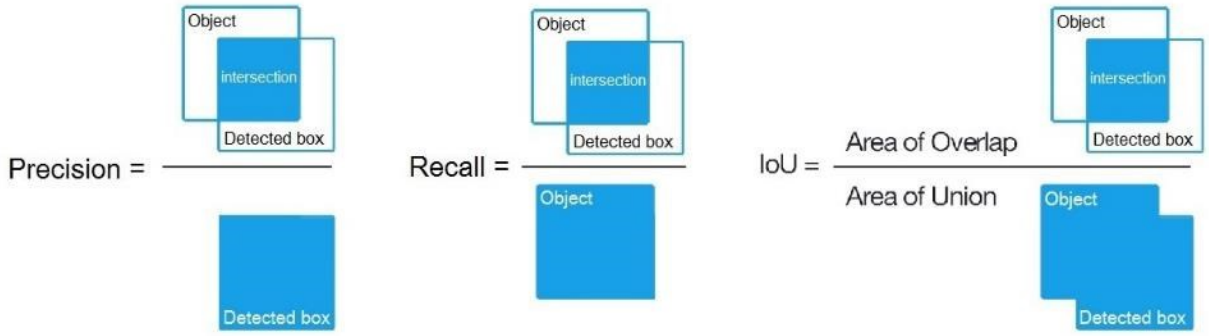

Figure 4.12. Precision, Recall, and IoU illustration

The **inference time** refers to the time it takes for a model to make a prediction on a single image, whilst the number of **frames per second** (fps) indicates the frequency at which inference is performed on consecutive images in a video stream. For real-time applications these are crucial metrics because excessive inference delay can lead to the machine being unable to respond in time. Inference time was calculated by running the models on a set of weed images and averaging the time over the number of images. On the other hand, fps was obtained by running the models on weed videos while recording the reciprocal of execution time for each frame. These two metrics vary among models as well as platforms, while the other metrics only vary among models.

4.3.8. Mobile Optimized Solution

The prediction speed is critical aspect of a real-time detection system, and due to the fact that in real scenario, the embedded computer will be running other applications for robot control in addition to the detection program, the inference speed may further be impacted. Other variants of deep learning models that have been optimized for speed have been developed, they achieve this by sacrificing some precision through reducing neural network size. YOLOv4 has a lightweight compressed version, YOLOv4-tiny built based on YOLOv4 but with a simpler network structure and reduced parameters to make it ideal for mobile and embedded devices.

YOLOv4-tiny can be used for faster training and inference than YOLOv4, however, its accuracy suffers. YOLOv4 was also compared to its lighter version YOLOv4-tiny for its viability on weed detection in embedded platform.

4.4 **Results**

4.4.1. Model Comparisons

The results, as shown in Table 4.2, when the models were evaluated on 600 labelled test images from the dataset (20% of the dataset) using COCO metrics, indicate that EfficientDet and CenterNet had similar performance with an overall mean average precision of 71.3% and 70.6%, respectively, which was better than YOLO with mAP of 61.6% at IoU = 0.5-0.95. This mAP is calculated by taking the average of mAP over IoU thresholds ranging from 0.5 to 0.95 with a step size of 0.05. At IoU = 0.5, EfficientDet outperformed all the other models (97.4%). However, the other models achieved satisfactory scores of 93.8% (CenterNet) and 93.4% (YOLOv4). Overall, EfficientDet had a slight edge over other models in terms of accuracy metrics.

Table 4.2. Model accuracy performance comparisons

Metric	**YOLOv4**	**CenterNet**	**EfficientDet**
mAP@ IoU=0.5-0.95	0.616	0.706	0.713
mAP@ IoU=0.5	0.934	0.938	0.974
mAP@ IoU=0.75	0.703	0.809	0.819
Average Recall	0.660	0.714	0.708

Visual observation showed no significant difference in detection except for few images where EfficientDet had better predictions, for example in Figure 4.13 and Figure 4.14, YOLOv4 and CenterNet failed to detect crowfoot grass, but EfficientDet detects it in Figure 4.15.

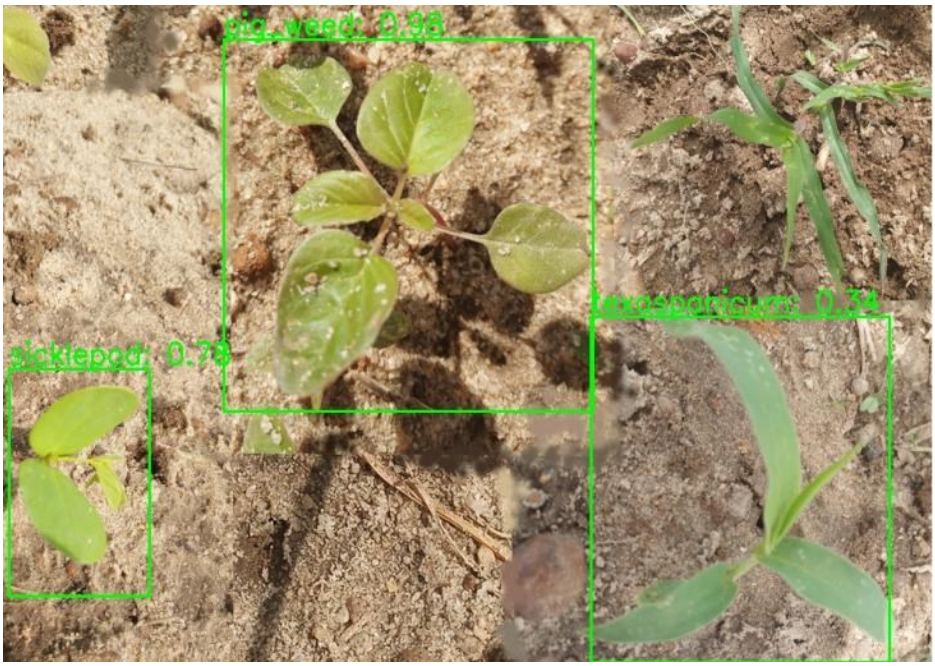

Figure 4.13. YOLOv4 detection – detects 3 weeds

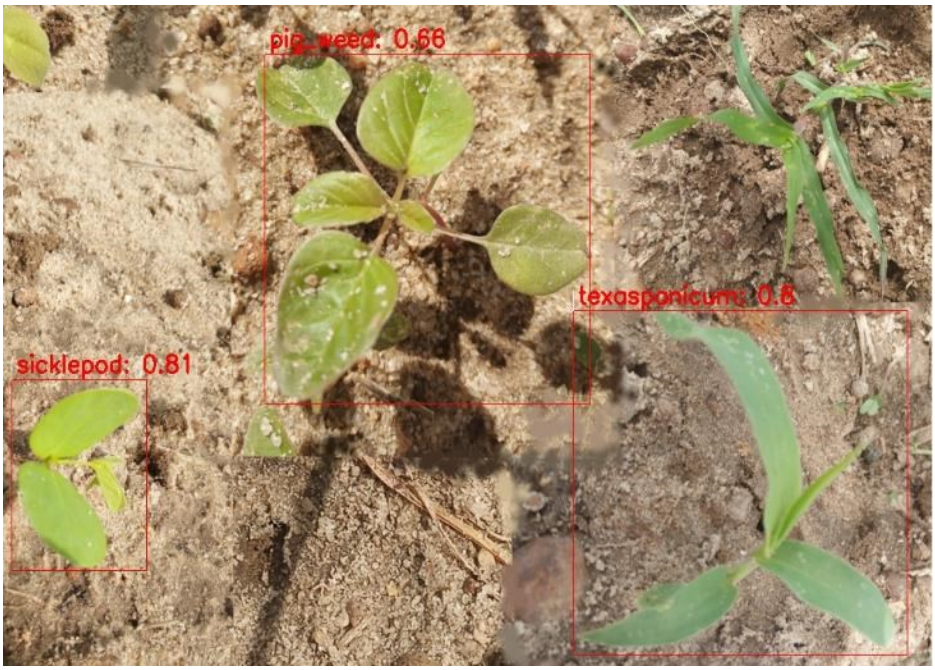

Figure 4.14. CenterNet detection – detects 3 weeds

Figure 4.15. EfficientDet detection - detects all 4 weeds

On performance in detecting individual weed species, the models did well on class evaluation using PASCAL VOC mAP @ IoU=0.5 metrics, except for CenterNet and EfficientDet when detecting purple nutsedge; they achieved mAP@0.5 scores of 0.06% and 0.07% respectively as shown in Table 4.3. This could be attributed to the limited number of training images for purple nutsedge and the similarity between yellow and purple nutsedge. However, YOLOv4 performed significantly better on purple nutsedge with mAP of 79.4% at IoU=0.5. This difference is evident even in visual inspections in Figure 4.16 and Figure 4.17 where Centernet and EfficientDet models detect only one of two purple nutsedge but YOLOv4 in Figure 4.18 successfully detect both weeds.

Table 4.3. Model mAP@0.5 for individual weed classes

Weed species	**YOLOv4**	**CenterNet**	**EfficientDet**
Smallflower morningglory	0.994	0.998	0.990
Sicklepod	1.000	0.998	1.000
Pitted morningglory	0.899	0.990	1.000
Ivyleaf morningglory	0.998	0.987	1.000
Florida pusley	1.000	1.000	1.000
Florida beggarweed	1.000	1.000	0.998
Texas panicum	0.999	0.999	1.000
Crabgrass	0.997	0.991	0.999
Crowfoot-grass	0.808	0.957	1.000
Goosegrass	1.000	0.967	1.000
Palmer amaranth	0.712	0.911	0.926
Yellow nutsedge	0.763	0.653	0.940
Purple nutsedge	0.794	0.0006	0.0007

Figure 4.16. Single purple nutsedge plant detected by CenterNet

Figure 4.17. Single purple nutsedge plant detected by EfficientDet

Figure 4.18. Two purple nutsedge plants detected by YOLOv4

4.4.2. Inference Time

For real-time robotic applications, the speed of detection is crucial. When the models were run on 600 images both on the deep learning PC and embedded computer, YOLOv4 performed significantly better on both platforms, as shown in Table 4.4 with an average of 18ms per image on the PC and importantly, just 80ms per image on the embedded computer. CenterNet performed better than EfficientDet on the PC, predicting at 44ms per image versus 66ms, however, EfficientDet outperformed CenterNet on the embedded computer achieving 102ms versus 140ms.

Table 4.4. Inference time (ms)

Platform	**YOLOv4**	**CenterNet**	**EfficientDet**
Deep Learning Computer	18	44	66
Jetson Xavier AGX	80	140	102

4.4.3. Frames Per Second (fps)

When the models were run on a video with a resolution 1280x720 on both platforms, YOLOv4 outperformed the other models, shown in Table 4.5, achieving 51 fps on PC and 14 fps on the embedded computer, while EfficientDet was better than CenterNet on embedded computer obtaining 12fps versus 8fps.

Table 4.5. Number of frames per seconds achieved

Platform	**YOLOv4**	**CenterNet**	**EfficientDet**
Deep Learning Computer	51	40	22
Jetson Xavier AGX	14	8	12

4.4.4. Improvement with YOLOv4-tiny

Regarding the balance of accuracy and speed, YOLOv4 performed better than the other models on embedded computer. An object detection speed of 14fps may suffice for many real-time applications; however, certain applications demand higher speed. An ideal model can identify and locate objects in real-time with rapid inference while maintaining a baseline level of accuracy. To assess this, YOLOv4-tiny model was trained on the same dataset as YOLOv4. During accuracy testing, YOLOv4-tiny achieved a precision of 81%, recall of 88% and a reduced mAP at Iou=0.5 of 89.2% as shown in Table 4.6. Impressively, when tested on the embedded computer, it achieved an inference time of 24.5ms and 52 frames per second, surpassing YOLOv4.

Table 4.6. YOLOv4-tiny evaluation results compared to YOLOv4 on embedded computer.

Metric	**YOLOv4-tiny**	**YOLOv4**
Precision	0.81	0.95
Recall	0.88	0.89
mAP @IoU=0.5	0.89	0.934
Inference on Jetson Xavier AGX (ms)	24.5	80
FPS on Jetson Xavier AGX	52	14

4.5 **Conclusion and Recommendations**

Three deep learning models - YOLOv4, EfficientDet, and CenterNet - were trained and tested for their effectiveness in detecting thirteen different species of weed using two platforms: a deep learning capable computer and an embedded computer. The experiment aimed to assess their suitability for real-time robotic applications. It was observed that, with a mean average precision of 93.4% at IoU threshold of 50%, an inference speed of 80ms, and 14 fps on an embedded computer, YOLOv4 is better suited for the real-time robotic applications due to its balanced performance between accuracy and inference speed. Furthermore, recognizing that some real-time robotic applications require higher speed without compromising the accuracy too much, a lightweight version of YOLOv4, YOLOv4-tiny was trained and tested in an embedded system. Despite its smaller size, YOLOv4-tiny impressively achieved a mean average precision of 89% at 50% IoU threshold which is approximately 4.7% less precise than YOLOv4. The model performed inference very rapidly on an embedded computer, with a speed of 24.5ms and 52 fps.

Due to its speed of detection in an embedded system and its satisfactory accuracy, YOLOv4-tiny is recommended for real time robotic applications that involve weed detection.

CHAPTER 5

THE INTEGRATION OF GPS AND VISUAL NAVIGATION FOR AUTONOMOUS NAVIGATION OF AN ACKERMAN STEERING MOBILE ROBOT IN COTTON FIELDS[3]

[3]Mwitta, C.,and Rains, G. To be submitted to *Smart Agricultural Technology*

5.1 **Abstract**

Autonomous navigation in agricultural fields poses a unique challenge due to the unpredictable nature of the outdoor environment. Different approaches have been attempted to combat the autonomous navigation task, each presenting its own unique challenges, such as GPS guidance with availability issues and inability to avoid obstacles, or several vision guidance techniques with their sensitivity to changes in light, weeds, and crop growth. Advances in hardware and software technology have provided an opportunity for more robust solutions to emerge. In this study three solutions to autonomous navigation in cotton fields are implemented. The first solution employed a path tracking algorithm pure pursuit to follow GPS coordinates to navigate a mobile robot between the rows in cotton fields. This solution effectively navigated the robot, generating a path with an average lateral distance deviation of 8.3cm from the pre-recorded path. The second solution utilized a deep learning model, a fully convolutional neural network for semantic segmentation, to detect the paths between cotton rows, and then navigate the mobile rover using a path planning algorithm called dynamic window approach (DWA). When tested for its performance in detecting paths between cotton rows, the trained deep learning model achieved a pixel accuracy of 93.5%, F1 score of 87.8%, and processed at 5 frames per second in an embedded computer used by the rover. In addition, the detected path in the image domain was successfully mapped to the ground coordinates using various computer vision techniques. The robot was able to navigate using DWA and the detected path with an average lateral deviation of 4.8cm from the desired path. Finally, the two solutions were combined for a more practical approach. GPS was employed as a global planner to map the field, while the deep learning model and DWA were used as local planner to navigate and make real-time decisions. This solution navigated the robot between cotton rows with an average lateral

distance error of 9.5cm. This solution presents a more practical way of navigating the robot autonomously between cotton field rows.

5.2 Introduction

The demand for increased production at a reduced cost in agriculture has necessitated the need for automation. Automation in agriculture improves farming efficiency, enhances safety, reduces costs, and reduces the need for human labor, ultimately leading to an increase in productivity. To achieve this, mobile robotic systems have been introduced in agricultural fields to automate tasks such as weeding, harvesting, spraying, scouting, planting, and monitoring. Driving these machines is a very demanding task, which involves steering to follow a path while operating the equipment (Heraud & Lange, 2009; Kise et al., 2005). Steering automation is a crucial step towards autonomous vehicles which allows more precise coordination between navigation in the field and the performance of the main operation such as harvesting, weeding, or other tasks.

Autonomous driving in the agricultural industry has seen significant breakthroughs recently, but compared to self-driving cars, the agricultural environment is significantly different in terms of complexity and diversity (Binbin et al., 2021). Most autonomous vehicles in agriculture utilize the Global Navigation Satellite System (GNSS) for navigation (Gao et al., 2018; Shalal et al., 2013). They determine their absolute position by utilizing real-time kinematic global position system (RTK-GPS) data and navigate by following a path formed from a series of pre-recorded GPS coordinates (Bakker et al., 2010; Fue, Porter, Barnes, Li, et al., 2020; Khan et al., 2018; Moeller et al., 2020; Stoll & Kutzbach, 2000). GPS guidance can work well as shown in (Bakker et al., 2010; Fue, Porter, Barnes, Li, et al., 2020; Khan et al., 2018; Moeller et al., 2020; Stoll & Kutzbach, 2000), however, weather, obstacles, and satellite availability can

affect its performance. Furthermore, without visual or ranging sensor, GPS navigation can be vulnerable to collisions in the field since it lacks obstacle detection.

Alternative solutions for autonomous navigation in agricultural fields have emerged with advances in computer vision technologies. Traditional computer vision algorithms have been used to detect either crop rows or the space between them as the path. Studies like (Ji & Qi, 2011; Rovira-Más et al., 2005) have utilized monocular RGB cameras to capture the scene and use computer vision algorithms to segment the images for crop row detection and path finding, others like (Kise et al., 2005) have used stereo vision to get a three-dimensional (3D) field image for crop row detection. Moreover, vision-based sensors like laser range finders which use LIDAR (Light Detection and Ranging) have been used by studies such as (Higuti et al., 2019; Hiremath et al., 2014) to follow crop rows in agricultural fields. Traditional computer vision techniques do not require extensive computational resources; however, they are sensitive to changes in illumination, and occlusion which can be exaggerated in outdoor agricultural environments. Additionally, color-based segmentation techniques are sensitive to weeds between crop rows, and most do not handle different crop growth stages well.

A reliable autonomous navigation system in agriculture would need to be robust against the challenging conditions in the field, such as changes in illumination, weather, occlusion, weed presence, and crop growth stages. Advances in deep learning technology have provided powerful and robust methods for distinguishing between crop rows and paths between rows. This is done through training deep learning models with extensive examples of images of different environmental scenery to improve future predictions. Many recent studies have utilized deep learning models as part of their autonomous navigation system in agriculture (Adhikari et al., 2020; Aghi et al., 2020; Bah et al., 2020; Cerrato et al., 2021; de Silva et al., 2021; Doha et al.,

2021). For example, (Adhikari et al., 2020) used a limited dataset and deep learning to develop a neural network that is robust against shadows, crop growth stages, and row spacing, however, it failed to generalize well to areas where crops had occluded the path. (Bah et al., 2020) developed a solution that combined convolutional neural network (CNN) and Hough transform to achieve crop row detection in UAV captured images, which was robust to weeds in the field.

Advances in road lane marking detection for self-driving vehicles has inspired studies which use deep learning based semantic segmentation. For example, (Adhikari et al., 2020; de Silva et al., 2021; Doha et al., 2021) utilized fully convolutional neural network (FCN) for semantic segmentation (Long et al., 2015), known as 'U-net' because of its 'U-like' structure (Ronneberger et al., 2015), and some computer vision algorithms to detect crop rows in agricultural fields. U-Net is a popular image segmentation algorithm known for not demanding a lot of data for training and having low latency in prediction. Most of these models were robust against shadows and row discontinuities but still struggled with changes in light conditions and presence of weeds.

After determining the paths' locations, the autonomous system needs to navigate by following the path through path planning and tracking. Different implementations of path planning and tracking have been deployed in agricultural settings to enable navigating the predicted paths. Solutions like pure pursuit path tracking (Fue, Porter, Barnes, Li, et al., 2020), Non-linear model predictive path tracking (Backman et al., 2012), sliding mode control for non-linear tracking (Tu et al., 2019), sliding window approach for path planning (Adhikari et al., 2020), genetic algorithms (Noguchi & Terao, 1997), and others have been implemented.

This paper explored using GPS, FCN for semantic segmentation, and a combination of both, while utilizing other computer vision algorithms to autonomously navigate a mobile robot

in a cotton field. The study also explored two path-planning and tracking algorithms, pure-pursuit (Coulter, 1992), and dynamic window approach (DWA) (Fox et al., 1997), on their effectiveness to follow the desired path while autonomously navigating the robot. Instead of detecting the crop rows, the FCN for semantic segmentation in this study concentrates on detecting the paths between the rows. The faster predictions feature of the model enables real-time path detection and planning for weeding, harvesting, and scouting in cotton. Moreover, to generate a path between cotton rows on the ground plane that the rover can follow, the detected path must be mapped from the image domain to ground coordinates. This study proposes a method for achieving that requirement.

5.3 **Materials and Methods**

5.3.1. Platform

The robotic platform used in this study was a 4-wheel Ackerman (car-like) steering ground rover (see Figure 5.1). The robot navigates between rows of cotton using various sensors, actuators, microcontrollers, and an embedded computer. Each of the rover's wheels is run by a 250W Pride Mobility wheelchair motor, with the two back wheels connected to Quadrature rotary encoders (CUI AMT 102) to provide feedback on wheel rotation. The motors are driven by two Cytron MDDS30 motor controllers and powered by two 20000mAh 6-cell Tunigy LIPO batteries. A linear servo (HDA8-50) is connected to the front wheels for steering. To track the rover's orientation two PhidgetSpatial Precision 3/3/3 High Resolution IMUs are mounted to the rover. These modules contain a 3-axis accelerometer, a 3-axis gyroscope, and a 3-axis compass. An Arduino Mega microcontroller controls these sensors and actuators. A single-band EMLID Reach RS+ RTK GNSS receiver is mounted to the rover for GPS navigation, while a Zed2 stereo camera (Stereo Labs) is utilized for visual navigation. The stereo camera has two image sensors

which allow it to capture normal RGB images, calculate depth of pixels in the image, and generate 3D point cloud. The rover also has a 2D cartesian arm that is used for various in-field tasks like harvesting, and weeding. The autonomous navigation system is run by an embedded computer (Nvidia Jetson Xavier AGX with 8-core ARM v8.2 64-bit CPU, 32GB of RAM, and a 512-core Volta GPU) which communicates with other components using Robotic Operating System [29] (ROS 1 – Noetic). ROS is a set of software frameworks for robot software implementation which provides processes presented as nodes in graph structure that are connected by edges known as topics. Topics carry and pass messages between nodes.

The RTK-GNSS receiver obtained corrections from another RTK GNSS receiver (EMLID Reach RS 2) which was set up as a base station at a fixed absolute position in the field. With base correction the rover can achieve centimeter-level precise position.

Figure 5.1. The robotic platform

5.3.2. Kinematics Modeling of the Robot

The robot uses front-wheel Ackerman steering mechanism (see Figure 5.2) which was designed to solve sideways tire slipping when following a curved path. The center of rotation (C)

is on the line extended from the rear axle intersecting the axes of the front wheels. When steering, the front inside wheel must turn a greater angle (θ_i) than the outside wheel (θ_o). The robot position is taken at the center of the rear axle (x_{robot}, y_{robot}).

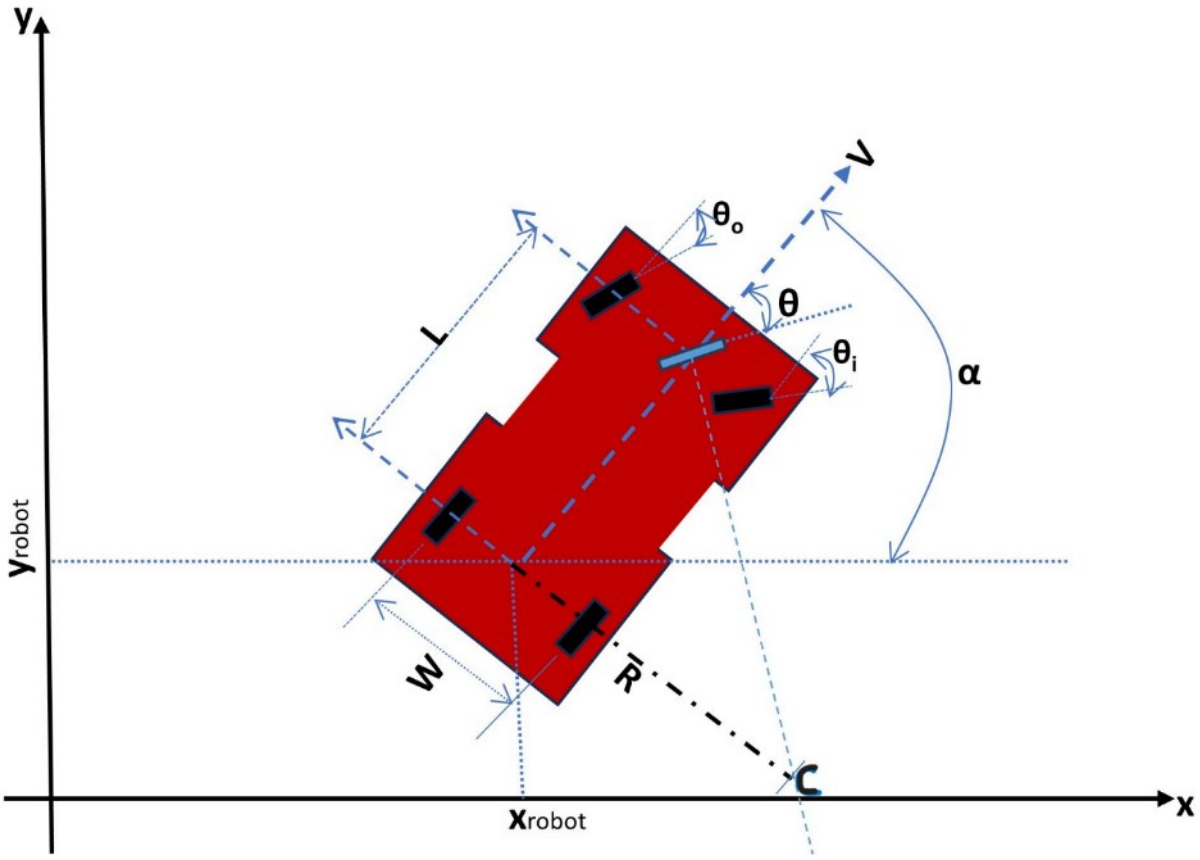

Figure 5.2. Ackerman Steering robot mechanism

The kinematics model considers the middle of the rear wheels as the robot's position where, R is the turning radius of the robot, L is the wheelbase (distance between rear and front wheels), W is the width of the robot, V is the linear velocity of the robot, $\propto$ is the heading, and θ ideal front wheel turning angle. The relationships are defined as follows:

$$\tan(\theta_i) = \frac{2Ltan(\theta)}{2L - Wtan(\theta)}$$

$$\tan(\theta_o) = \frac{2Ltan(\theta)}{2L + Wtan(\theta)}$$

$$\dot{X}_{robot} = Vcos(\propto)$$

$$\dot{Y}_{robot} = Vsin(\propto)$$

$$\dot{\propto} = \frac{V}{L}\tan(\theta)$$

5.3.3. GPS Navigation

5.3.3.1. Sensor Fusion using Extended Kalman Filter

Extended Kalman Filter (EKF) is an algorithm that efficiently estimates the internal state of a non-linear dynamic system from a series of noisy measurements. Derived from Kalman filter (Kalman, 1960) which can only estimate linear systems, EKF is a well-known non-linear state estimator which has been implemented in many studies (Moore & Stouch, 2016; Smith et al., 1962; Wan & Nelson, 2001). Our goal is to accurately estimate the pose and velocity of the robot over time by fusing multiple noisy sensors. Considering, the robot's state (pose) at time t, x_t, f as a non-linear transition function, w_t the process noise (normally distributed), z_t, the measurement received from sensors at time t, h as a non-linear sensor model, v_t the measurement noise, and u_t as the control, the process and measurements can be described with two equations.

$$x_t = f(x_{t-1}, u_t) + w_t$$

$$z_t = h(x_t) + v_t$$

The time step, Δt depends on the speed of updating the filter. The filter was updated at a frequency of 20 Hz, which implies a time step of 50ms.

The EKF implementation fused continuous data from encoders, IMUs and GPS using the ROS package Robot_localization (Moore & Stouch, 2016). Robot_localization package accepts position, linear velocity, angular velocity, linear acceleration, and angular acceleration data from sensors and then estimates the robot's pose and velocity. Two nodes; a state estimation node

EKF_localization_node and a sensor processing node NavSat_Transform node (see Figure 5.3) implemented in Robot_Localization were fed sensor data to estimate the local and global pose and velocity of the robot. Data from two IMU topics (*/imu1/data* and */imu2/data*) fused with the odometry topic *(/enc_odom*) obtained the two encoder readings and kinetic modeling equations were fused by the EKF_localization_node to get locally accurate odometry estimates in the topic */odometry/filtered/local*. The NavSat_Transform_Node transformed geographic coordinates (latitude, longitude) into robot's world frame and produced GPS odometry topic */odometry/gps* from fusing data from GPS topic */gps/fix*, IMU topic */imu2/data*, and the local estimate from EKF_Localization_node /odometry/filtered/local. The GPS odometry */odometry/gps* was then fed to EKF_Localization_node to obtain an accurate and complete global state (*/odometry/filtered/global*).

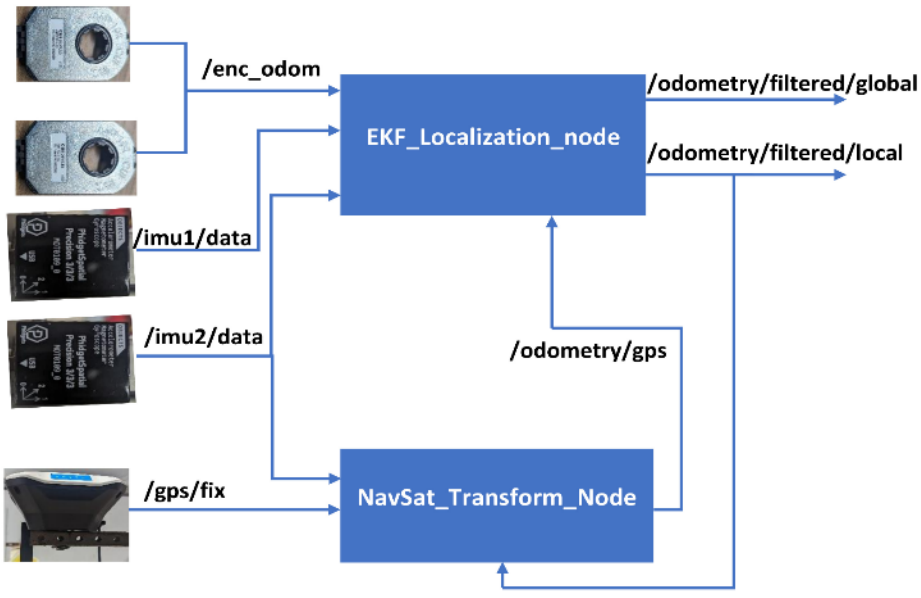

Figure 5.3. ROS – Robot_localization package implementation

5.3.3.2. Path Generation

The paths between cotton rows are represented by pre-recorded GPS points where the robot was driven at the UGA Tifton Campus fields located at (31.471987 N, 83.527951 W) in

Tifton, GA. The GPS points were converted to UTM (Universal Transverse Mercator) format which represent the latitude and longitude values in meters instead of degrees. To get smooth paths the UTM points were connected using cubic spline interpolation method (McKinley & Levine, 1998). This method utilizes a third-degree polynomial to connect points and generate other points in between, which enabled us to generate points with a resolution of 3cm.

5.3.3.3. Modified Pure Pursuit Path Tracking

After a path is generated, the robot needs to follow that path through tracking its own pose and determine the steering angle needed to remain on the desired path. One of the well-known path-tracking algorithms is pure pursuit. Pure pursuit (Coulter, 1992; Fue, Porter, Barnes, Li, et al., 2020; Park et al., 2014; W. J. Wang et al., 2017) is a geometric path tracking controller. It follows a look-ahead target point at a fixed distance on the reference path. The target point (Goal point as shown in Figure 5.4) along the desired path is selected at a distance L_d from the position of the rover which is taken at the center of the rear axle.

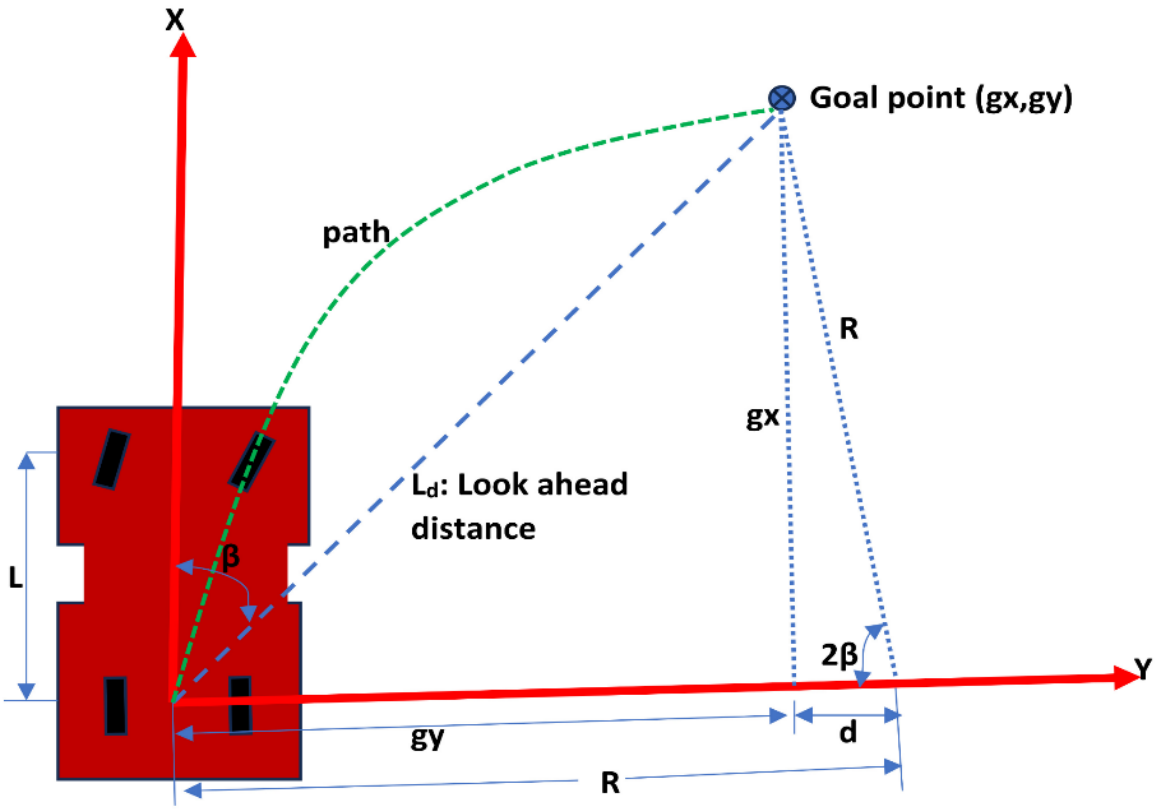

Figure 5.4. Pure pursuit mechanism

With the aim of making the robot steer at a correct angle θ to get to the target point, the geometric relationships were calculated. Considering the angle between the robot's heading and the look-ahead line as β, the robot traverses a curved path of radius R. From Figure 5.4, the relationships are defined below:

$$R = |gy| + d$$

$$d^2 + gx^2 = R^2$$

$$gx^2 + gy^2 = {L_d}^2$$

Solving these equations, results into,

$$R = \frac{{L_d}^2}{2 \times |gy|}$$

But,

$$\sin(\beta) = \frac{|gy|}{L_d}$$

So,

$$R = \frac{L_d}{2\sin(\beta)}$$

From the robot kinematics, the relationship between R, wheelbase R, and the steering angle θ,

$$R = \frac{L}{\tan(\theta)}$$

So, the steering angle θ can be calculated as:

$$\theta = \arctan\left(\frac{2Lsin(\beta)}{L_d}\right)$$

The pure pursuit controller ignores dynamic forces on the vehicle and assumes constant speed, however, at shorter look-ahead distances, the controller would be dangerously aggressive at high speeds which lead to instability. So, the algorithm was modified to set the robot's speed depending on the steering angle calculated, the speed V_r is set inversely proportional to the steering angle θ by a gain K_s.

$$V_r = K_s \times \theta$$

5.3.3.4. Speed Control Using PID

Since the field surface is uneven and contains some washed out gullies, maintaining velocity of the rover is challenging. A PID controller (Proportional, Integral, and Derivative) (Ang et al., 2005; L. Wang, 2020) was used for speed control. A PID controller continuously computes the difference between a desired setpoint value and a measured variable, then applies correction on the control value based on three pre-tuned gains, proportional, integral, and derivative. For speed control, the control value at time t, $u(t)$ is the motor command. Given the

current velocity of the robot $V_C(t)$, the PID system calculates the motor command required by the robot to reach the desired targeted velocity $V_T(t)$, using the three gains, proportional gain K_p, integral gain K_i, and derivative gain K_d.

The error value $e(t)$ is given by:

$$e(t) = V_T(t) - V_C(t)$$

The motor command $u(t)$ is obtained from:

$$u(t) = K_p e(t) + K_i \int_0^t e(\tau)\, d\tau + K_d \frac{de(t)}{dt}$$

The PID controller was tuned to find the values of the three gains that achieved desired performance, by iteratively adjusting the gains while monitoring the step response of the rover. The time step was set at 50ms.

The overall navigation process using pursuit is summarized in Figure 5.5

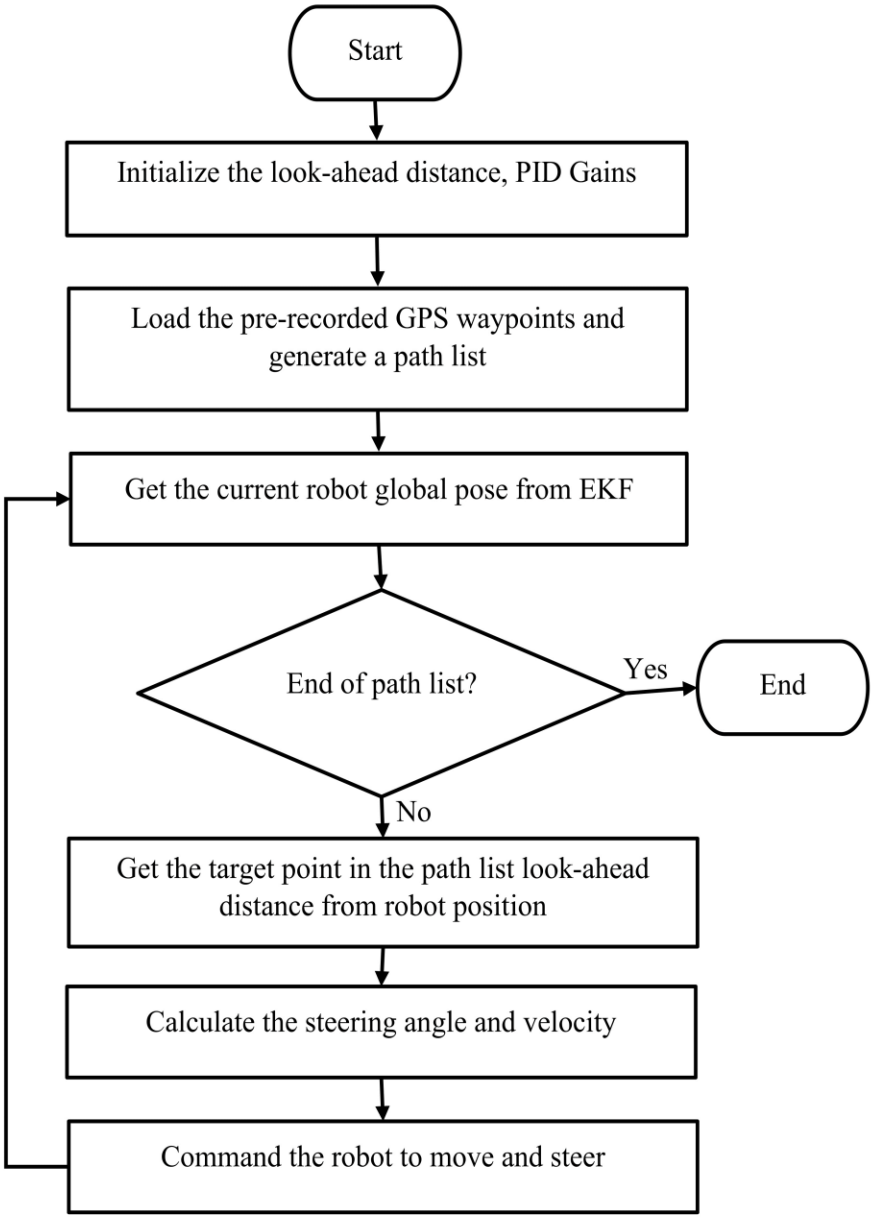

Figure 5.5. Autonomous navigation using pure pursuit and GPS process.

5.3.4. Visual Navigation using Deep Learning

Unlike GPS-based navigation systems, visual navigation systems are robust to interference, high resolution, and low cost. With vision, obstacle avoidance can also be implemented. Vision technology can be utilized to detect paths or crop rows in the field.

5.3.4.1. Path Detection using Fully Convolutional Network (FCN) for Semantic Segmentation

FCN for semantic segmentation, Figure 5.6, classifies each pixel in an image to a predefined class. The network consists of two parts. The first part is the convolution/encoder network which uses an object classification network such as VGG Net [37], as a backbone to shrink the spatial resolution of feature maps in the image and detect the important features. The second part is the deconvolutional/decoder network which up-samples and increases the spatial resolution of the features to classify each pixel from the original image into a class. The input to the FCN is an image and the output is another image (a segmentation mask) which has the same size as an input image with each pixel representing a predefined class.

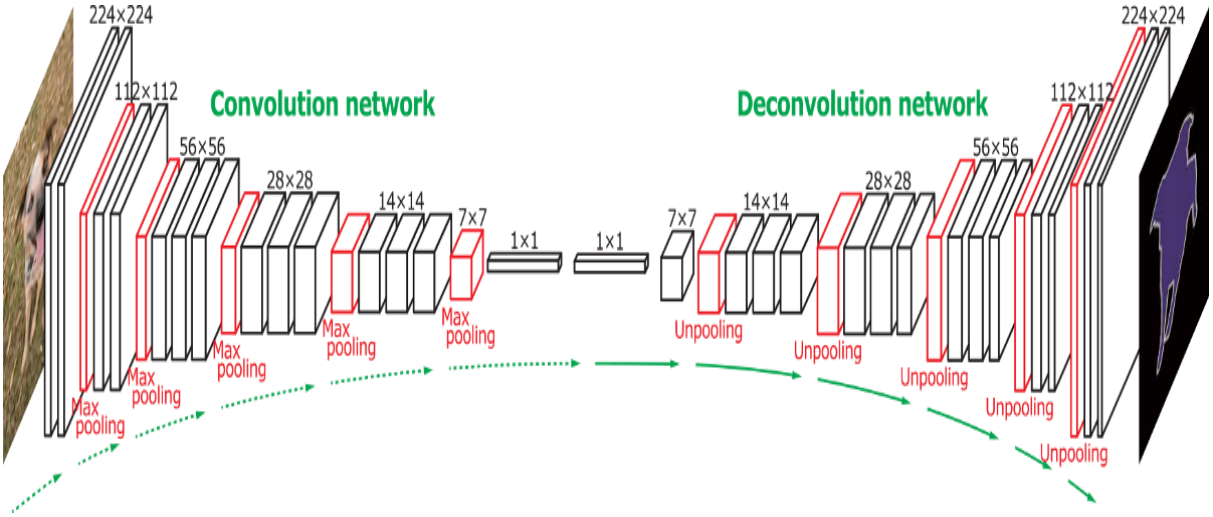

Figure 5.6. A fully convolutional neural network structure (image source (Noh et al., 2015))

For path detection, the image of cotton rows (Figure 5.7 **A**) is fed into the network, and the network predicts the segmentation mask as shown in Figure 5.7 **B,** with the white pixels representing the path between the rows.

Figure 5.7. Cotton rows and paths (**A**), Expected segmentation mask (**B**)

5.3.4.1.1. Model Creation

Cotton rows images (resolution 1280 x 720 pixels) were acquired from the University of Georgia Tifton Campus cotton field (31°28'N 83°31'W) using a ZED2 stereo camera (stereolabs.com) mounted on a rover at different cotton growth stages, times of the day, and camera angles.

More than 400 images were labeled to indicate the path between cotton rows (see Figure 5.8) using Label Studio software (https://labelstud.io/).

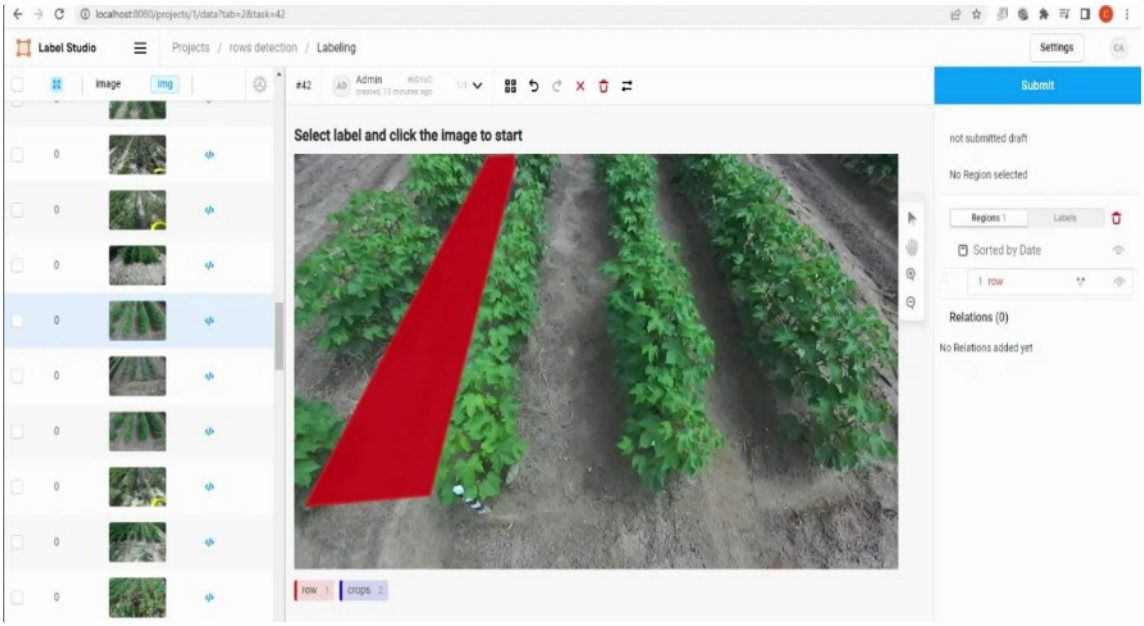

Figure 5.8. Image labelling with Label studio

Since only paths were considered, there was only one segmentation class. The labeled dataset was randomly split into training dataset (80%), validation dataset (10%), and testing dataset (10%).

The FCN segmentation model was trained on a training dataset while being validated on a validation dataset. The model was trained on a deep learning computer (32–cores Intel I9, 2 Nvidia RTX 2080 GPUs, 128GB RAM). After training, the model was run on the testing dataset to test its performance.

5.3.4.2. Robot Navigation

The FCN model predicts the path between the cotton rows and outputs the segmentation mask which is just physical pixels in the image domain that represents the path. For the rover to navigate, its position on the ground relative to the detected path must be known together with the next target coordinates, so the detected path in the image plane must be mapped to the ground plane. Figure 5.9 shows this process.

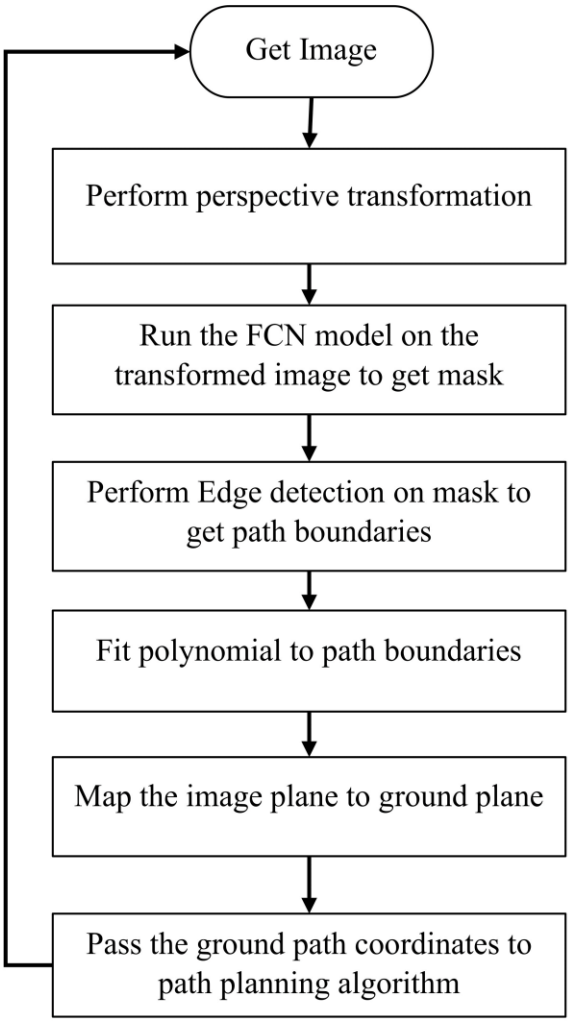

Figure 5.9. Context of the process to detect path and map to ground coordinates.

The image from the ZED2 stereo camera in front of the rover (Figure 5.10) was acquired. The camera was mounted at a height of 1.5 meters from the ground and inclined at an angle of 25° from the vertical axis. The left image sensor of the ZED2 stereo camera was used as a reference axis, the resolution of the image was 1280x720 pixels. ZED2 has a field of view (FOV) of 110° (H) x 70° (V) x 120° (D).

Figure 5.10. Acquired image from the front camera

From camera perspective, parallel lines appear to converge further away from the camera lens which make the path between cotton rows appear narrower away from the camera lens. To get accurate parallel lines, perspective transform of the image is required. Perspective-transform maps image points to new image points with a new perspective. The cotton rows image is transformed to a bird's-eye view that represent the rows seen from above (Figure 5.11) (only the path between the center two rows is targeted).

Figure 5.11. Bird's eye view of the image

To detect the path, the FCN model was run on the transformed image to produce a segmentation mask (Figure 5.12) with the white pixels representing the path in the image.

Figure 5.12. A segmentation mask of the transformed image

To find the path boundaries, edge detection was performed on the segmentation mask to get the pixels that represent the left and right boundaries of the detected path (Figure 5.13). Canny edge detection algorithm (Canny, 1986) was applied to the mask to get the edges between path (white pixels).

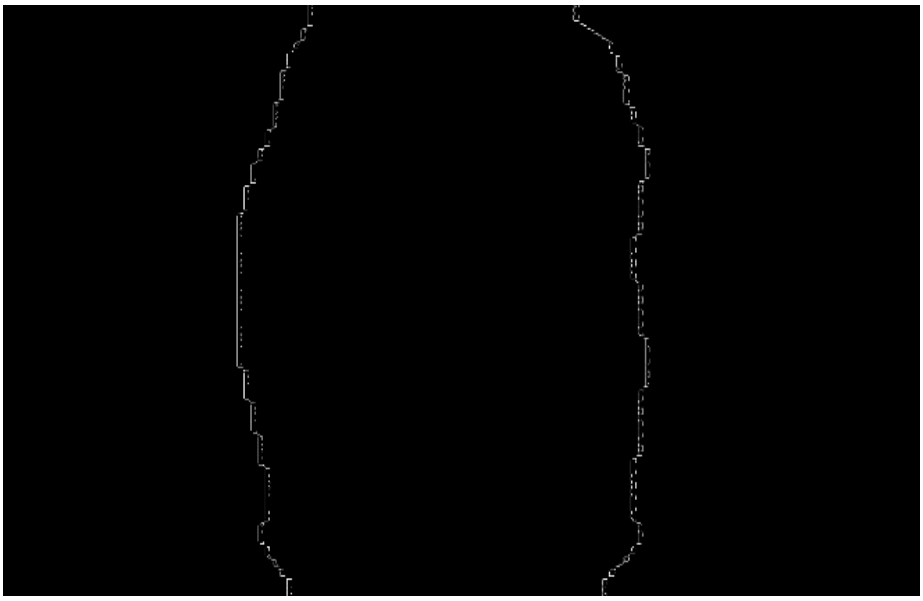

Figure 5.13. Edge detection result on the segmentation mask

To be able to map the path detected in the image domain to the ground plane, a plane representing the detected path in the image domain is needed. Since we already have the pixels representing the detected path boundaries, we fit polynomials to those pixels to get the left and right lines which form a plane (Figure 5.14). A second order polynomial is fitted to the boundaries to account for the chance that the rows may be curved.

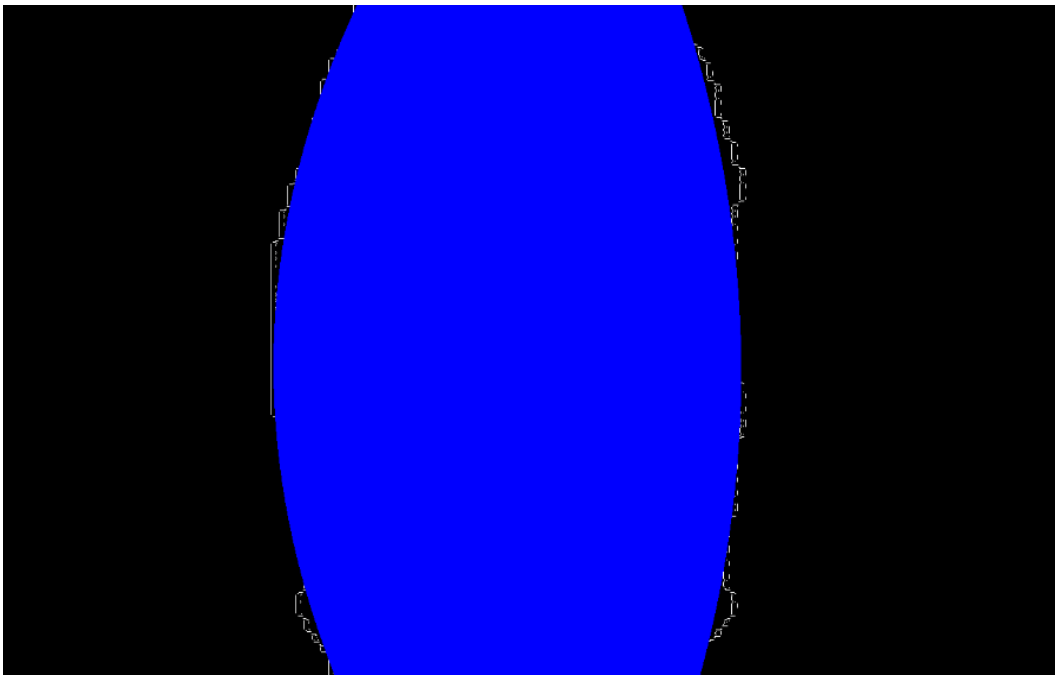

Figure 5.14. Polynomial fitted into left and right path boundaries.

Since the camera FOV, resolution, and position with respect to the rover is known, the pixels in the image domain (u, v) were mapped to the (x, y) coordinates on the ground plane. Establishing our ground coordinates origin directly below the camera center (Figure 5.15) with the camera height h meters from the ground, inclined at $\emptyset$ from the vertical axis, vertical FOV angle of θ , horizontal FOV angle of φ , and resolution $(H \times W)$, the (x, y) coordinates on the ground mapped from the (u, v) pixel coordinates are given by the following equations:

$$x = h \times \left(\tan(\emptyset - {}^{\theta}/_{2}) + {}^{(H-u)}/_{H} \times (\tan(\emptyset + {}^{\theta}/_{2}) - \tan(\emptyset - {}^{\theta}/_{2})) \right)$$

$$y = h \times \left(\left({}^{(2v-W)}/_{W} \right) \times tan\, {}^{\varphi}/_{2} \right)$$

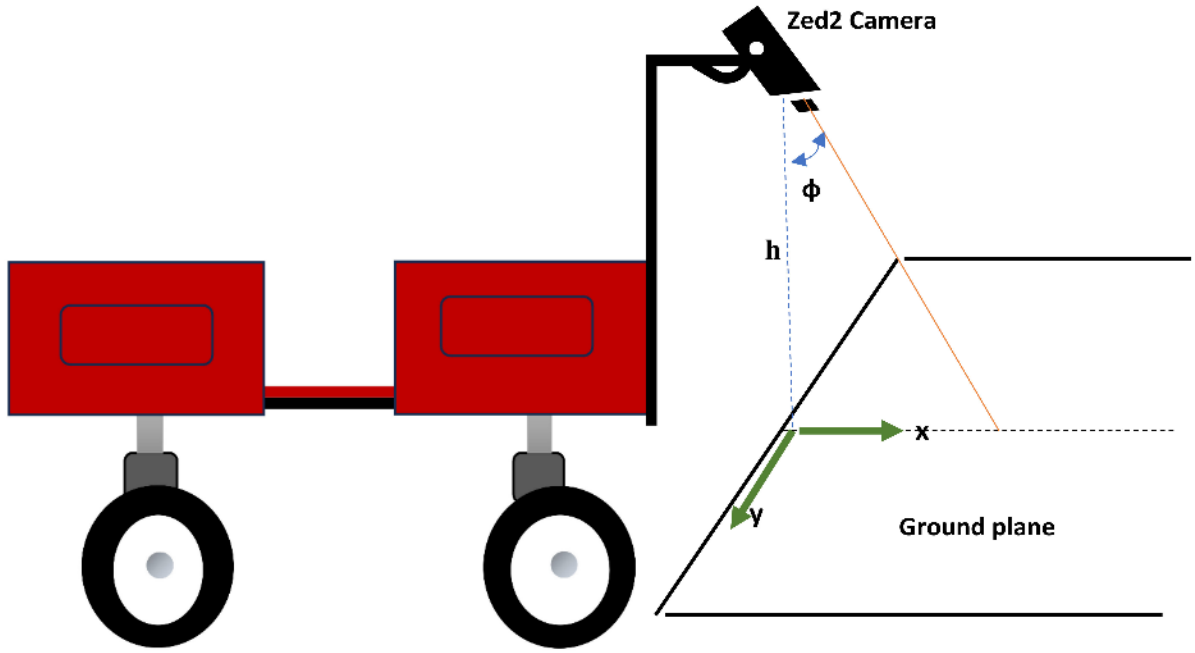

Figure 5.15. Camera setup with respect to ground plane.

5.3.4.3. Path Planning with Dynamic Window Approach (DWA)

The DWA (Fox et al., 1997) is a velocity-based local path planning algorithm that tries to find the optimal collision-free velocities for the robot to navigate. This algorithm takes the robot's kinematics into consideration when deciding a solution. Considering the limited accelerations of the motors, the search space for a solution is done in a 'dynamic window' which contains only the velocities that can be reached within the next time interval (Figure 5.16). The algorithm works by generating trajectories determined by translational and rotational velocities (υ,ω), then selecting admissible velocities which avoid obstacles or can make the robot stop before it reaches an obstacle. The dynamic window created contains only the admissible

velocities that can be reached within a short time interval given the limited dynamics of the robot.

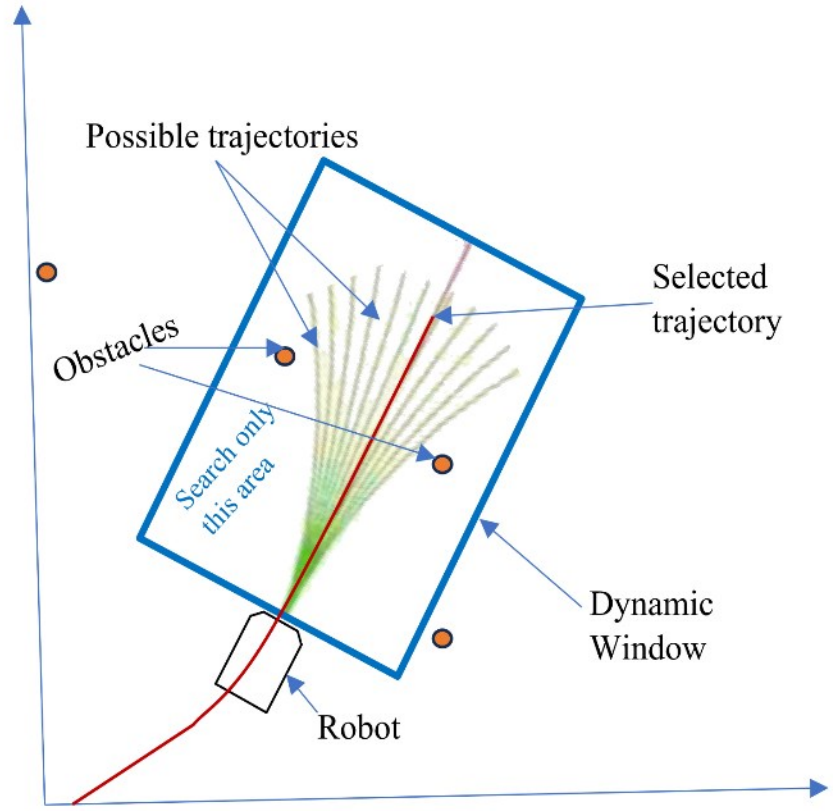

Figure 5.16. Dynamic window approach

Because of its obstacle avoidance nature, DWA can be used to navigate the robot between cotton rows and avoid running over the rows by treating them as obstacles. So, points along the detected path boundaries are sampled and fed to the algorithm as obstacles, then the generated trajectory avoids those points.

DWA considers three main parameters for optimization: The first parameter is Heading. It measures how close the robot's direction is to the targeted goal location. The algorithm prefers the direction that moves the robot closer to the goal. Another parameter is Obstacle distance, which measures the distance to the closest obstacle on the trajectory, smaller distances increase

the robot's desire to move around them. The third parameter is the forward velocity of the robot, the algorithm tries to choose the highest admissible velocity for fast movement. In general, the algorithm finds a set of linear and angular velocities (v, ω) that optimize the objective function $F(v, w)$ containing heading with gain α, obstacle distance with gain β, and velocity with gain γ.

$$F(v, w) = \delta(\alpha.heading(v, \omega) + \beta.obstacle(v, \omega) + \gamma.velocity(v, \omega))$$

Navigation in the cotton field using DWA was done by continuously giving the algorithm a goal point which is a point along the center line (2.0 m ahead of the robot position) of the predicted path by FCN network. The obstacles were represented by the sampled points on the path boundaries as seen in Figure 5.17.

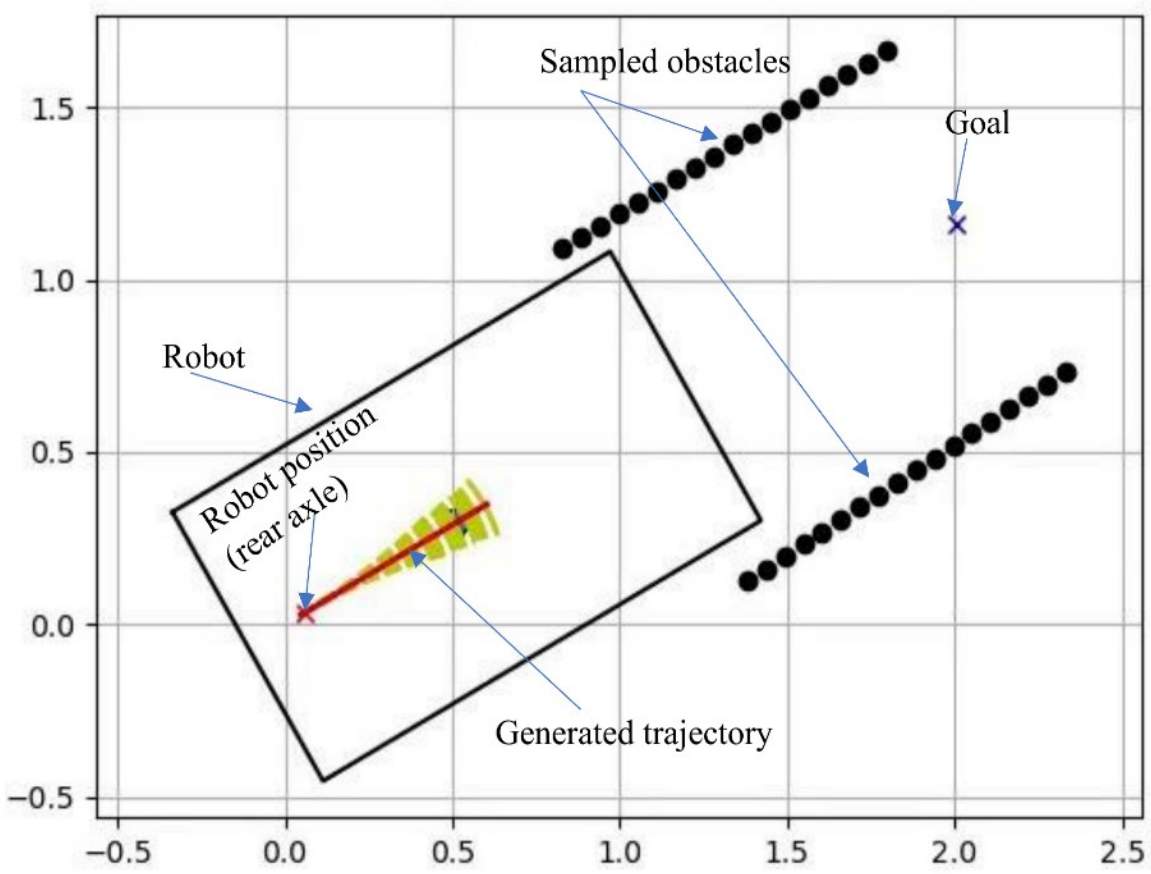

Figure 5.17. Path boundaries points sampled to represent obstacles in DWA algorithm.

5.3.5. GPS and FCN Network Navigation Combination

The FCN network navigation has the advantage of stability and since the path is observed in real-time, the robot can plan to account for any dynamic changes in real-time while navigating between the rows. However, it does not know the overall map of the field which can be challenging especially when the robot is turning to go to another row. Global path planning is ideal for this situation. Despite its shortcomings, GPS can easily map the entire field. A better solution is to leverage the advantages of both GPS and deep learning by combining them. GPS can be used for global planning to map the entire field, while deep learning acts as a local planner, to detect paths between the rows in real-time, navigate and avoid obstacles. So, the robot follows the GPS global path while adjusting its movement based on the visual observation.

This solution was implemented by getting the target goals from pre-recorded GPS coordinates, using FCN to detect the path between the rows, then finding the velocities (v,w) that approach the goal but not collide with obstacles.

5.3.6. Experiments

To test the solutions, experiments were conducted in University of Georgia Tifton campus cotton fields located at (31°28'N 83°31'W).

5.3.6.1. GPS Navigation Experiment

The robot was run manually first between rows of cotton field, turn at the end and come back through another pair of rows, skipping one row because of robot's turning radius as in Figure 5.18, while recording the GPS coordinates to form pre-recorded way-points. Then the robot was autonomously driven following the recorded pattern using pure pursuit. This was repeated four times. The robot's GPS position was recorded while navigating for comparison with the path followed.

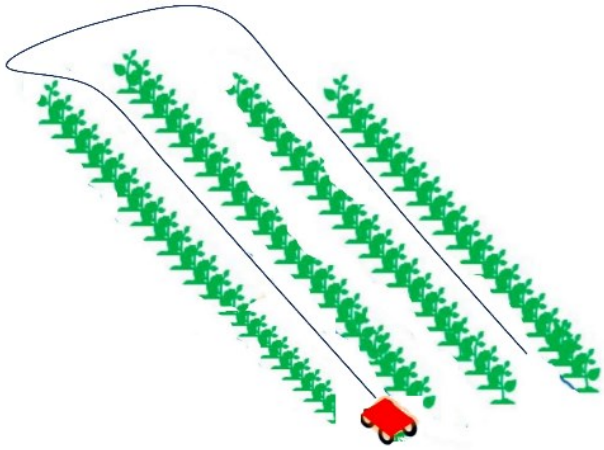

Figure 5.18. Robot's movement pattern in the field

5.3.6.2. FCN and DWA Experiment

Firstly, the fully convolutional neural network for semantic segmentation model was tested on testing dataset for its accuracy in detecting the paths between the rows. Then, in the cotton field, utilizing the model to detect path and DWA to navigate, the robot was run four times between cotton rows. The ideal path (center line between the rows) and the robot's position was recorded for comparisons.

5.3.6.3. FCN and GPS Combination Experiment

Using the pre-recorded GPS coordinates from the GPS experiment as the desired path, the rover navigated between the rows following the coordinates while restricting its movement based on the path detection information and DWA planning. When the robot does not detect the path, for example, at the end of the rows, the robot uses GPS only solution to navigate until it detects the path again.

5.3.7. Evaluation Metrics

The FCN network for semantic segmentation model was evaluated using Pixel Accuracy, Intersection over Union (Jaccard Index), F1 score (Dice coefficient), Precision, Recall, inference time, and number of frames per second (fps) metrics.

Pixel accuracy represents the percentage of pixels in the image that are classified correctly.

Precision measures how well the positive predictions match the ground truth.

$$Precision = \frac{True\ positives}{True\ positives + False\ positives}$$

Recall measures how many relevant predictions are made out of all predictions.

$$Recall = \frac{True\ positives}{True\ positives + False\ negatives}$$

Intersection over Union (IoU) indicates the overlap of the predicted bounding box coordinates to the ground truth box, see Figure 5.19.

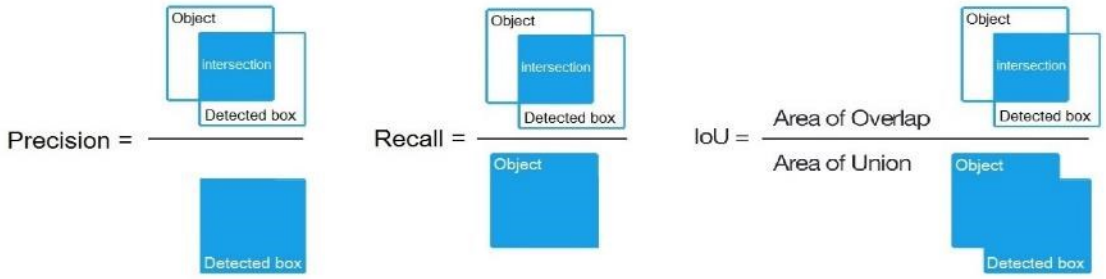

Figure 5.19. Precision, recall, and IoU demonstration

F1 score is calculated from precision and recall representing the model's accuracy.

$$F1\ score = 2\frac{Precision \times Recall}{Precision + Recall}$$

Inference time measures the time it takes for a model to make a prediction on a single image, and frames per second indicate the frequency at which inference is performed on consecutive images in a video stream. The inference time and fps were tested on the robot's embedded computer (Nvidia Jetson Xavier AGX) for real-field experience.

To evaluate the accuracy of the robot's path following ability, a trajectory similarity measure was used. This method samples points along the path and calculates the lateral distance error

between the desired path and the path generated by robot's movement (see Figure 5.20). The points along the path were sampled at 0.05m distances, then the lateral error was evaluated.

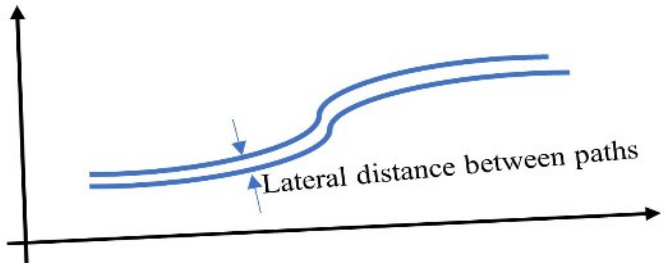

Figure 5.20. Similarity metric - lateral distance error

5.4 **Results**

5.4.1. FCN Model Accuracy

Table 5.1 shows the model performance results when it was tested on testing dataset. The model performed well with a pixel accuracy of 93.5%, F1 score of 87.8%, and IoU of 79.5%. However, the model was relatively slow on robot's embedded computer which attained a reference time of 182 ms and 5fps.

Table 5.1. FCN model performance evaluation results

Metric	Value
Pixel Accuracy	0.935
Intersection over union	0.795
Precision	0.908
Recall	0.859
F1 score	0.878
Inference time (ms) – embedded computer	182
Frames per second (fps) – embedded computer	5

Visual observation (Figure 5.21) showed that the model was able to detect paths between cotton rows and was robust to camera angles, cotton growth stages, weeds, and occlusions in the field.

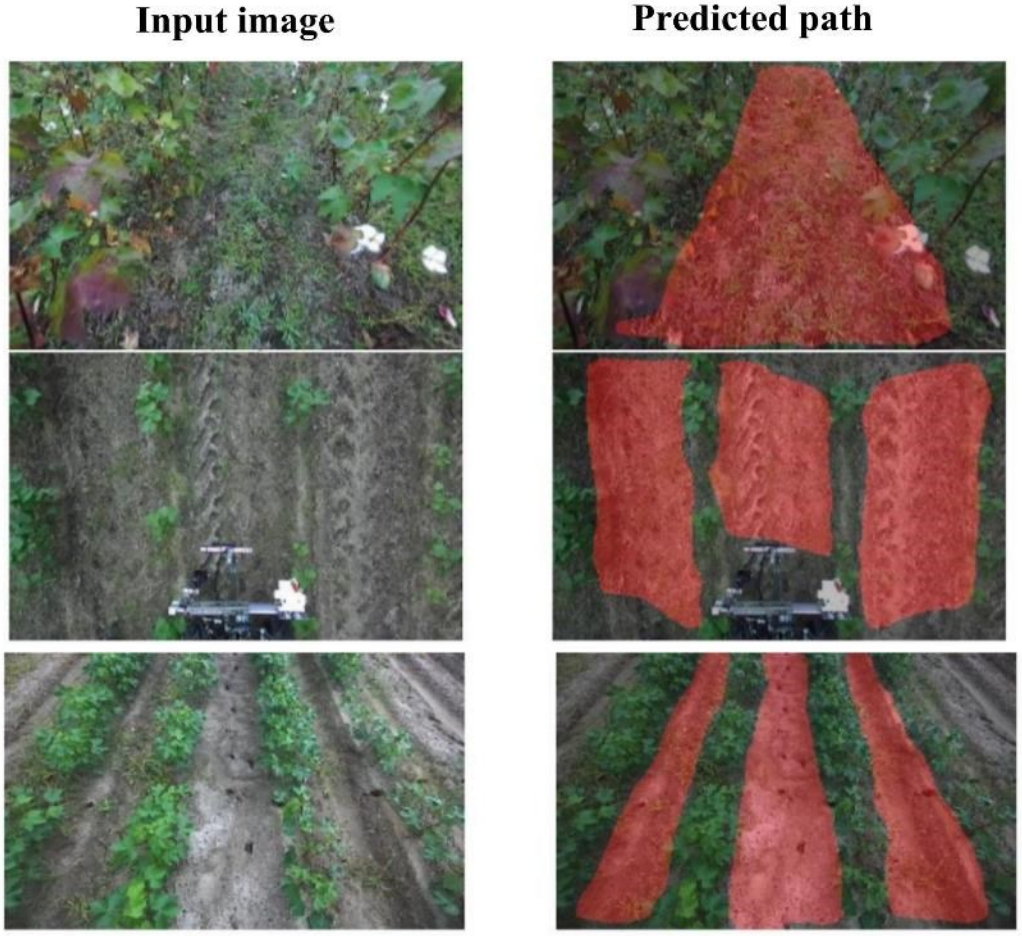

Figure 5.21. Examples of tested images on the FCN model and their predicted results

The process to map detected path in image domain to ground coordinates worked when tested on field images, the algorithm isolated a single row, found a path and mapped it into ground coordinates as in Figure 5.22.

Figure 5.22. Path detected between cotton rows and mapped to ground plane.

5.4.2. Navigation Experiments

The robot was able to follow the pre-recorded GPS coordinates in the field using pure pursuit path tracking algorithm (Figure 5.23). The shape of the trajectory at end-of-row turning is due to the large turn radius of the robot as it tries to go to the next plot. There were slight deviations when the robot was turning, which is demonstrated by the deviation errors in Figure 5.24. The lateral deviation errors for trials seem to peak around turning locations. The average lateral deviation was 8.3 cm which is good for navigating the field.

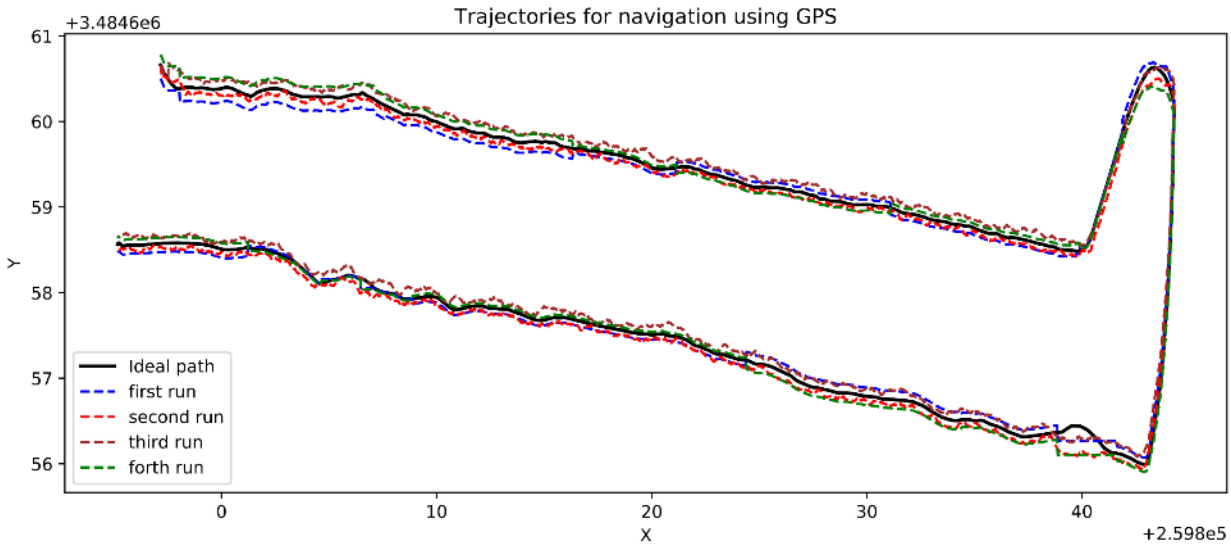

Figure 5.23. Trajectories generated by pure pursuit following GPS path.

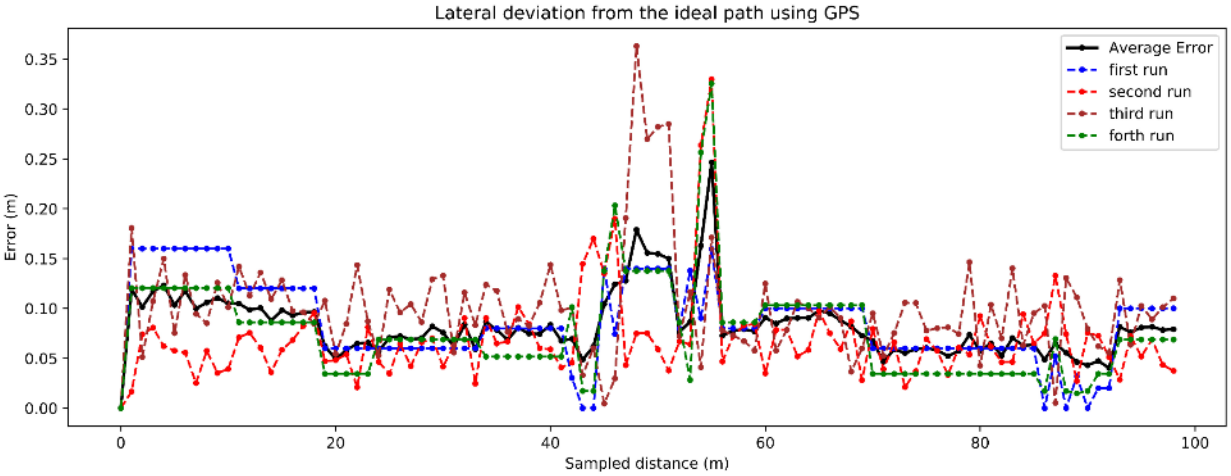

Figure 5.24. Latteral distance error of the paths generated by the robot using GPS and pure pursuit.

Using DWA and deep learning, the robot was able to follow the ideal straight path (center line between the rows), as demonstrated in Figure 5.25, with an impressive average lateral deviation of 4.8cm as in Figure 5.26

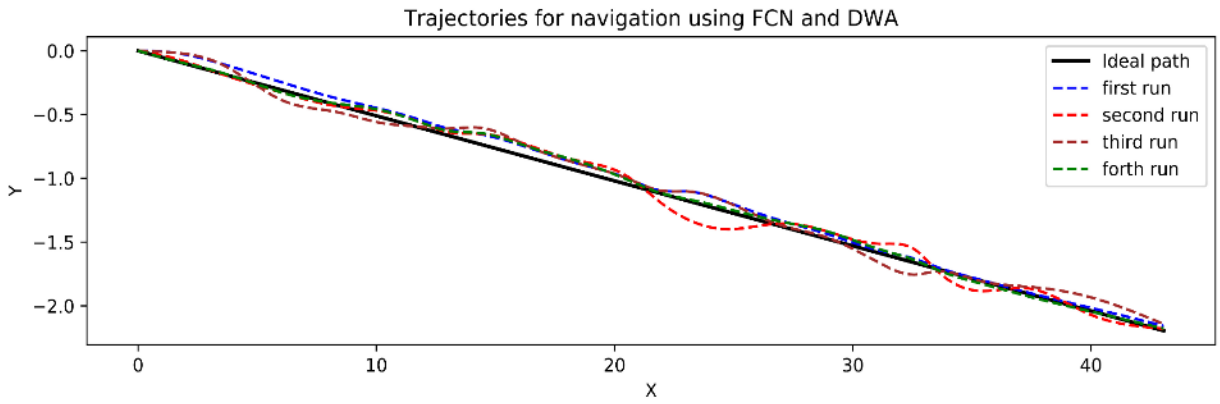

Figure 5.25. Trajectories generated using FCN and DWA

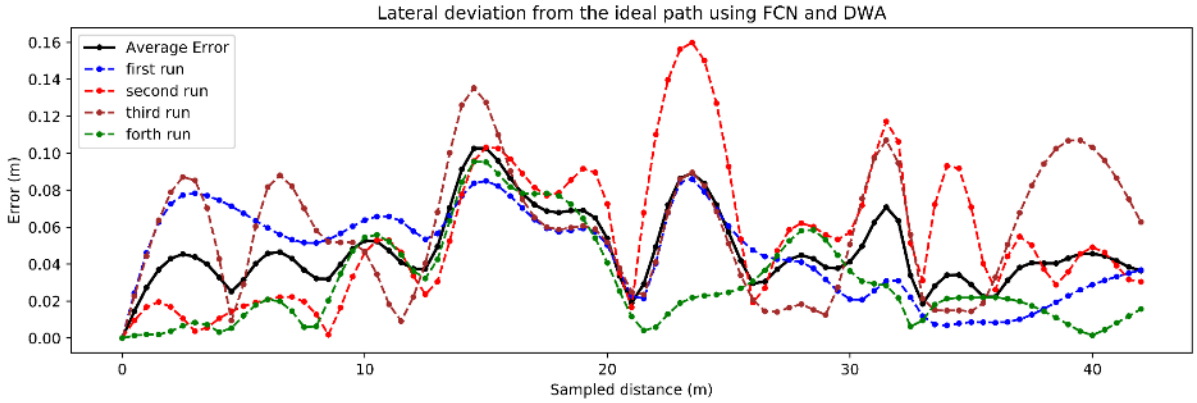

Figure 5.26. Latteral distance errors by FCN and DWA

With a combination of GPS and FCN, the robot successfully followed the GPS coordinates as a global path while performing path detection and avoided obstacles (rows). It can be observed in Figure 5.27, the path profiles for all the runs look the same because they were trying to go straight forced by the DWA local planner while the GPS coordinates were not as straight. The average lateral deviation was 12.1cm which was higher than the other solutions, however, it was skewed at the turning locations as shown in Figure 5.28, and by the pre-recorded GPS points not making a smooth straight path. The average deviation of row following separately was 9.5cm, while that of end-of-row turning was 14.6cm. This was still the best

method since it can move the robot straight between the rows and avoid running over crops while following the GPS global map. Table 5.2 summarizes the deviations.

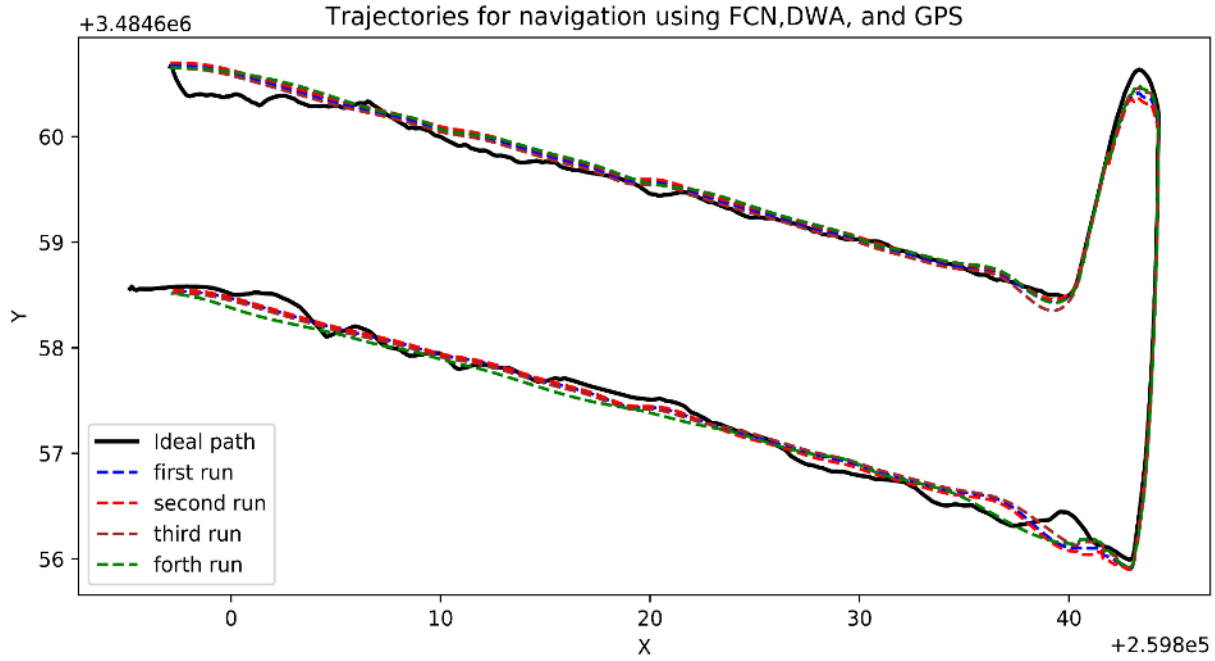

Figure 5.27. Trajectories generated by a combination of FCN, DWA and GPS

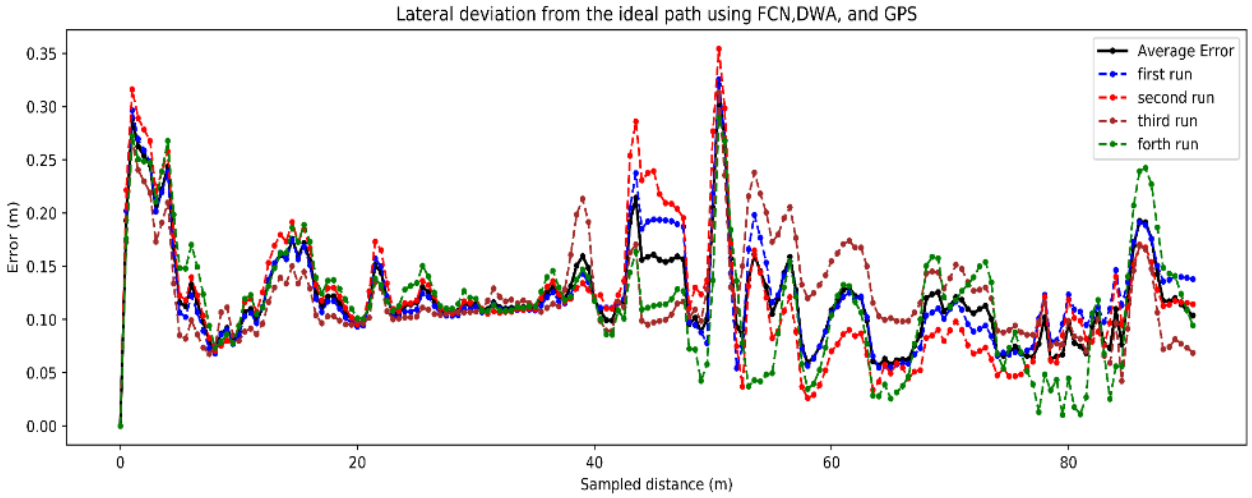

Figure 5.28. Lateral distance deviations by combining FCN, DWA, and GPS

Table 5.2. Autonomous navigation solutions comparison

Solution	Average lateral deviation (cm)
GPS and pure pursuit	8.3
Deep learning and DWA	4.8
GPS, deep learning, and DWA	12.1

5.5 **Conclusion**

Autonomous navigation in cotton fields using GPS and visual navigation techniques was successfully implemented and tested in a cotton field. In GPS navigation, a pure pursuit path tracking algorithm was used to follow pre-recorded GPS coordinates in the field. The solution was able to follow the path generated by the coordinates with an average lateral distance error of 8.3cm. In visual navigation a deep learning model, fully convolutional neural network for semantic segmentation model was trained to detect paths between cotton rows, then a local path planning algorithm, dynamic window approach (DWA) used the detected path to navigate the robot. The model achieved a pixel accuracy of 93.5%, F1 score of 87.8%, and 5 frames per second speed on an embedded computer used by the robot. Moreover, the detected paths were successfully mapped to the ground coordinates for robot navigation. When tested in the field, using dynamic window approach path planning technique, the solution was able to navigate the robot autonomously with an average lateral deviation of 4.8cm from the desired path. Leveraging the advantages of each solution, GPS with its global mapping ability, and visual navigation with its ability to detect paths in real-time and avoid obstacles, a combination of both solutions was implemented, with GPS used for global path planning to map the field, and visual navigation and DWA used for local path planning to navigate and make decisions in real-time. The combined

solution was able to follow the path with an average lateral distance deviation of 9.5cm when following the row, and 14.6cm when turning at the end of the row.

Combining GPS and visual navigation proved to be the desirable solution due to its ability to autonomously navigate the robot throughout the entire field using GPS mapping and the potential to avoid dynamic obstacles in real-time.

CHAPTER 6

AUTONOMOUS DIODE LASER WEEDING MOBILE ROBOT IN COTTON FIELD USING DEEP LEARNING, VISUAL SERVOING AND FINITE STATE MACHINE[4]

[4]Mwitta, C., Rains, G., and Prostko, E. To be submitted to *Frontiers in Robotics and AI*

6.1 **Abstract**

Small autonomous robotic platforms can be utilized in agricultural environments to target weeds in their early stages of growth and eliminate them. Autonomous solutions reduce the need for labor, cut costs, and enhance productivity. In order to eliminate the need for chemicals in weeding, and other solutions that can interfere with the crop's growth, lasers have emerged as a viable alternative. Lasers can precisely target weed stems, effectively eliminating or stunting their growth. In this study an autonomous robot that employs a diode laser for weed elimination was developed and its performance in removing weeds in a cotton field was evaluated. The robot utilized a combination of visual servoing for motion control, the Robotic operating system (ROS) finite state machine implementation (SMACH) to manage its states, actions, and transitions. Furthermore, the robot utilized deep learning for weed detection, as well as navigation when combined with GPS and dynamic window approach path planning algorithm. Employing its 2D cartesian arm, the robot positioned the laser diode attached to a rotating pan-and-tilt mechanism for precise weed targeting. In a cotton field, without weed tracking, the robot achieved an overall weed elimination rate of 47% in a single pass, with a 9.5 second cycle time per weed treatment when the laser diode was positioned parallel to the ground. When the diode was placed at a 10°downward angle from the horizontal axis, the robot achieved a 63% overall elimination rate on a single pass with 8 seconds cycle time per weed treatment. With the implementation of weed tracking using DeepSORT tracking algorithm, the robot achieved an overall weed elimination rate of 72.35% at 8 seconds cycle time per weed treatment. These results provide strong evidence of the feasibility of autonomous weed elimination using low-cost diode lasers and small robotic platforms.

6.2 **Introduction**

Weeding in agricultural fields can be a challenging and expensive task while also being a crucial predictor of productivity. Weeds can have detrimental effects on crop yield, causing heavy economic losses (Oerke, 2006; Pimentel et al., 2000), and in most cases, even higher losses than pathogens and invertebrate pests (Oerke, 2006).

Chemical weeding, manual weeding, and mechanical weeding have been the common practices for weed control in agricultural fields (Chauvel et al., 2012). Chemical weeding has been the most effective and most used weed control method (Buhler et al., 2000; Gianessi & Reigner, 2007). However, weeds have evolved resistance to many chemistries, posing a threat to productivity (Powles et al., 1996; Shaner, 2014). Moreover, there are concerns about the negative impacts of the chemicals on the environment (Colbach et al., 2010). Mechanical weeding approaches are not very efficient and can interfere with crop activities, potentially causing crop injury (Fogelberg & Gustavsson, 1999), while manual weeding is associated with high labor costs (Bastiaans et al., 2008; Schuster et al., 2007).

Weeding can be labor-intensive, necessitating the hiring and management of labor. As evidence shows, labor costs in agriculture are increasing rapidly due to labor shortages (Guthman, 2017; Richards, 2018; Zahniser et al., 2018). Without alternative methods that are less labor-reliant, the development of agriculture will fall short of demand. Thanks to technology, multiple potential solutions have been investigated and implemented including taking advantage of autonomous robots to deliver management tools. The affordability of artificial intelligence, computer processors and sensors has enabled the automation of various agricultural tasks, including weeding, planting, and harvesting (Oliveira et al., 2021).

Autonomous weeding in agricultural fields demands high precision in effectively identifying the weeds, navigating the robot, and removing the weeds. These tasks are made difficult by the outdoor nature of the agricultural environment, which is subject to constant changes in illumination, weather, uneven terrain, and occlusion. Various techniques have been employed in attempts to overcome these challenges. For example, (McCool et al., 2018) implemented mechanical and spraying mechanisms in their autonomous weed management robot, Agbot II, and utilized color segmentation in their weed detection. (Blasco et al., 2002) used machine vision algorithms to identify weeds and remove them with an electric discharge. Furthermore, (Pérez-Ruíz et al., 2014) introduced an autonomous mechanical weeding robot to remove intra-row weeds using movable hoes, utilizing odometry data and pre-programmed crop planting pattern, while (Florance Mary & Yogaraman, 2021) drilled the weeds to the ground with their autonomous robot that utilized deep learning computer algorithms for weed detection.

Most of these solutions have high potential for interfering with crop growth by disturbing the soil or injuring the crop. A more precise method of targeting and removing weeds is crucial for weed management efficiency. Laser technology has emerged as a potential solution for precise targeted elimination of weeds. Treating weeds with lasers has proved effective in eliminating them or stunting their growth (Heisel et al., 2001; Kaierle et al., 2013; Marx et al., 2012; Mathiassen et al., 2006; Mwitta et al., 2022). Narrow beams from lasers can remove both inter-row and intra-row with precision targeting.

The development of autonomous laser weeding robots is still a relatively new endeavor being studied. For example, (Xiong et al., 2017) developed a prototype of an autonomous laser weeding robot that utilized color-segmentation for weed identification, fast path-planning algorithms, and two laser pointers to target weeds in an indoor environment, achieving a hit rate

of 97%. However, there have been relatively few examples of applications in outdoor field environments.

In this study, we developed and tested an autonomous weeding Ackerman-steered robot with a 2-degrees of freedom Cartesian manipulator, stereo vision system, and a diode laser mounted on a pan-and-tilt mechanism. This research builds upon our previous study (Mwitta et al., 2022), which observed that inexpensive low-powered laser diodes can be used as a weed control mechanism, leading to portable inexpensive robotic platforms.

The study analyzes the robot's real-time weeding performance in a cotton field, as well as the control systems and decision-making processes involved.

6.3 **Materials and Methods**

6.3.1. The Platform Setup

The robot (see Figure 6.1) used in this study was an electric-powered 4-wheel Ackerman-steered rover with a 2D cartesian manipulator mounted on the front. The robot was developed to navigate between crop rows of 90 cm or more in agricultural fields. The robot had a length of 123 cm and width of 76 cm (without peripherals attached).

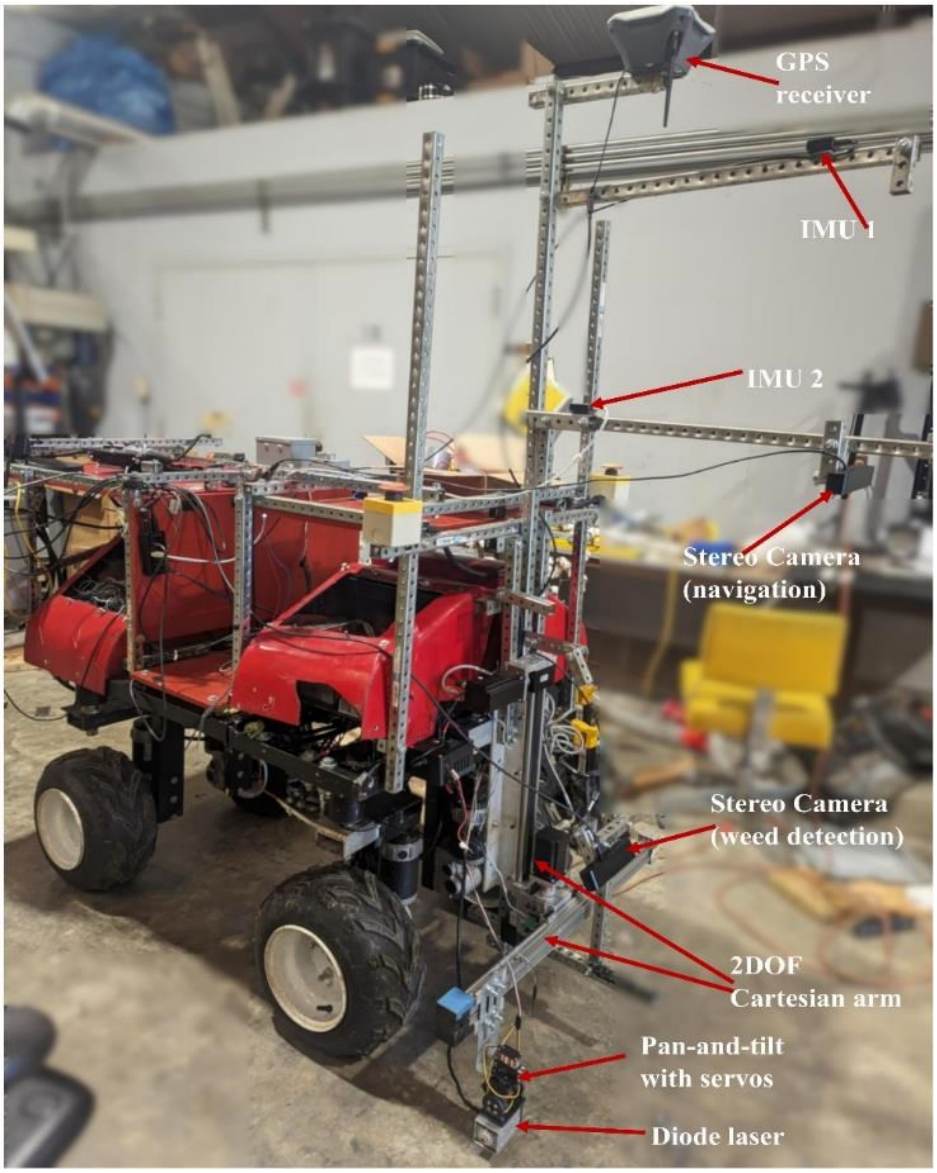

Figure 6.1. The robot platform for laser weeding

The robot had four main controllers (see contextual diagram; Figure 6.2) which controlled all the sensors and actuators mounted on the robot: A master controller for coordination of all robot activities, a rover controller for navigation, an arm controller for manipulation, and a laser controller for weed elimination.

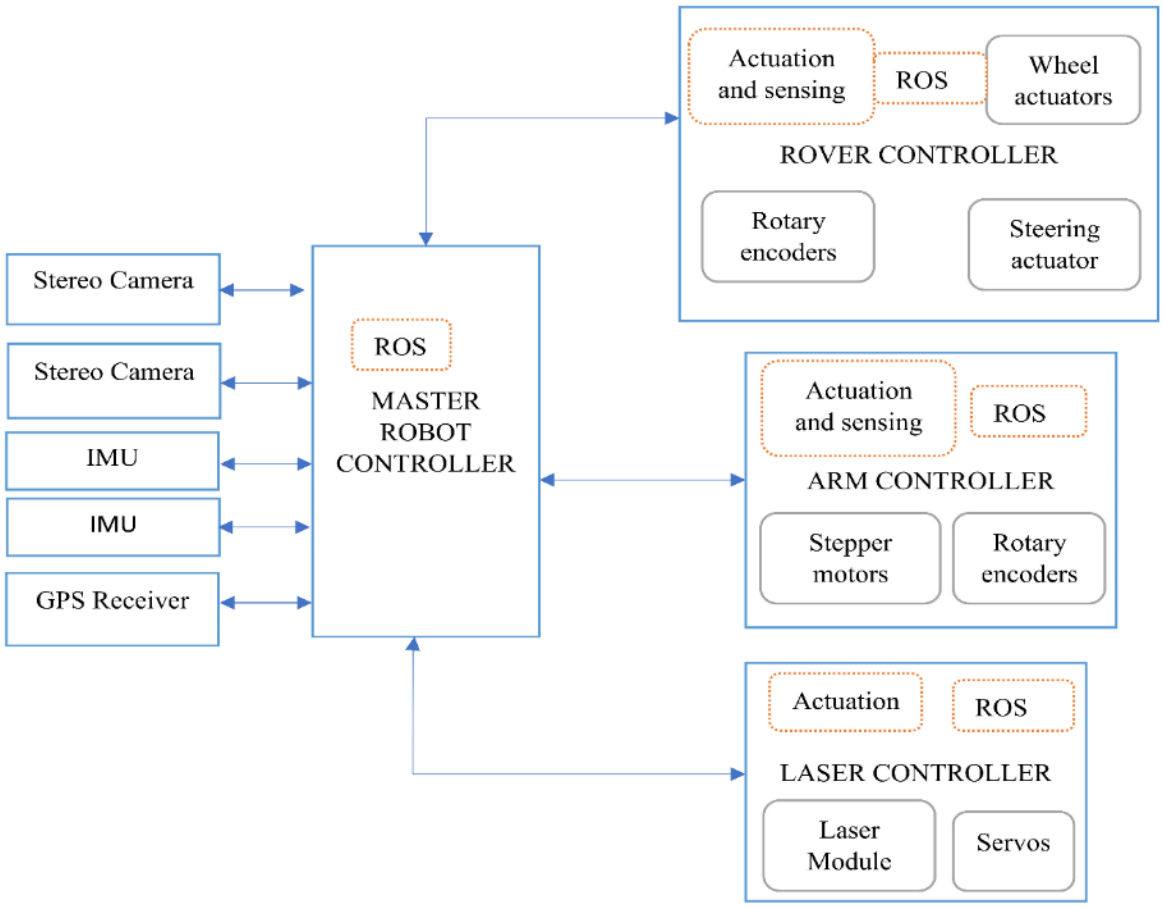

Figure 6.2. Contextual block diagram of the autonomous laser weeding robot

6.3.1.1. Master Robot Controller

An embedded computer (Nvidia Jetson Xavier AGX) was used as the central processor of the robot. Equipped with an 8-core ARM v8.2 64-bit CPU, 32GB of RAM, and a 512-core Volta GPU with tensor cores, this embedded computer delivered the needed performance, and enabled creation and deployment of end-to-end AI robotic applications while not demanding a lot of power (under 30W). The computer was responsible for all the autonomous operations, such as receiving and interpreting data from sensors like the stereo cameras, IMUs, and GPS, running deep learning models for weed detection, path planning and navigation between rows, and controlling the Arduino microcontrollers which were directly connected to relays and drivers for

sensors and actuators, by sending commands and receive sensors information. The information exchange between the computer and other modules was done using Robotic Operating System (Quigley et al., 2009) (ROS 1 - Noetic). The computer was powered by a 22000mAh 6-cell Tunigy LIPO battery.

A single-band EMLID Reach RS+ RTK GNSS receiver (see Figure 6.3 A) was mounted on the rover and connected to the embedded computer for robot's GPS position tracking, field mapping, and navigation.

To track the robot's orientation, two PhidgetSpatial Precision 3/3/3 high resolution inertia measurement units (IMUs) (Figure 6.3 B) were mounted on the robot. The IMUs contained a 3-axis accelerometer, 3-axis gyroscope, and 3-axis compass for precise estimation of robot's orientation.

A B

Figure 6.3. GPS receiver (A) and IMU (B) used in the platform

Two stereo cameras (Zed 2 and Zed 2i) from Stereo Labs, were mounted on the robot and connected to the embedded computer. Each of the stereo cameras featured two image sensors that allowed for the capture of normal RGB images, depth images, and 3D point clouds, facilitating 3D pixel depth estimation. Additionally, they were equipped with internal IMUs capable of tracking their orientations.

The Zed 2 camera was utilized for detecting paths between cotton rows, enabling visual navigation, while the Zed 2i camera was employed for weed detection in the field and the determination of their 3D locations relative to the camera. These cameras published ROS topics for RGB images and point cloud, to which the embedded computer subscribed. To obtain the 3D location of detected weed, the Zed ROS coordinate frames (see Figure 6.4) were utilized. The Zed 2i camera publishes a 3D point cloud that contained (x, y, z) values representing the center of the detected weed. Since the camera is mounted at an angle $\theta = 25^0$ from the vertical axis (see Figure 6.5), the position values published had been rotated on camera's y-axis. To obtain the actual perpendicular distances, the values needed to be rotated back (rotated $-\theta$ degrees by y-axis). The rotation matrix by y is given by:

$$R_y(-\theta) = \begin{bmatrix} \cos(-\theta) & 0 & \sin(-\theta) \\ 0 & 1 & 0 \\ -\sin(-\theta) & 0 & \cos(-\theta) \end{bmatrix}$$

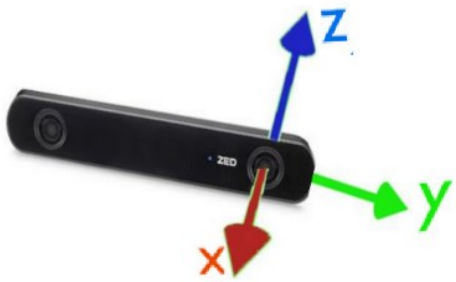

Figure 6.4. Zed camera ROS coordinate frames

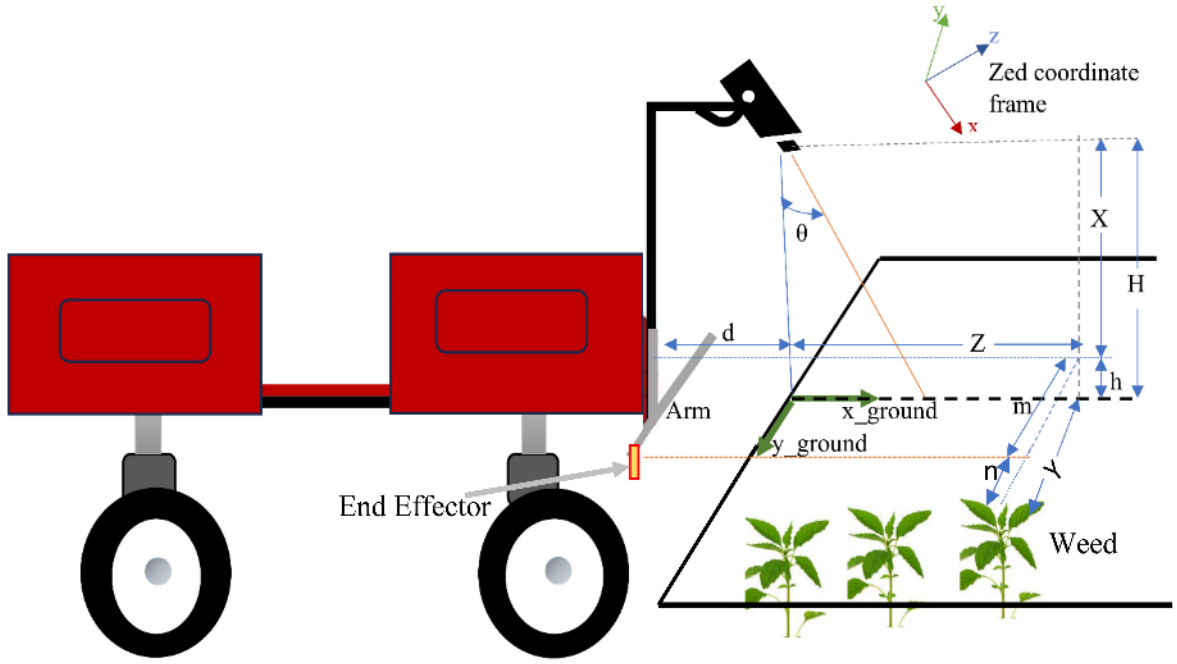

Figure 6.5. Camera setup on the rover

The distances (X, Y, Z) are given by:

$$\begin{bmatrix} X \\ Y \\ Z \end{bmatrix} = R_y(-\theta) \begin{bmatrix} x \\ y \\ z \end{bmatrix}$$

With rover to camera distance (d), camera to end-effector distance (m), and camera to ground height (H), all known, the important distances are calculated as follows:

$$Rover\ to\ weed\ distance = d + Z$$

$$End\ effector\ to\ weed\ (n) = Y - m$$

$$Weed\ height\ (h) = H - X$$

6.3.1.2.Rover Controller

An Arduino Mega microcontroller controlled the driving and steering of the robot. ROS was used to communicate with the embedded computer. Each of the robot wheels was run by a 250W Pride Mobility wheelchair motor with the two back wheels connected to Quadrature rotary encoders (CUI AMT 102), to provide feedback on wheel rotation. The motors were driven by

two Cytron MDDS30 motor controllers and powered by two 20000mAh 6-cell Tunigy LIPO batteries. A linear servo (HDA8-50) was connected to the front wheels for steering. The robot could also be manually controlled using an IRIS+ RC transmitter which communicated with an FrSky X8R receiver connected to the Arduino.

The robot used Ackerman steering geometry (see Figure 6.6) to track its position, orientation, and velocity.

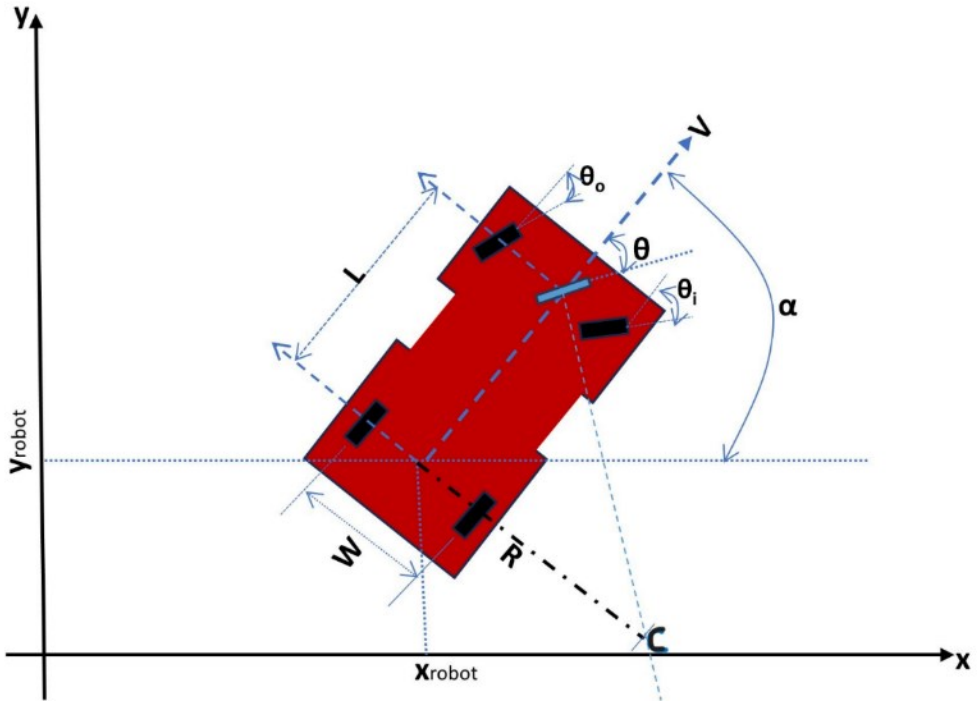

Figure 6.6. Ackerman steering geometry

With R, the turning radius of the robot, L the wheelbase, W the width of the robot, V the linear velocity of the robot, $\propto$ the heading, and θ ideal front wheel turning angle (θ_i, θ_o as inside and outside tire turn angle). The kinematics of the robot are described as below:

$$\tan(\theta_i) = \frac{2Ltan(\theta)}{2L - Wtan(\theta)}$$

$$\tan(\theta_o) = \frac{2Ltan(\theta)}{2L + Wtan(\theta)}$$

$$\dot{X}_{robot} = Vcos(\propto)$$

$$\dot{Y}_{robot} = Vsin(\propto)$$

$$\dot{\propto} = \frac{V}{L}\tan(\theta)$$

To maintain velocity on uneven agricultural terrain, the robot employed a PID (Proportional, Integral, and Derivative) controller (Ang et al., 2005; L. Wang, 2020). A PID controller continuously computes the difference between a desired setpoint value and a measured variable, subsequently applying corrections to the control value based on three pre-tuned gains: proportional, integral, and derivative. The PID controller was also used to move the robot to a specific position. For instance, when the position of the detected weed relative to the robot's end-effector was determined, the robot had to move a certain distance to align the end-effector with the weed for elimination. The PID controller made sure the robot didn't overshoot or undershoot the desired position. The feedback (measured value) was obtained from the fused wheel encoders.

The PID system calculates the motor command required by the robot to reach the desired target, whether it is velocity or position, using three gains: proportional gain K_p, integral gain K_i, and derivative gain K_d. Given the error $e(t)$ as the difference between the current value and the target value, the motor command $u(t)$ was calculated as follows:

$$u(t) = K_p e(t) + K_i \int_0^t e(\tau)\, d\tau + K_d \frac{de(t)}{dt}$$

The PID controller was tuned to find the values of the three gains (K_p, K_i, K_d) that achieved desired performance, by iteratively adjusting the gains while monitoring the step response of the rover.

Due to sensor noise, the accurate estimation of the robot's pose employs an extended Kalman filter (EKF) (Smith et al., 1962). The EKF is designed to fuse multiple noisy sensors, resulting in a precise estimate of the robot's pose. Considering, the robot's state (pose) at time t as x_t, a non-linear transition function denoted by f, process noise w_t (normally distributed), the measurement received from sensors at time t as z_t, a non-linear sensor model labelled as h, measurement noise v_t (normally distributed), and control u_t, the process and measurements can be described using two equations:

$$x_t = f(x_{t-1}, u_t) + w_t$$

$$z_t = h(x_t) + v_t$$

The EKF implementation fused continuous data from encoders, IMUs and GPS using the ROS package Robot_localization (Moore & Stouch, 2016). Robot_localization package accepts data including position, linear velocity, angular velocity, linear acceleration, and angular acceleration from sensors, and then estimates robot's pose and velocity. It utilizes two ROS nodes: a state estimation node EKF_localization_node and a sensor processing node NavSat_Transform node (see Figure 6.7). These nodes work together to fuse the sensor data and publish an accurate estimate of the robot's pose and velocity.

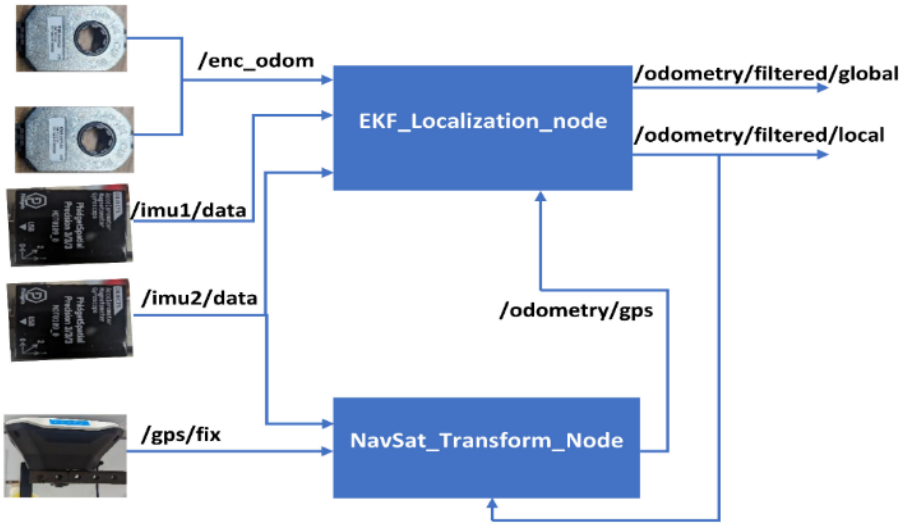

Figure 6.7. Fusing sensor data with Robot_localization ROS package

Using ROS, the rover controller published the position and velocity topics and subscribed to motor command topics from the master controller.

6.3.1.3.Arm Controller

The robotic manipulator was a 2D cartesian system consisting of two Igus drylin® belt drive cantilever axis rails (ZAW-1040 horizontally oriented, and ZLW-1040 vertically oriented), driven by two Igus drylin® NEMA 17 stepper motors. These motors were controlled by two SureStep STP-DRV-6575 stepper drivers and featured internal rotary encoders to track the position of the rails. The arm was controlled by an Arduino Mega microcontroller which communicated with the embedded computer using ROS. The arm controller published the arm position topic, to which the master controller subscribed. It also subscribed to the arm control topic from the master controller, receiving commands to move to a specific target position.

The manipulator could move left, right, up, and down, with each axis controlled by its respective PID controller. However, the manipulator's movement was constrained by the arm kinematics, allowing translation in two axes only.

For visual servoing, the robot utilized the inverse kinematics of both the arm and rover. Solving the inverse kinematics problem for the robot involved accounting for both the arm movement (X, Y) and the rover movement (Z). Consequently, given the (*xw, yw, zw*) coordinates of the weed obtained from the stereo camera, the robot had to move a distance of (X, Y, Z) to reach the weed (see Figure 6.8).

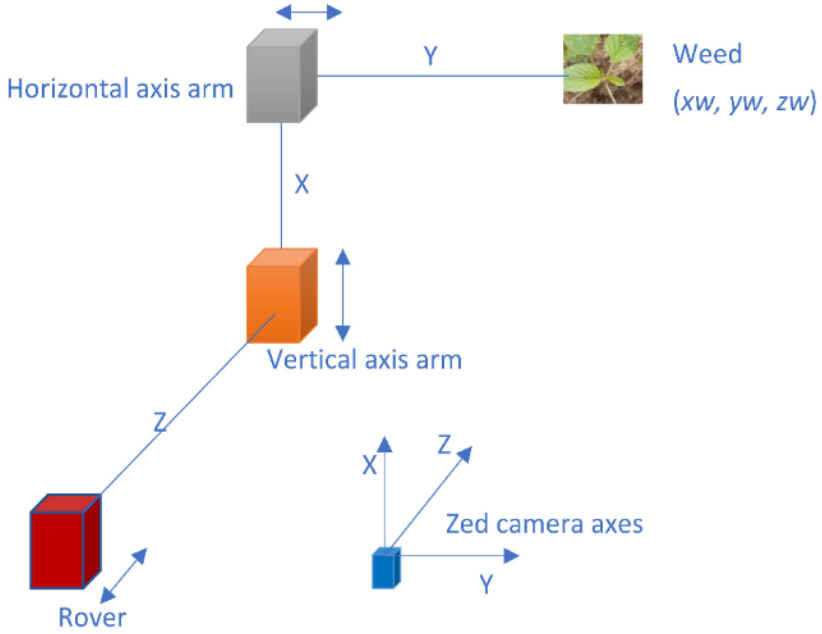

Figure 6.8. Inverse kinematics of the robot

6.3.1.4.Laser Controller

An Arduino Uno was responsible for controlling the release of laser beam from a diode laser. The diode laser was attached to a pan-and-tilt unit, which was controlled by two HSB-9380TH brushless servos, allowing it to rotate to different orientations (see Figure 6.9). The Arduino communicated with the computer through ROS.

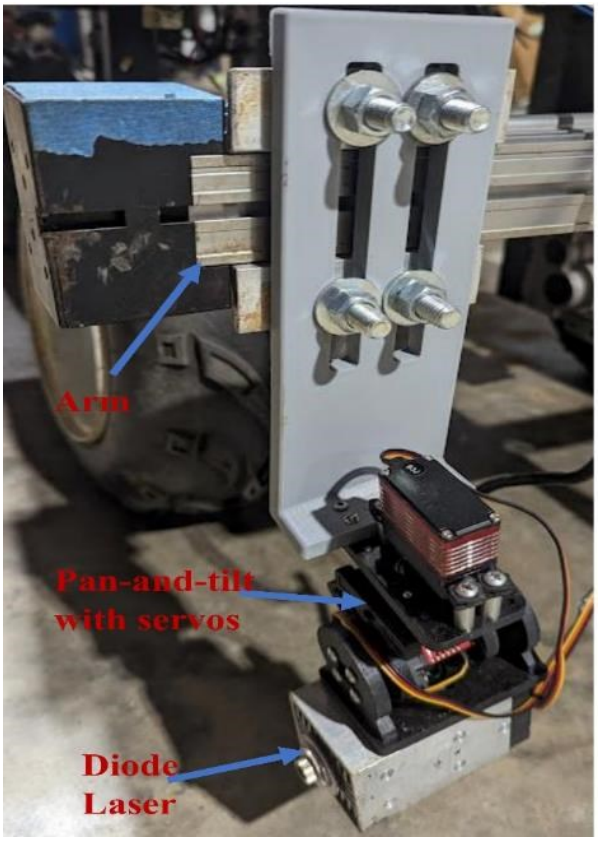

Figure 6.9. Laser module attached to the arm

Due to the challenge of precisely targeting the weed stem, the servos would dither the diode dither back-and-forth at a speed of 10 times per second at an angle of approximately 10°. This motion increased the cross-section area of the laser beam and maximized the laser beam's contact with the weed stem (see Figure 6.10). The beam formed about 1cm cross-section at the weed stem approximately 3mm above the ground.

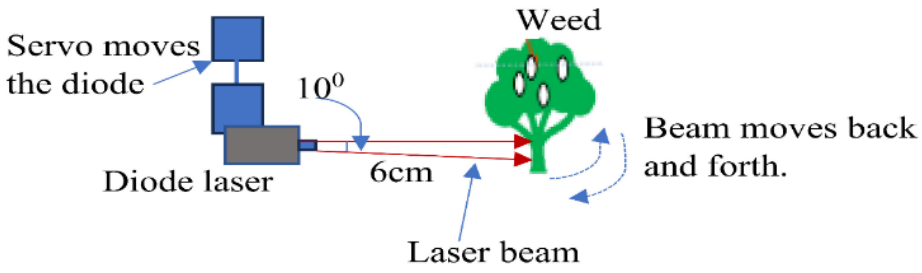

Figure 6.10. Dithering mechanism of the diode laser

6.3.2. Weed Detection using YOLOv4-tiny

YOLOv4-tiny detection model was trained and utilized for detecting Palmer Amaranth (Amaranthus palmeri) weed species in the cotton field. YOLOv4-tiny is a lightweight, compressed version of YOLOv4 (Bochkovskiy et al., 2020), designed with a simpler network structure and reduced parameters to make it ideal for deployment on mobile and embedded devices. Since the robot was powered by an embedded computer, a lighter network was necessary to ensure faster inference times. Additionally, performance test on weed detection demonstrated that YOLOv4-tiny was only approximately 4.7% less precise than YOLOv4. However, it offered significantly faster inference, achieving 52 frames per second (fps) on the embedded computer (see Table 6.1)

Table 6.1. Comparisons between YOLOv4-tiny and YOLOv4 weed detection performance.

Metric	**YOLOv4-tiny**	**YOLOv4**
Precision	0.81	0.95
Recall	0.88	0.89
mAP @IoU=0.5	0.89	0.93
Inference on Jetson Xavier AGX (ms)	24.5	80
FPS on Jetson Xavier AGX	52	14

Images from the left lens of Zed 2i stereo camera were passed to YOLOv4-tiny model for detecting palmer amaranth weeds. The model performed well in detecting the weeds (see Figure 6.11), even when there were shadows (as shown in Figure 6.12). However, the model faced challenges in direct sunlight, resulting in excessive reflections and significant shadows (as seen

in Figure 6.13). This issue was more prevalent during the afternoons one hour after solar zenith and approximately 3 hours before sunset.

Figure 6.11. Palmer amaranth weed detection in the cotton field

Figure 6.12. Detecting weeds in presence of shadows

Figure 6.13. Sunlight brightness and shadows hindering weed detection

6.3.3. Navigation in Cotton Fields

The robot employed a combination of GPS and visual navigation to navigate between the rows of cotton.

A fully convolutional neural network (FCN) for semantic segmentation model (Long et al., 2015) was trained to detect paths between cotton rows in the field. The model achieved a pixel accuracy of 93.5% on the testing dataset. The detected path between the cotton rows was then mapped from the image domain to the ground plane to obtain the points on the ground that the robot could traverse (see Figure 6.14)

Figure 6.14. Path detected between cotton rows and mapped to the ground plane

GPS was employed as a global planner to map the entire field and acquire pre-recorded coordinates of the path that the robot should follow (as seen in Figure 6.15).

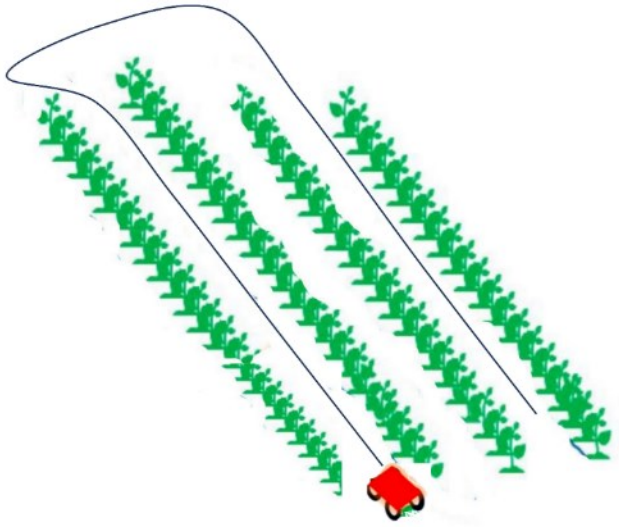

Figure 6.15. The robot's movement pattern in the field

A local path planner, the Dynamic Window Approach (DWA) (Fox et al., 1997), was used to navigate between the rows and avoid running over crops based on the path detected by FCN. The DWA algorithm aims to find the optimal collision-free velocities for the robot's navigation, taking the robot's kinematics into account. The ground coordinates of the detected

path boundaries were sampled and treated as obstacles in the DWA algorithm (see Figure 6.16 and Figure 6.17)

Figure 6.16. Path between cotton rows detected by FCN

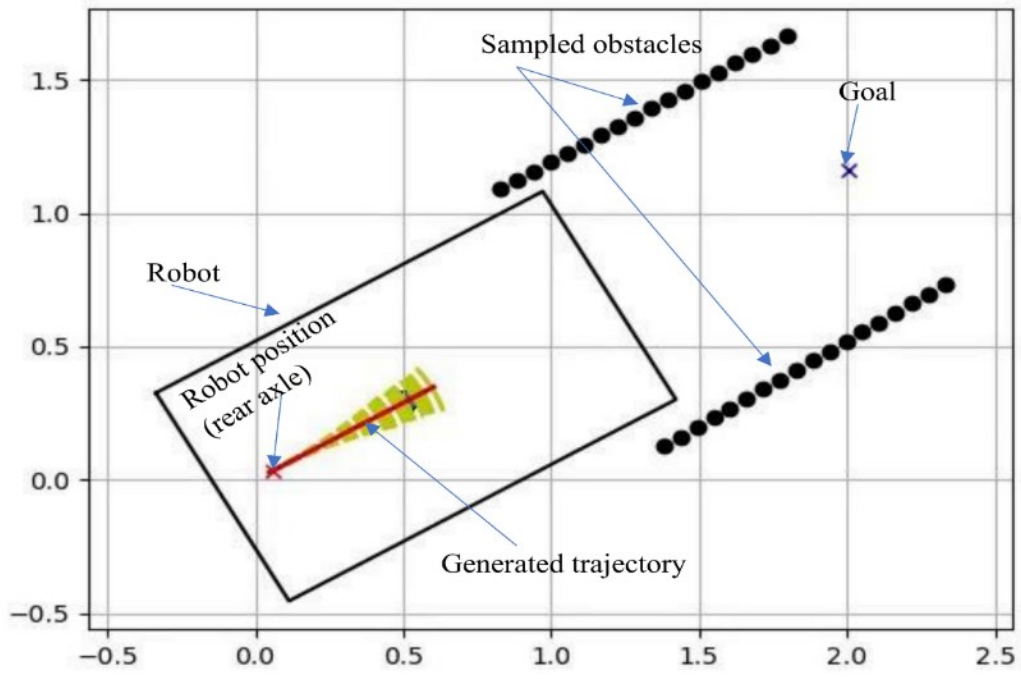

Figure 6.17. Sampled path boundaries treated as obstacles by the DWA algorithm

In summary, the robot attempted to follow the global GPS map of pre-recorded GPS coordinates while simultaneously avoiding obstacles, represented by the path boundaries from FCN model-detected path, using the DWA algorithm. During field testing, this approach navigated the robot with an average lateral distance error of 12.1 cm between the desired path and the robot's actual path.

6.3.4. Overall Robot Control with Finite State Machine

To model the order of task execution and the flow of information between the robot controllers, the master controller (embedded computer) utilized ROS python library SMACH to create a Finite State Machine (FSM). An FSM is used to model logic and can be in a specific state from a finite set of possible states at any given point. Furthermore, it can transition to another state by accepting input and producing output.

The autonomous weeding robot tasks were modeled into seven states (actions), with eight transitions from one state to another (see Figure 6.18). The states were built in a task-level architecture, allowing the robotic system to transition smoothly from one state to another.

The system begins at the entry state ("get image"), if the system fails to obtain an image from Zed 2i camera, it exits. Otherwise, the weed detection model searches for weeds in the image. If no weed is detected, the system continues navigating between the rows while attempting to acquire another image and run the weed detection program. When a weed is detected, the system obtains the 3D coordinates (*x, y, z*) of the weed relative to the camera and calculates the forward distance from the rover to the weed, as well as the lateral distance of the weed relative to the laser module attached on the arm. The rover then moves to the weed and orients the arm with the weed. Subsequently, the arm moves laterally to within 6cm from the weed. At this point, the system emits a laser beam for a defined duration while the servos

oscillate to increase the contact area with the weed stem. The arm then returns to its initial position to avoid colliding with cotton in the rows during movement. Then FSM transitions back to the beginning state to start all over.

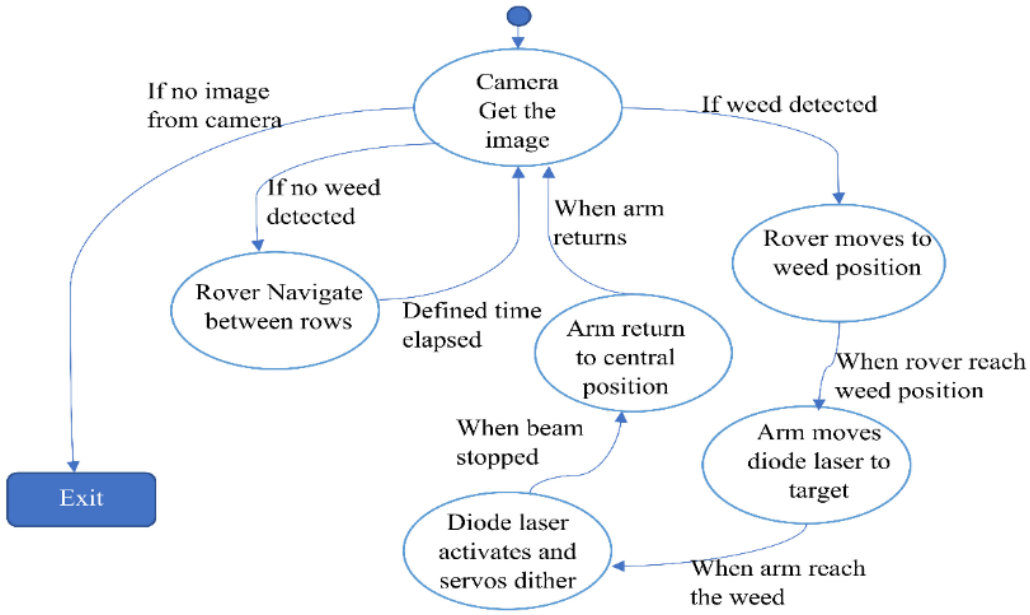

Figure 6.18. Finite State Machine of the laser weeding robot

6.3.5. Real-time Tracking of Weeds using DeepSORT Algorithm

Relying solely on the PID system to align the robot with the weed position has the drawback of occasional overshooting or undershooting the desired position. While the dithering of the pan-and-tilt mechanism mitigates part of this problem by increasing the cross-section area of the beam, the unevenness of the agricultural environment can lead the PID system to miss the target by a greater margin than dithering can compensate for. To address this issue, tracking the detected weeds across subsequent frames increases the likelihood of accurately targeting the weed with a laser beam. This is achieved by using the servos on the pan-and-tilt mechanism to point the laser in the direction of the closest weed. Even if the PID system overshoots or undershoots the position, tracking provides the final position of the target relative to the diode's

position. The servos then compensate for any error by directing the diode laser towards the targeted weed.

DeepSORT (Wojke et al., 2018), an evolution of the SORT (Simple Online and Realtime Tracking) algorithm (Bewley et al., 2016), enhances object tracking by incorporating a deep learning metric as an appearance descriptor to extract features from images. SORT is a multi-object tracking algorithm that links objects from one frame to another using detections from object detection model, Kalman Filter (Kalman, 1960) for predicting object movements, a data association algorithm (Hungarian algorithm (Kuhn, 1955)) for associating tracks with detected objects, and a distance metric (Mahalanobis distance) for quantifying the association. DeepSORT introduces the appearance feature vector, which accounts for object appearances and offsets some of the Kalman filter's limitations in tracking occluded objects or objects viewed from different viewpoints.

The feature descriptor needs a feature extractor, which is a deep learning model that can classify and match features of the objects that are tracked. In this study, a Siamese neural network (Koch et al., 2015) was used as a feature extractor. Siamese networks are renowned for their proficiency in feature matching, by ranking similarities between inputs using a convolutional architecture. The Siamese network model was trained on a dataset of palmer amaranth weed species to learn their features, achieving an accuracy of 89% when evaluated on testing dataset.

DeepSORT performed effectively in conjunction with YOLOv4-tiny as the object detector, assigning ID to every weed detected (see Figure 6.19). It attempted to track and maintain the same ID for each weed in subsequent frames. When tested with videos collected by the rover in the field, DeepSORT achieved a Multiple Object Tracking Accuracy (MOTA) of

69.8%. By observing each frame t in a series of frames, with FN representing false negatives, FP representing false positives, IDS denoting ID switches, and GT signifying the ground truth object count, the $MOTA$ is calculated by the following formula:

$$MOTA = 1 - \frac{\sum_t FN_t + FP_t + IDS_t}{\sum_t GT_t}$$

Figure 6.19. ID assigned to detected weeds by the DeepSORT tracking algorithm

Despite the strong performance of the DeepSORT algorithm, challenges persisted, including issues with ID switching and missed detections in the field. Addressing these challenges calls for further training and parameter tuning to enhance the algorithm's robustness and reliability.

6.3.6. Experiments

To evaluate the effectiveness of the autonomous laser weeding robot, three main experiments were conducted in University of Georgia Tifton campus cotton fields located at (31°28'N 83°31'W). In the first two experiments, around 20 Palmer amaranth plants per plot were transplanted in five 30-feet plots (as illustrated in Figure 6.20). For the third experiment,

around 10 Palmer amaranth plants were transplanted per plot in five 15-feet plots. This reduction in weed density was due to the experiment being conducted later in the growing season.

The weeds used in the experiments were collected from the University of Georgia research fields near Ty Ty, GA (31.509730N, 83.655880W) between one to two weeks after emergence. The laser treatments were administered by the robot in 4 plots, while the fifth plot was left as a control. The autonomous rover navigated between the cotton rows, attempting to detect weeds in real-time and treating them with laser beam. After treatments, the weeds were observed for a week. A 5W 450nm diode laser (measured 5cm from the laser lens using a Gentec Pronto-50-W5 portable laser power meter.) was employed for the treatments. The laser was equipped with a G7 lens and was powered by a 2200mAh LiPo battery and a constant current source of 4A and a voltage of 12V. The robot positioned the laser diode approximately 6mm distance from the weed stem before releasing the beam, which made the beam width approximately 4mm at the weed stem.

The laser treatment duration was 2 seconds, resulting in a dosage of 10 Joules (2s*5W). This was selected to maximize the weed elimination potential based on the results from our previous study (Mwitta et al., 2022), that showed 100% laser effectiveness at approximately 10 Joules regardless of the diameter of the weed stem (at early stages of growth).

Figure 6.20. Palmer amaranth plants transplanted in cotton field

6.3.6.1.First Experiment

In the first experiment, the laser module was attached to the arm, positioned parallel to the ground (see Figure 6.21). However, due to the distance from bottom of the laser module and the laser mouth, which was approximately 3cm, the laser module needed to be in contact with the ground for the beam to hit the weed stem, unless the weed exceeded a height of about 4cm. Consequently, during navigation, the arm was raised, and it was lowered when treating the weed to prevent the module from scraping against the ground. The laser treatment duration for each weed was set at 2 seconds. The rover moved at a speed of 0.5 mph, and the robot used a PID controller to reach the target position after detecting the weed.

Figure 6.21. Diode laser setup parallel to the ground

6.3.6.2.Second Experiment

The second experiment closely resembled the first one, but the laser module was placed at an angle of 10° downward from the horizontal axis (see Figure 6.22). This adjustment reduced the arm's up and down movements, thereby increasing the likelihood of targeting even shorter weeds effectively and reducing cycle time between weeds. The laser beam also terminated at the ground, increasing safety from stray laser.

Figure 6.22. The laser module attachment at an angle, and the laser module attached to it

6.3.6.3.Third Experiment

In the third experiment, DeepSORT tracking was implemented to track the weeds as the robot moved towards the target. The laser configuration remained the same as in the second experiment. Preliminary experiments were conducted in a controlled indoor environment using 15 weeds, to check how tracking influenced the targeting of weeds. Then, the robot was tested in the cotton field.

6.3.7. Evaluation Metrics

Several metrics were used to evaluate the effectiveness of the robot in targeting and killing weeds. The accuracy metrics included:

- Total number of detections: All the detections reported by the model.
- True positives: All the detections that were correct.
- False positives: All the detections reported by the model as the targeted weed but were not the targeted weed.
- Laser beam hits: The total number of weeds that the robot attempted to hit and succeeded in hitting them with the laser beam.
- Laser beam misses: The total number of weeds that the robot attempted to hit with the laser beam but missed.
- Hit and killed: The number of weeds which were hit by the laser beam and killed.
- Hit and survived: The number of weeds which were hit by the laser beam but survived.
- Percentage killed after hit: The percentage of the weeds killed out of all that were hit by the laser beam.
- Percentage of weeds killed in the plot: The percentage of weeds killed out of all the weeds in the plot.

The speed of operation was measured by the total treatment cycle, which was the total time per single treatment in the worst-case scenario.

6.4 **Results and Discussion**

6.4.1 Experiment 1

Table 6.2 shows the results for the first experiment in the field. The biggest challenge was aiming on target (see Figure 6.23 and Figure 6.24 on laser aiming), about 34% of all laser treatments were a miss because of either the weed being shorter than the minimum height, or rover overshooting/undershooting the position due to imperfect sensors (camera, wheel encoders), or a combination of both (The hit rate was 66%). The detection model had a precision of 84%, most of the false positives were due to some other plants in the row resembling Palmer amaranth, and the detection misses were due to inconsistencies of illumination in the outside environment. This was minimized by performing the experiments in the morning hours before solar zenith. The laser treatment performed well when the weed was hit, with 87% of the treated weeds killed, but the overall kill rate on a single pass was reduced to 47% due to misses in detection and aiming.

The robot achieved a total treatment cycle time of 9.5 seconds per weed treatment. The time distribution per task is shown on Table 6.3

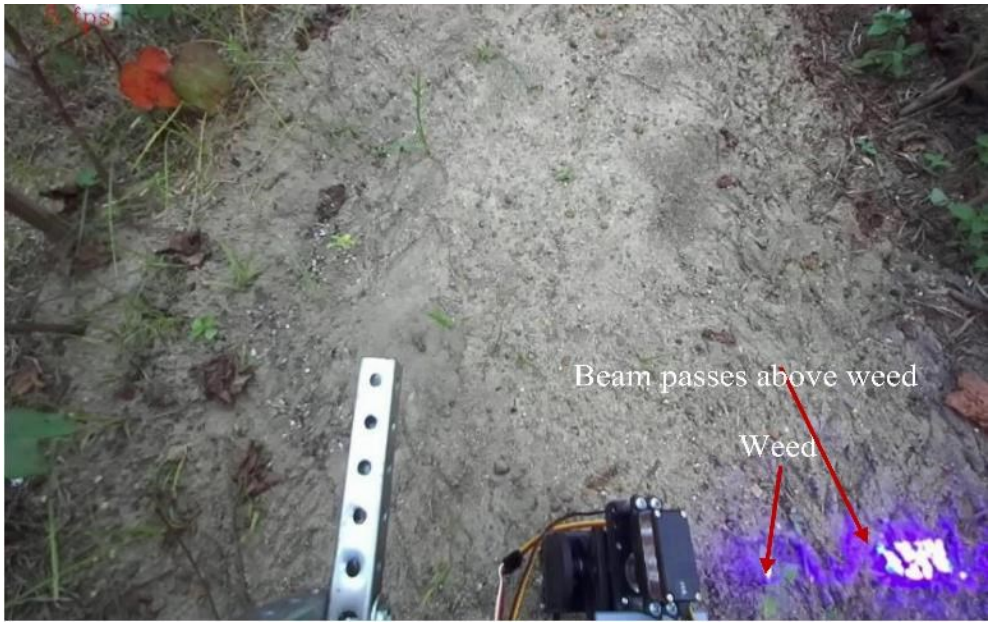

Figure 6.23. Laser beam turned on and slightly misses the weed stem

Figure 6.24. Top view of laser module targeting a weed

Table 6.2. Treatment results for the first experiment

Plot No.	Number of weeds	Total number of detections	True Positives	False positives	Laser beam hits	Laser beam misses	Hit and killed	Hit and survived	Percentage Killed after hit	Percentage of weeds killed in the plot
1	21	23	18	5	12	6	10	2	83.33	47.6
2	20	19	16	3	9	5	9	0	100	45
3	23	21	20	1	13	7	10	3	76.92	43.47
4	25	25	20	5	15	5	13	2	86.66	52

Table 6.3. Time distribution per task for the first experiment

Action	Maximum time spent (s)
Weed detection	Real-time
Rover moves to target	3
Arm moves to target	3
Laser treatment	2
Arm retract	1.5
Total treatment cycle	9.5

6.4.2 Experiment 2

From Table 6.4, the detection precision was increased to 91% due to retraining the model with additional images from the first experiment. Only about 19% of detected weeds were missed by the laser with an 81% hit rate. The kill percentage for the treated weeds was about the same (88%), but the overall kill rate on a single pass increased to 63%.

The total treatment cycle time was reduced to 8 seconds (see Table 6.5) due to reduced arm movements with the configuration in Figure 6.25.

Figure 6.25. Laser configuration on rover for second experiment

Table 6.4. Treatment results for second experiment

Plot No.	Number of weeds	Total number of detections	True Positives	False positives	Laser beam hits	Laser beam miss	Hit and killed	Hit and survived	Percentage Killed after hit	Percentage of weeds killed in the plot
1	23	22	21	1	18	3	16	2	88.88	69.57
2	22	22	19	3	14	5	12	2	85.71	54.54
3	26	24	22	2	17	5	14	3	82.35	53.80
4	19	19	17	2	15	2	14	1	93.33	73.68

Table 6.5. Time distribution per task in second experiment

Action	Maximum time spent (s)
Weed detection	Real-time
Rover moves to target	3
Arm moves to target	2
Laser treatment	2
Arm retract	1
Total treatment cycle	8

6.4.3 Experiment 3

The preliminary experiments in a controlled environment achieved a 93% hit rate through tracking (see Figure 6.26), and the servos rotating the diode to point in the direction of the weed (see Figure 6.27) even when the PID system overshoot/undershot the position.

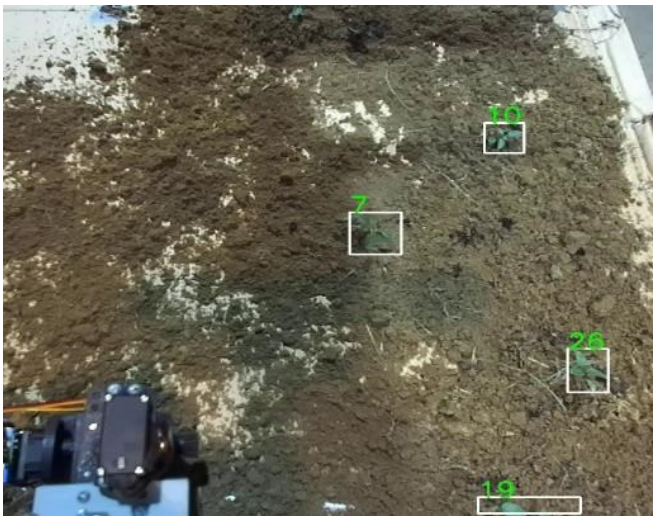

Figure 6.26. Tracking assigning IDs to the weeds

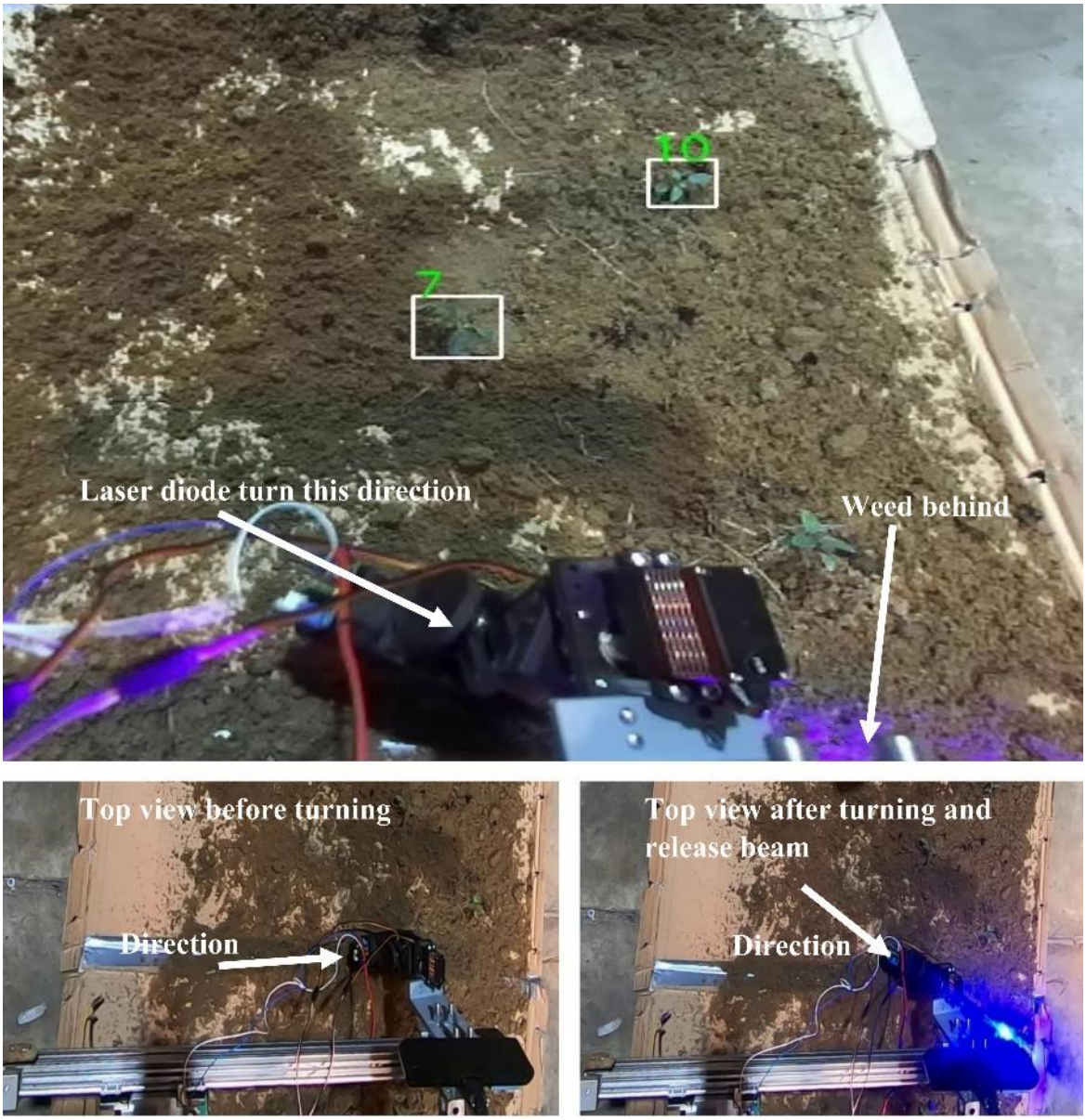

Figure 6.27. Servos rotate the diode laser to compensate the robot overshooting weed position

In the cotton field, as shown in Table 6.6, the hit rate was increased through tracking to 83.7%, and the overall kill rate for a single pass was significantly increased to 72.35%. The treatment cycle time remained the same as in experiment 2, see Table 6.7

Table 6.6. Treatment results for third experiment

Plot No.	Number of weeds	Total number of detections	True Positives	False positives	Laser beam hits	Laser beam miss	Hit and killed	Hit and survived	Percentage Killed after hit	Percentage of weeds killed in the plot
1	11	12	10	1	8	2	8	0	100	72.7
2	9	8	8	0	7	1	6	1	85.71	66.7
3	10	12	10	2	9	1	8	1	88.9	80.0
4	10	13	9	3	7	2	7	0	100	70.0

Table 6.7. Time distribution per task in the third experiment

Action	Maximum time spent (s)
Weed detection and tracking	Real-time
Rover moves to target	3
Arm moves to target	2
Laser treatment	2
Arm retract	1
Total treatment cycle	8

There was still more than 30% ID switching which proved to be a challenge for the tracking algorithm. In future studies, the model will need to be trained more on the field data obtained from the experiments in addition to tuning of parameters to reduce the ID switching problem.

6.5 **Conclusion**

In this study, an autonomous diode laser weeding robot was developed and tested in a cotton field. The robot used was an Ackerman-steering ground rover with a 2D cartesian arm that carried a diode laser attached to a pan-and-tilt mechanism to target Palmer amaranth stems for elimination. Real-time weed detection using YOLOv4-tiny model was employed to detect weeds. The position of the detected weed was determined by the point cloud from Zed 2i stereo camera. The robot used GPS, FCN for semantic segmentation and DWA path planning algorithm to navigate between cotton rows.

Without weed tracking in the field, the robot achieved a hit rate of 66% and 47% overall weed kill rate on a single pass at 9.5 second cycle time per weed treatment when the laser diode was positioned parallel to the ground. A hit rate of 81% with 63% overall kill rate on a single pass at 8 seconds cycle time per weed treatment was achieved when the diode was placed at a 10° downward angle. Using DeepSORT weed tracking tracking algorithm, a preliminary investigation in a controlled environment showed a hit rate of 93%, however, when tested in the field, the robot achieved a hit rate of 83.7% with an overall kill rate of 72.4% at 8 seconds cycle time per weed treatment.

The aim of the study was to develop an affordable system that can be deployed in the field multiple times throughout the season and target weeds at early stages of growth without using chemicals and invasive methods. Despite some minor shortcomings, this platform proves

the viability of the concept. Some shortcomings can be alleviated with multiple passes to increase the kill rate. Furthermore, the rover was moving at a slow speed of 0.5 mph to give the system more time to react and decrease the motion blur to the cameras. The speed and cycle time can be increased in future research with an improved detection model and tracking solution to align the manipulator and the weed precisely.

CHAPTER 7

CONCLUSIONS, LIMITATIONS AND FUTURE WORK

7.1 **Conclusions**

The autonomous diode laser weeding robot was successfully demonstrated in this dissertation. The robot can effectively navigate between cotton rows, detecting weeds, localizing, and eliminating the weeds with laser beam. This is among the first robot of its kind to be developed and tested in an agricultural field. Satisfactory performance in the field was observed, however, the treatment cycle of 8 second per weed is relatively slow. In its current state, the system and methodologies can be used in the field and as a tool for weed control research.

7.2 **Limitations**

A few limitations for the systems and methodologies were observed. These were as follows:

1. The steering system using a linear actuator had a slow response, making navigation control difficult.
2. The stereo camera images for weed detection and navigation were satisfactory only when the robot was moving approximately 0.5mph.
3. The cartesian arm was relatively slow (approximately 14cm/s), contributing to the slow treatment cycle.
4. The embedded computer struggled when running a combination of different programs at the same time, for example navigation, detection, and tracking. This delayed robot's response to control commands and data from sensors.

5. Under bright direct sunlight and shadows, the stereo cameras were not effective.
6. The diode laser powers used required an extended laser treatment time (dosage) for effective weed elimination.

7.3 Future Work

This dissertation's experimental results proved the viability of using inexpensive low-powered diode lasers on an autonomous robot for weed elimination. The developed systems and algorithms for robot control, weed detection, navigation, tracking, and laser treatment can be improved by collecting more data, more training and testing of models, and utilizing new emerging technologies in robotics and Artificial Intelligence especially in the self-driving car industry. Due to limitations in time and scope of this dissertation, detailed information on future studies is listed as follows:

1. Experimenting with multiple passes of the robot in the field to make sure the weeds are eliminated. This will be more viable when the treatment cycle time is improved.
2. Collecting more extensive data representing the periods when the machine learning algorithms struggled to detect weeds such as when weeds are in direct sunlight during the middle of the day and then training models on the collected data to improve the algorithms detection performance.
3. Exploring 3D point clouds for path detection and navigation
4. Developing obstacle avoidance system to avoid collisions when the robot is navigating autonomously.
5. Conducting more experiments to validate the developed system under different field conditions and with different weed species.

6. Developing a multi-pronged robotic system with multiple end-effectors that decide what elimination method to use based on detected weed species known characteristics and location along the rows.
7. Developing a weed mapping system that can map weed locations and type in the field prior to treatment.
8. As the $/W of laser diodes decreases, more powerful laser diodes should be tested to minimize required treatment time.
9. Developing a method that decides on the amount of dosage (Joules) to treat the weed based on weed size.

REFERENCES

Abadi, M., Barham, P., Chen, J., Chen, Z., Davis, A., Dean, J., Devin, M., Ghemawat, S., Irving, G., Isard, M., Kudlur, M., Levenberg, J., Monga, R., Moore, S., Murray, D. G., Steiner, B., Tucker, P., Vasudevan, V., Warden, P., … Zheng, X. (2016). TensorFlow: A system for large-scale machine learning. *Proceedings of the 12th USENIX Symposium on Operating Systems Design and Implementation, OSDI 2016*.

Adhikari, S. P., Kim, G., & Kim, H. (2020). Deep neural network-based system for autonomous navigation in paddy field. *IEEE Access*, *8*. https://doi.org/10.1109/ACCESS.2020.2987642

Aghi, D., Mazzia, V., & Chiaberge, M. (2020). Local motion planner for autonomous navigation in vineyards with a RGB-D camera-based algorithm and deep learning synergy. *Machines*, *8*(2). https://doi.org/10.3390/MACHINES8020027

Ahlgren, S. (2004). Environmental impact of chemical and mechanical weed control in agriculture - a comparing study using Life Cycle Assessment (LCA) methodology. In *SIK-rapport* (Vol. 719, Issue 719). SIK Institutet för livsmedel och bioteknik. http://ri.diva-portal.org/smash/get/diva2:942850/FULLTEXT01.pdf

Allmendinger, A., Spaeth, M., Saile, M., Peteinatos, G. G., & Gerhards, R. (2022). Precision Chemical Weed Management Strategies: A Review and a Design of a New CNN-Based Modular Spot Sprayer. In *Agronomy* (Vol. 12, Issue 7). https://doi.org/10.3390/agronomy12071620

Andreasen, C., Scholle, K., & Saberi, M. (2022). Laser Weeding With Small Autonomous Vehicles: Friends or Foes? *Frontiers in Agronomy*, *4*, 12. https://doi.org/10.3389/fagro.2022.841086

Andy Bunn, M. K. (2017). A language and environment for statistical computing. *R Foundation for Statistical Computing*, *10*(1), 11–18. http://www.gnu.org/copyleft/gpl.html.%0Ahttp://www.r-project.org/%0Ahttp://www.r-project.org

Ang, K. H., Chong, G., & Li, Y. (2005). PID control system analysis, design, and technology. *IEEE Transactions on Control Systems Technology*, *13*(4). https://doi.org/10.1109/TCST.2005.847331

Aravind, R., Daman, M., & Kariyappa, B. S. (2016). Design and development of automatic weed detection and smart herbicide sprayer robot. *2015 IEEE Recent Advances in Intelligent Computational Systems, RAICS 2015*. https://doi.org/10.1109/RAICS.2015.7488424

Asad, M. H., & Bais, A. (2020). Weed detection in canola fields using maximum likelihood classification and deep convolutional neural network. *Information Processing in Agriculture*, *7*(4). https://doi.org/10.1016/j.inpa.2019.12.002

Bachmann, F. (2003). Industrial applications of high power diode lasers in materials processing. *Applied Surface Science*, *208–209*(1), 125–136. https://doi.org/10.1016/S0169-4332(02)01349-1

Backman, J., Oksanen, T., & Visala, A. (2012). Navigation system for agricultural machines: Nonlinear Model Predictive path tracking. *Computers and Electronics in Agriculture*, *82*. https://doi.org/10.1016/j.compag.2011.12.009

Bah, M. D., Hafiane, A., & Canals, R. (2020). CRowNet: Deep Network for Crop Row Detection in UAV Images. *IEEE Access*, *8*. https://doi.org/10.1109/ACCESS.2019.2960873

Bakker, T., Asselt, K., Bontsema, J., Müller, J., & Straten, G. (2010). Systematic design of an autonomous platform for robotic weeding. *Journal of Terramechanics*, *47*(2). https://doi.org/10.1016/j.jterra.2009.06.002

Barawid, O. C., Mizushima, A., Ishii, K., & Noguchi, N. (2007). Development of an Autonomous Navigation System using a Two-dimensional Laser Scanner in an Orchard Application. *Biosystems Engineering*. https://doi.org/10.1016/j.biosystemseng.2006.10.012

Bastiaans, L., Paolini, R., & Baumann, D. T. (2008). Focus on ecological weed management: What is hindering adoption? In *Weed Research*. https://doi.org/10.1111/j.1365-3180.2008.00662.x

Bawden, O., Kulk, J., Russell, R., McCool, C., English, A., Dayoub, F., Lehnert, C., & Perez, T. (2017). Robot for weed species plant-specific management. *Journal of Field Robotics*, *34*(6), 1179–1199. https://doi.org/10.1002/rob.21727

Bechar, A., & Vigneault, C. (2016). Agricultural robots for field operations: Concepts and components. In *Biosystems Engineering*. https://doi.org/10.1016/j.biosystemseng.2016.06.014

Behmann, J., Mahlein, A. K., Rumpf, T., Römer, C., & Plümer, L. (2015). A review of advanced machine learning methods for the detection of biotic stress in precision crop protection. In *Precision Agriculture*. https://doi.org/10.1007/s11119-014-9372-7

Berge, T. W., Goldberg, S., Kaspersen, K., & Netland, J. (2012). Towards machine vision based site-specific weed management in cereals. *Computers and Electronics in Agriculture*, *81*, 79–86. https://doi.org/10.1016/j.compag.2011.11.004

Bewley, A., Ge, Z., Ott, L., Ramos, F., & Upcroft, B. (2016). Simple online and realtime tracking. *2016 IEEE International Conference on Image Processing (ICIP)*, 3464--3468.

Bhattacharya, P., & Gavrilova, M. L. (2008). Roadmap-based path planning - Using the voronoi diagram for a clearance-based shortest path. *IEEE Robotics and Automation Magazine*. https://doi.org/10.1109/MRA.2008.921540

Binbin, X., Jizhan, L., Meng, H., Jian, W., & Zhujie, X. (2021). Research progress on Autonomous Navigation Technology of Agricultural Robot. *2021 IEEE 11th Annual International Conference on CYBER Technology in Automation, Control, and Intelligent Systems, CYBER 2021*. https://doi.org/10.1109/CYBER53097.2021.9588152

Blasco, J., Aleixos, N., Roger, J. M., Rabatel, G., & Moltó, E. (2002). AE—Automation and Emerging Technologies: Robotic Weed Control using Machine Vision. *Biosystems Engineering*, *83*(2).

Bochkovskiy, A., Wang, C.-Y., & Liao, H.-Y. M. (2020). YOLOv4: Optimal Speed and Accuracy of Object Detection. *ArXiv Preprint ArXiv:2004.10934*. http://arxiv.org/abs/2004.10934

Buhler, D. D., Liebman, M., & Obrycki, J. J. (2000). Theoretical and practical challenges to an IPM approach to weed management. *Weed Science*. https://doi.org/10.1614/0043-1745(2000)048[0274:tapcta]2.0.co;2

Canny, J. (1986). A Computational Approach to Edge Detection. *IEEE Transactions on Pattern Analysis and Machine Intelligence*, *PAMI-8*(6). https://doi.org/10.1109/TPAMI.1986.4767851

Cao, P. M., Hall, E. L., & Zhang, E. (2003). Soil sampling sensor system on a mobile robot. *Intelligent Robots and Computer Vision XXI: Algorithms, Techniques, and Active Vision*. https://doi.org/10.1117/12.516367

Cerrato, S., Mazzia, V., Salvetti, F., & Chiaberge, M. (2021). A deep learning driven algorithmic pipeline for autonomous navigation in row-based crops. *ArXiv Preprint ArXiv:211.03816*.

Chauvel, B., Guillemin, J. P., Gasquez, J., & Gauvrit, C. (2012). History of chemical weeding from 1944 to 2011 in France: Changes and evolution of herbicide molecules. *Crop Protection*, *42*. https://doi.org/10.1016/j.cropro.2012.07.011

Chechliński, Ł., Siemiątkowska, B., & Majewski, M. (2019). A system for weeds and crops identification—reaching over 10 fps on raspberry pi with the usage of mobilenets, densenet and custom modifications. *Sensors (Switzerland)*, *19*(17). https://doi.org/10.3390/s19173787

Chen, D., Lu, Y., Li, Z., & Young, S. (2022). Performance evaluation of deep transfer learning on multi-class identification of common weed species in cotton production systems. *Computers and Electronics in Agriculture*, *198*. https://doi.org/10.1016/j.compag.2022.107091

Christensen, S., SØgaard, H. T., Kudsk, P., NØrremark, M., Lund, I., Nadimi, E. S., & JØrgensen, R. (2009). Site-specific weed control technologies. *Weed Research*. https://doi.org/10.1111/j.1365-3180.2009.00696.x

Colbach, N., Kurstjens, D. A. G., Munier-Jolain, N. M., Dalbiès, A., & Doré, T. (2010). Assessing non-chemical weeding strategies through mechanistic modelling of blackgrass (*Alopecurus myosuroides* Huds.) dynamics. *European Journal of Agronomy*, *32*(3). https://doi.org/10.1016/j.eja.2009.11.005

Coleman, G., Betters, C., Squires, C., Leon-Saval, S., & Walsh, M. (2021). Low Energy Laser Treatments Control Annual Ryegrass (*Lolium rigidum*). *Frontiers in Agronomy*, *2*. https://doi.org/10.3389/fagro.2020.601542

Coulter, R. C. (1992). Implementation of the pure pursuit path tracking algorithm. *Carnegie Mellon University, The Robotics Institute*.

Culliney, T. W. (2005). Benefits of classical biological control for managing invasive plants. In *Critical Reviews in Plant Sciences* (Vol. 24, Issue 2). https://doi.org/10.1080/07352680590961649

Davies, E., Garlow, A., Farzan, S., Rogers, J., & Hu, A. P. (2018). Tarzan: Design, Prototyping, and Testing of a Wire-Borne Brachiating Robot. *IEEE International Conference on Intelligent Robots and Systems*. https://doi.org/10.1109/IROS.2018.8593823

de Silva, R., Cielniak, G., & Gao, J. (2021). *Towards agricultural autonomy: crop row detection under varying field conditions using deep learning. arXiv preprint arXiv:2109.08247.*

Deery, D., Jimenez-Berni, J., Jones, H., Sirault, X., & Furbank, R. (2014). Proximal remote sensing buggies and potential applications for field-based phenotyping. In *Agronomy*. https://doi.org/10.3390/agronomy4030349

Délye, C., Jasieniuk, M., & Le Corre, V. (2013). Deciphering the evolution of herbicide resistance in weeds. In *Trends in Genetics*. https://doi.org/10.1016/j.tig.2013.06.001

Doha, R., Al Hasan, M., Anwar, S., & Rajendran, V. (2021). Deep Learning based Crop Row Detection with Online Domain Adaptation. *Proceedings of the ACM SIGKDD International Conference on Knowledge Discovery and Data Mining*. https://doi.org/10.1145/3447548.3467155

dos Santos Ferreira, A., Matte Freitas, D., Gonçalves da Silva, G., Pistori, H., & Theophilo Folhes, M. (2017). Weed detection in soybean crops using ConvNets. *Computers and Electronics in Agriculture*. https://doi.org/10.1016/j.compag.2017.10.027

Duan, K., Bai, S., Xie, L., Qi, H., Huang, Q., & Tian, Q. (2019). CenterNet: Keypoint triplets for object detection. *Proceedings of the IEEE International Conference on Computer Vision*, *2019-Octob*, 6568–6577. https://doi.org/10.1109/ICCV.2019.00667

Everingham, M., Van Gool, L., Williams, C. K. I., Winn, J., & Zisserman, A. (2010). The pascal visual object classes (VOC) challenge. *International Journal of Computer Vision*, *88*(2). https://doi.org/10.1007/s11263-009-0275-4

Farzan, S., Hu, A. P., Davies, E., & Rogers, J. (2018). Modeling and control of brachiating robots traversing flexible cables. *Proceedings - IEEE International Conference on Robotics and Automation*. https://doi.org/10.1109/ICRA.2018.8461036

Florance Mary, M., & Yogaraman, D. (2021). Neural Network Based Weeding Robot for Crop and Weed Discrimination. *Journal of Physics: Conference Series*, *1979*(1). https://doi.org/10.1088/1742-6596/1979/1/012027

Fogelberg, F., & Gustavsson, A. M. D. (1999). Mechanical damage to annual weeds and carrots by in-row brush weeding. *Weed Research*, *39*(6). https://doi.org/10.1046/j.1365-3180.1999.00163.x

Fox, D., Burgard, W., & Thrun, S. (1997). The dynamic window approach to collision avoidance. *IEEE Robotics and Automation Magazine*, *4*(1). https://doi.org/10.1109/100.580977

François Chollet. (2015). *Keras*. https://keras.io

Fue, K., Porter, W., Barnes, E., Li, C., & Rains, G. (2020). Autonomous navigation of a center-articulated and hydrostatic transmission rover using a modified pure pursuit algorithm in a cotton field. *Sensors (Switzerland)*, *20*(16). https://doi.org/10.3390/s20164412

Fue, K., Porter, W., Barnes, E., & Rains, G. (2020). An Extensive Review of Mobile Agricultural Robotics for Field Operations: Focus on Cotton Harvesting. *AgriEngineering*. https://doi.org/10.3390/agriengineering2010010

Gao, X., Li, J., Fan, L., Zhou, Q., Yin, K., Wang, J., Song, C., Huang, L., & Wang, Z. (2018). Review of wheeled mobile robots' navigation problems and application prospects in agriculture. In *IEEE Access* (Vol. 6). https://doi.org/10.1109/ACCESS.2018.2868848

Gerhards, R., & Christensen, S. (2003). Real-time weed detection, decision making and patch spraying in maize, sugarbeet, winter wheat and winter barley. In *Weed Research* (Vol. 43, Issue 6, pp. 385–392). https://doi.org/10.1046/j.1365-3180.2003.00349.x

Gerhards, R., & Oebel, H. (2006). Practical experiences with a system for site-specific weed control in arable crops using real-time image analysis and GPS-controlled patch spraying. *Weed Research*, *46*(3). https://doi.org/10.1111/j.1365-3180.2006.00504.x

Gianessi, L. P., & Reigner, N. P. (2007). The Value of Herbicides in U.S. Crop Production. *Weed Technology*. https://doi.org/10.1614/wt-06-130.1

Grimstad, L., & From, P. J. (2017). The Thorvald II agricultural robotic system. *Robotics*. https://doi.org/10.3390/robotics6040024

Guthman, J. (2017). Paradoxes of the Border: Labor Shortages and Farmworker Minor Agency in Reworking California's Strawberry Fields. *Economic Geography*, *93*(1). https://doi.org/10.1080/00130095.2016.1180241

Hamill, A. S., Holt, J. S., & Mallory-Smith, C. A. (2004). Contributions of Weed Science to Weed Control and Management 1 . *Weed Technology*, *18*(sp1). https://doi.org/10.1614/0890-037x(2004)018[1563:cowstw]2.0.co;2

Hannan, M. W., Burks, T. F., & Bulanon, D. M. (2007). A real-time machine vision algorithm for robotic citrus harvesting. *2007 ASABE Annual International Meeting, Technical Papers*. https://doi.org/10.13031/2013.23429

Hasan, A. S. M. M., Sohel, F., Diepeveen, D., Laga, H., & Jones, M. G. K. (2021). A survey of deep learning techniques for weed detection from images. In *Computers and Electronics in Agriculture*. https://doi.org/10.1016/j.compag.2021.106067

Heisel, T., Schou, J., Andreasen, C., & Christensen, S. (2002). Using laser to measure stem thickness and cut weed stems. *Weed Research*, *42*(3). https://doi.org/10.1046/j.0043-1737.2002.00282.x

Heisel, T., Schou, J., Christensen, S., & Andreasen, C. (2001). Cutting weeds with a CO_2 laser. *Weed Research*, *41*(1), 19–29. https://doi.org/10.1046/j.1365-3180.2001.00212.x

Heraud, J. A., & Lange, A. F. (2009). Agricultural automatic vehicle guidance from horses to GPS: How we got here, and where we are going. *ASABE Distinguished Lecture Series - Agricultural Automatic Vehicle Guidance from Horses to GPS: How We Got Here, and Where We Are Going*.

Higuti, V. A. H., Velasquez, A. E. B., Magalhaes, D. V., Becker, M., & Chowdhary, G. (2019). Under canopy light detection and ranging-based autonomous navigation. *Journal of Field Robotics*, *36*(3). https://doi.org/10.1002/rob.21852

Hiremath, S. A., van der Heijden, G. W. A. M., van Evert, F. K., Stein, A., & Ter Braak, C. J. F. (2014). Laser range finder model for autonomous navigation of a robot in a maize field

using a particle filter. *Computers and Electronics in Agriculture*, *100*, 41–50. https://doi.org/10.1016/j.compag.2013.10.005

Jensen, M. A. F., Bochtis, D., Sorensen, C. G., Blas, M. R., & Lykkegaard, K. L. (2012). In-field and inter-field path planning for agricultural transport units. *Computers and Industrial Engineering*, *63*(4). https://doi.org/10.1016/j.cie.2012.07.004

Ji, R., & Qi, L. (2011). Crop-row detection algorithm based on Random Hough Transformation. *Mathematical and Computer Modelling*, *54*(3–4). https://doi.org/10.1016/j.mcm.2010.11.030

Kaierle, S., Marx, C., Rath, T., & Hustedt, M. (2013). Find and Irradiate - Lasers Used for Weed Control. *Laser Technik Journal*, *10*(3), 44–47. https://doi.org/10.1002/latj.201390038

Kalman, R. E. (1960). A new approach to linear filtering and prediction problems. *Journal of Fluids Engineering, Transactions of the ASME*, *82*(1). https://doi.org/10.1115/1.3662552

Khan, N., Medlock, G., Graves, S., & Anwar, S. (2018). GPS Guided Autonomous Navigation of a Small Agricultural Robot with Automated Fertilizing System. *SAE Technical Papers*, *2018-April*. https://doi.org/10.4271/2018-01-0031

Kise, M., Zhang, Q., & Rovira Más, F. (2005). A stereovision-based crop row detection method for tractor-automated guidance. *Biosystems Engineering*, *90*(4). https://doi.org/10.1016/j.biosystemseng.2004.12.008

Koch, G., Zemel, R., & Salakhutdinov, R. (2015). Siamese Neural Networks for One Shot Image Learning. *ICML Deep Learning Workshop*.

Kondo, N., & Ting, K. C. (1998). Robotics for Plant Production. *Artificial Intelligence Review*. https://doi.org/10.1007/978-94-011-5048-4_12

Kuhn, H. W. (1955). The Hungarian method for the assignment problem. *Naval Research Logistics Quarterly*, *2*(1–2). https://doi.org/10.1002/nav.3800020109

Li, Y., Li, J., Zhou, W., Yao, Q., Nie, J., & Qi, X. (2022). Robot Path Planning Navigation for Dense Planting Red Jujube Orchards Based on the Joint Improved A* and DWA Algorithms under Laser SLAM. *Agriculture (Switzerland)*, *12*(9). https://doi.org/10.3390/agriculture12091445

Lin, T. Y., Maire, M., Belongie, S., Hays, J., Perona, P., Ramanan, D., Dollár, P., & Zitnick, C. L. (2014). Microsoft COCO: Common objects in context. *Lecture Notes in Computer Science (Including Subseries Lecture Notes in Artificial Intelligence and Lecture Notes in Bioinformatics)*, *8693 LNCS*(PART 5). https://doi.org/10.1007/978-3-319-10602-1_48

Long, J., Shelhamer, E., & Darrell, T. (2015). Fully convolutional networks for semantic segmentation. *Proceedings of the IEEE Computer Society Conference on Computer Vision and Pattern Recognition*, *07-12-June-2015*. https://doi.org/10.1109/CVPR.2015.7298965

Longchamps, L., Panneton, B., Samson, G., Leroux, G. D., & Thériault, R. (2010). Discrimination of corn, grasses and dicot weeds by their UV-induced fluorescence spectral signature. *Precision Agriculture*, *11*(2). https://doi.org/10.1007/s11119-009-9126-0

Macé, K., Morlon, P., Munier-Jolain, N., & Quéré, L. (2007). Time scales as a factor in decision-making by French farmers on weed management in annual crops. *Agricultural Systems*. https://doi.org/10.1016/j.agsy.2006.04.007

Mahmud, M. S. A., Abidin, M. S. Z., Mohamed, Z., Rahman, M. K. I. A., & Iida, M. (2019). Multi-objective path planner for an agricultural mobile robot in a virtual greenhouse environment. *Computers and Electronics in Agriculture*, *157*. https://doi.org/10.1016/j.compag.2019.01.016

Marx, C., Pastrana Pérez, J. C., Hustedt, M., Barcikowski, S., Haferkamp, H., & Rath, T. (2012). Investigations on the absorption and the application of laser radiation for weed control. *Landtechnik*, *67*(2), 95–101. https://doi.org/10.15150/lt.2012.277

Mathiassen, S. K., Bak, T., Christensen, S., & Kudsk, P. (2006). The Effect of Laser Treatment as a Weed Control Method. *Biosystems Engineering*, *95*(4), 497–505. https://doi.org/10.1016/j.biosystemseng.2006.08.010

McCool, C., Beattie, J., Firn, J., Lehnert, C., Kulk, J., Bawden, O., Russell, R., & Perez, T. (2018). Efficacy of Mechanical Weeding Tools: A Study into Alternative Weed Management Strategies Enabled by Robotics. *IEEE Robotics and Automation Letters*, *3*(2), 1184–1190. https://doi.org/10.1109/LRA.2018.2794619

McKinley, S., & Levine, M. (1998). Cubic spline interpolation. *College of the Redwoods*, *45*(1), 1049–1060.

Mehdizadeh, M., Mushtaq, W., Siddiqui, S. A., Ayadi, S., Kaur, P., Yeboah, S., Mazraedoost, S., Al-Taey, D. K. A., & Tampubolon, K. (2021). Herbicide residues in agroecosystems: Fate, detection, and effect on non-target plants. In *Reviews in Agricultural Science* (Vol. 9, pp. 157–167). https://doi.org/10.7831/ras.9.0_157

Moeller, R., Deemyad, T., & Sebastian, A. (2020). Autonomous Navigation of an Agricultural Robot Using RTK GPS and Pixhawk. *2020 Intermountain Engineering, Technology and Computing, IETC 2020*. https://doi.org/10.1109/IETC47856.2020.9249176

Monkman, G. J. (1995). Robot Grippers for Use With Fibrous Materials. *The International Journal of Robotics Research*. https://doi.org/10.1177/027836499501400204

Monta, M., Kondo, N., & Shibano, Y. (1995). Agricultural robot in grape production system. *Proceedings - IEEE International Conference on Robotics and Automation*. https://doi.org/10.1109/robot.1995.525635

Moore, T., & Stouch, D. (2016). A generalized extended Kalman filter implementation for the robot operating system. *Advances in Intelligent Systems and Computing*, *302*, 335–348. https://doi.org/10.1007/978-3-319-08338-4_25

Mwitta, C., Rains, G. C., & Prostko, E. (2022). Evaluation of Diode Laser Treatments to Manage Weeds in Row Crops. *Agronomy*, *12*(11). https://doi.org/10.3390/agronomy12112681

Nguyen Thanh Le, V., Apopei, B., & Alameh, K. (2019). Effective plant discrimination based on the combination of local binary pattern operators and multiclass support vector machine methods. *Information Processing in Agriculture*, *6*(1). https://doi.org/10.1016/j.inpa.2018.08.002

Noguchi, N., & Terao, H. (1997). Path planning of an agricultural mobile robot by neural network and genetic algorithm. *Computers and Electronics in Agriculture*, *18*(2–3). https://doi.org/10.1016/s0168-1699(97)00029-x

Noh, H., Hong, S., & Han, B. (2015). Learning Deconvolution Network for Semantic Segmentation. *2015 IEEE International Conference on Computer Vision (ICCV)*, 1520–1528. https://doi.org/10.1109/ICCV.2015.178

Oerke, E. C. (2006). Crop losses to pests. In *Journal of Agricultural Science* (Vol. 144, Issue 1). https://doi.org/10.1017/S0021859605005708

Oliveira, L. F. P., Moreira, A. P., & Silva, M. F. (2021). Advances in agriculture robotics: A state-of-the-art review and challenges ahead. In *Robotics* (Vol. 10, Issue 2). https://doi.org/10.3390/robotics10020052

Park, M. W., Lee, S. W., & Han, W. Y. (2014). Development of lateral control system for autonomous vehicle based on adaptive pure pursuit algorithm. *International Conference on Control, Automation and Systems*. https://doi.org/10.1109/ICCAS.2014.6987787

Pedersen, S. M., Fountas, S., Have, H., & Blackmore, B. S. (2006). Agricultural robots - System analysis and economic feasibility. *Precision Agriculture*. https://doi.org/10.1007/s11119-006-9014-9

Pérez-Ruíz, M., Slaughter, D. C., Fathallah, F. A., Gliever, C. J., & Miller, B. J. (2014). Co-robotic intra-row weed control system. *Biosystems Engineering*, *126*. https://doi.org/10.1016/j.biosystemseng.2014.07.009

Peteinatos, G. G., Reichel, P., Karouta, J., Andújar, D., & Gerhards, R. (2020). Weed identification in Maize, sunflower, and potatoes with the aid of convolutional neural networks. *Remote Sensing*, *12*(24). https://doi.org/10.3390/rs12244185

Pimentel, D., Lach, L., Zuniga, R., & Morrison, D. (2000). Environmental and economic costs of nonindigenous species in the United States. In *BioScience*. https://doi.org/10.1641/0006-3568(2000)050[0053:EAECON]2.3.CO;2

Powles, S. B., Preston, C., Bryan, I. B., & Jutsum, A. R. (1996). Herbicide Resistance: Impact and Management. *Advances in Agronomy*, *58*(C). https://doi.org/10.1016/S0065-2113(08)60253-9

Quigley, M., Conley, K., Gerkey, B., Faust, J., Foote, T., Leibs, J., Wheeler, R., & Ng, A. Y. (2009). ROS: an open-source Robot Operating System. *ICRA Workshop on Open Source Software*, *3*(3.2).

Rahaman, M. M., Chen, D., Gillani, Z., Klukas, C., & Chen, M. (2015). Advanced phenotyping and phenotype data analysis for the study of plant growth and development. In *Frontiers in Plant Science*. https://doi.org/10.3389/fpls.2015.00619

Rao, Y., He, L., & Zhu, J. (2017). A residual convolutional neural network for pan-shaprening. *RSIP 2017 - International Workshop on Remote Sensing with Intelligent Processing, Proceedings*. https://doi.org/10.1109/RSIP.2017.7958807

Redmon, J. (n.d.). *Darknet: Open Source Neural Networks in C*. http://pjreddie.com/darknet/

Redmon, J., Divvala, S., Girshick, R., & Farhadi, A. (2016). You only look once: Unified, real-time object detection. *Proceedings of the IEEE Computer Society Conference on Computer Vision and Pattern Recognition*, *2016-December*. https://doi.org/10.1109/CVPR.2016.91

Reiser, D., Sehsah, E. S., Bumann, O., Morhard, J., & Griepentrog, H. W. (2019). Development of an autonomous electric robot implement for intra-row weeding in vineyards. *Agriculture (Switzerland)*. https://doi.org/10.3390/agriculture9010018

Richards, T. J. (2018). Immigration reform and farm labor markets. *American Journal of Agricultural Economics*, *100*(4). https://doi.org/10.1093/ajae/aay027

Richter, O., Zwerger, P., & Böttcher, U. (2002). Modelling spatio-temporal dynamics of herbicide resistance. *Weed Research*. https://doi.org/10.1046/j.1365-3180.2002.00262.x

Rodríguez, F., Moreno, J. C., Sánchez, J. A., & Berenguel, M. (2012). Grasping in agriculture: State-of-the-art and main characteristics. In *Mechanisms and Machine Science*. https://doi.org/10.1007/978-1-4471-4664-3_15

Ronneberger, O., Fischer, P., & Brox, T. (2015). U-net: Convolutional networks for biomedical image segmentation. *Lecture Notes in Computer Science (Including Subseries Lecture*

Notes in Artificial Intelligence and Lecture Notes in Bioinformatics), *9351*. https://doi.org/10.1007/978-3-319-24574-4_28

Rovira-Más, F., Zhang, Q., Reid, J. F., & Will, J. D. (2005). Hough-transform-based vision algorithm for crop row detection of an automated agricultural vehicle. *Proceedings of the Institution of Mechanical Engineers, Part D: Journal of Automobile Engineering*, *219*(8). https://doi.org/10.1243/095440705X34667

Rueda-Ayala, V., Rasmussen, J., & Gerhards, R. (2010). Mechanical weed control. *Precision Crop Protection-the Challenge and Use of Heterogeneity*, 279--294.

Safren, O., Alchanatis, V., Ostrovsky, V., & Levi, O. (2007). Detection of green apples in hyperspectral images of apple-tree foliage using machine vision. *Transactions of the ASABE*. https://doi.org/10.13031/2013.24083

Sahin, H., & Yalınkılıc, M. (2017). Using Electric Current as a Weed Control Method. *European Journal of Engineering Research and Science*, *2*(6). https://doi.org/10.24018/ejers.2017.2.6.379

Sankaran, S., Khot, L. R., Espinoza, C. Z., Jarolmasjed, S., Sathuvalli, V. R., Vandemark, G. J., Miklas, P. N., Carter, A. H., Pumphrey, M. O., Knowles, R. R. N., & Pavek, M. J. (2015). Low-altitude, high-resolution aerial imaging systems for row and field crop phenotyping: A review. In *European Journal of Agronomy*. https://doi.org/10.1016/j.eja.2015.07.004

Schuster, I., Nordmeyer, H., & Rath, T. (2007). Comparison of vision-based and manual weed mapping in sugar beet. *Biosystems Engineering*, *98*(1). https://doi.org/10.1016/j.biosystemseng.2007.06.009

Shah, T. M., Nasika, D. P. B., & Otterpohl, R. (2021). Plant and weed identifier robot as an agroecological tool using artificial neural networks for image identification. *Agriculture (Switzerland)*. https://doi.org/10.3390/agriculture11030222

Shalal, N., Low, T., McCarthy, C., & Hancock, N. (2013). A Review of Autonomous Navigation Systems in Agricultural Environments. *SEAg 2013: Innovative Agricultural Technologies for a Sustainable Future*.

Shaner, D. L. (2014). Lessons Learned From the History of Herbicide Resistance. *Weed Science*, *62*(2). https://doi.org/10.1614/ws-d-13-00109.1

Shapira, U., Herrmann, I., Karnieli, A., & Bonfil, D. J. (2013). Field spectroscopy for weed detection in wheat and chickpea fields. *International Journal of Remote Sensing*, *34*(17). https://doi.org/10.1080/01431161.2013.793860

Shorten, C., & Khoshgoftaar, T. M. (2019). A survey on Image Data Augmentation for Deep Learning. *Journal of Big Data*, *6*(1). https://doi.org/10.1186/s40537-019-0197-0

Simonyan, K., & Zisserman, A. (2015). Very deep convolutional networks for large-scale image recognition. *3rd International Conference on Learning Representations, ICLR 2015 - Conference Track Proceedings*.

Sivakumar, A., Modi, S., Gasparino, M., Ellis, C., Baquero Velasquez, A., Chowdhary, G., & Gupta, S. (2021). *Learned Visual Navigation for Under-Canopy Agricultural Robots*. https://doi.org/10.15607/rss.2021.xvii.019

Sivakumar, A. N. V., Li, J., Scott, S., Psota, E., Jhala, A. J., Luck, J. D., & Shi, Y. (2020). Comparison of object detection and patch-based classification deep learning models on mid-to late-season weed detection in UAV imagery. *Remote Sensing*, *12*(13). https://doi.org/10.3390/rs12132136

Smith, G. L., Schmidt, S. F., & McGee, L. A. (1962). Application of Statistical Filter Theory to the Optimal Estimation of Position and Velocity on Board a Circumlunar Vehicle. In *NASA technical report*.

Sori, H., Inoue, H., Hatta, H., & Ando, Y. (2018). Effect for a paddy weeding robot in wet rice culture. *Journal of Robotics and Mechatronics*, *30*(2). https://doi.org/10.20965/jrm.2018.p0198

Stoll, A., & Kutzbach, H. D. (2000). Guidance of a forage harvester with GPS. *Precision Agriculture*, *2*(3). https://doi.org/10.1023/A:1011842907397

Sujaritha, M., Annadurai, S., Satheeshkumar, J., Kowshik Sharan, S., & Mahesh, L. (2017). Weed detecting robot in sugarcane fields using fuzzy real time classifier. *Computers and Electronics in Agriculture*. https://doi.org/10.1016/j.compag.2017.01.008

Tai, K., El-Sayed, A. R., Shahriari, M., Biglarbegian, M., & Mahmud, S. (2016). State of the art robotic grippers and applications. In *Robotics*. https://doi.org/10.3390/robotics5020011

Tan, M., Pang, R., & Le, Q. V. (2020). EfficientDet: Scalable and efficient object detection. *Proceedings of the IEEE Computer Society Conference on Computer Vision and Pattern Recognition*, 10778–10787. https://doi.org/10.1109/CVPR42600.2020.01079

TensorFlow. (2022). *TensorFlow 2 Model Zoo*. https://github.com/tensorflow/models/blob/master/research/object_detection/g3doc/tf2_detection_zoo.md

Timmons, F. L. (1970). A History of Weed Control in the United States and Canada. *Weed Science*, *18*(2). https://doi.org/10.1017/s0043174500079807

Tu, X., Gai, J., & Tang, L. (2019). Robust navigation control of a 4WD/4WS agricultural robotic vehicle. *Computers and Electronics in Agriculture*, *164*. https://doi.org/10.1016/j.compag.2019.104892

Utstumo, T., Urdal, F., Brevik, A., Dørum, J., Netland, J., Overskeid, Ø., Berge, T. W., & Gravdahl, J. T. (2018). Robotic in-row weed control in vegetables. *Computers and Electronics in Agriculture*, *154*. https://doi.org/10.1016/j.compag.2018.08.043

Wan, E. A., & Nelson, A. T. (2001). Dual Extended Kalman Filter Methods. In *Kalman Filtering and Neural Networks*. https://doi.org/10.1002/0471221546.ch5

Wang, L. (2020). Basics of PID Control. In *PID Control System Design and Automatic Tuning using MATLAB/Simulink*. https://doi.org/10.1002/9781119469414.ch1

Wang, W. J., Hsu, T. M., & Wu, T. S. (2017). The improved pure pursuit algorithm for autonomous driving advanced system. *2017 IEEE 10th International Workshop on Computational Intelligence and Applications, IWCIA 2017 - Proceedings*, *2017-December*. https://doi.org/10.1109/IWCIA.2017.8203557

Wise, A. M., Grey, T. L., Prostko, E. P., Vencill, W. K., & Webster, T. M. (2009). Establishing the Geographical Distribution and Level of Acetolactate Synthase Resistance of Palmer Amaranth (*Amaranthus palmeri*) Accessions in Georgia. *Weed Technology*. https://doi.org/10.1614/wt-08-098.1

Wojke, N., Bewley, A., & Paulus, D. (2018). Simple online and realtime tracking with a deep association metric. *Proceedings - International Conference on Image Processing, ICIP*, *2017-September*. https://doi.org/10.1109/ICIP.2017.8296962

Wöltjen, C., Haferkamp, H., Rath, T., & Herzog, D. (2008). Plant growth depression by selective irradiation of the meristem with CO2 and diode lasers. *Biosystems Engineering*, *101*(3), 316–324. https://doi.org/10.1016/j.biosystemseng.2008.08.006

Xiong, Y., Ge, Y., Liang, Y., & Blackmore, S. (2017). Development of a prototype robot and fast path-planning algorithm for static laser weeding. *Computers and Electronics in Agriculture*, *142*. https://doi.org/10.1016/j.compag.2017.11.023

Yang, C. C. (2000). Application of artificial neural networks in image recognition and classification of crop and weeds. *Canadian Biosystems Engineering / Le Genie Des Biosystems Au Canada*.

Yu, J., Sharpe, S. M., Schumann, A. W., & Boyd, N. S. (2019). Deep learning for image-based weed detection in turfgrass. *European Journal of Agronomy*. https://doi.org/10.1016/j.eja.2019.01.004

Zahniser, S., Taylor, J. E., Hertz, T., & Charlton, D. (2018). Farm Labor Markets in the United States and Mexico Pose Challenges for U. S. Agriculture. *USDA Economic Research Service*, *201*.

Zhang, Z., Noguchi, N., Ishii, K., Yang, L., & Zhang, C. (2013). Development of a robot combine harvester for wheat and paddy harvesting. *IFAC Proceedings Volumes (IFAC-PapersOnline)*. https://doi.org/10.3182/20130327-3-jp-3017.00013

Zhao, Y. dong, Sun, Y. rui, Cai, X., Liu, H., & Lammers, P. S. (2012). Identify Plant Drought Stress by 3D-Based Image. *Journal of Integrative Agriculture*. https://doi.org/10.1016/S2095-3119(12)60116-6

Zheng, Y., Zhu, Q., Huang, M., Guo, Y., & Qin, J. (2017). Maize and weed classification using color indices with support vector data description in outdoor fields. *Computers and Electronics in Agriculture*, *141*. https://doi.org/10.1016/j.compag.2017.07.028

Zhu, W., & Zhu, X. (2009). The application of support vector machine in weed classification. *Proceedings - 2009 IEEE International Conference on Intelligent Computing and Intelligent Systems, ICIS 2009*, *4*. https://doi.org/10.1109/ICICISYS.2009.5357638

Zhuang, F., Qi, Z., Duan, K., Xi, D., Zhu, Y., Zhu, H., Xiong, H., & He, Q. (2021). A Comprehensive Survey on Transfer Learning. In *Proceedings of the IEEE* (Vol. 109, Issue 1). https://doi.org/10.1109/JPROC.2020.3004555